Université de Lille

École Doctorale Mathématiques, sciences du numérique et de leurs interactions

Institut de Recherche Inria Lille - Nord Europe

Thèse préparée par **Meysam Mayahi**
en vue de l'obtention du grade de **Docteur en Informatique**
Discipline **Informatique et Applications**

Protocoles de communication basés sur un paradigme alternatif pour les appareils mobiles sans fil

---

Thèse soutenue le 12/12/2022 devant le jury composé de :

Valeria LOSCRI Chargée de recherche HDR, Inria	**Directrice de thèse**
Mohammad-Ali KHALIGHI Professeur associé, Ecole Centrale Marseille	**Rapporteur**
Pierre COMBEAU Professeur associé, XLIM	**Rapporteur**
Luc CHASSAGNE Professeur, Université de Versailles Saint-Quentin	**Examinateur**
Virginie DENIAU Directrice de recherche, Université Gustave Eiffel	**Examinatrice**
Antoine GALLAIS Professeur, INSA Hauts-de-France	**Examinateur et Président**

University of Lille
Doctoral School MAthematics and DIgital Sciences
Research Institute Inria Lille - Nord Europe

Thesis prepared by **Meysam Mayahi**
with the view of obtaining the degree of **PhD in Computer Science**
Discipline **IT and Applications**

Communication Protocols Based on Alternative Paradigm for Wireless Mobile Devices

---

Thesis defended the 12/12/2022 in-front of the jury comprised of:

Valeria LOSCRI	**Supervisor**
Permanent Researcher, Inria	
Mohammad-Ali KHALIGHI	**Rapporteur**
Associate Professor, Ecole Centrale Marseille	
Pierre COMBEAU	**Rapporteur**
Associate Professor, XLIM	
Luc CHASSAGNE	**Examiner**
Professor, Université de Versailles Saint-Quentin	
Virginie DENIAU	**Examiner**
Research Director, Université Gustave Eiffel	
Antoine GALLAIS	**Examiner and President**
Professor, INSA Hauts-de-France	

يَقِينًا كُلُّهُ خَيْرٌ

Preface

During the last decade, the exponential growth of mobile devices and wireless applications induced an enormous demand for radio frequency (RF) technologies which in return requires more and more resources from both the connecting devices and the supporting network infrastructures. Spectrum crunch is a term referred to the network traffic overload and the infrastructure ability to meet the user demands because of limited resources. In recent years, many strategies have been adopted to make the most of these precious resources, such as reusing the available frequency band, and/or discovering new bands such as millimeter and Tera-hertz waves. Meanwhile, the Visible Light Communications (VLC) demonstrate huge capacity to supplement the conventional RF technology, including unlicensed and free massive spectrum band, which provides the communication service along with illumination at a convenient price. Despite its vast potential applications and available infrastructures, VLC is still in its infancy and has a long way to pave in order to join the heterogeneous architectures. At this time, the majority of scientific research has been conducted around the physical and data link layers with emphasis on the point to point communication, while the development on the upper layers has been partially neglected. Certainly, the stable connection at the "decent rate" is the key objective of the medium access control layer which is acquired through different techniques such as handover, multiple access, association, disassociation and adaptive modulation and coding schemes. In this doctoral dissertation entitled as "Communication protocols based on alternative paradigm for wireless mobile devices", VLC has been initially used to address vehicular communication challenges as a main application at MAC layer, by integrating VLC and cellular vehicular to everything (C-V2X). The main contributions of this PhD thesis are as follows: 1- study and derive a communication model for outdoor VLC applications using open source simulating tools, 2- design and apply link adaptive protocols to associate, transmit and modify the communication session in VLC mobile scenarios, 3- develop, implement and test the interference based handover mechanism in small scale testbed, 4- comprehensive comparison between LTE-V2X and V2LC performances in ad-hoc regime, 5- design and perform the RF-V2LC protocol for cooperative VLC and LTE in vehicular network. These contributions have been performed through deep understanding of the up to date literature, interpret, compare and analyze the recent associated researches and developments in order to provide the reliable outcomes in VLC communication protocols for mobile devices.

Contents

List of Figures

List of Tables

introduction 1

The ever-increasing number of mobile devices and wireless applications induces an extensive demand for Radio Frequency (RF) spectrum. According to [1] The total number of global mobile subscribers will grow from 5.1 billion (66 percent of the world's population) in 2018 to 5.7 billion (71 percent of the world's population) by 2023. During the same period, connected home applications will have nearly half or 48 percent of Machine-to-Machine (M2M) share by 2023 and connected car applications will grow the fastest at a Compound Annual Growth Rate (CAGR) of 30 percent. Higher cost and limited free RF spectrum to host further mobile data traffic call for an alternative communication medium to offload traffic from the RF spectrum and provide more capacity.

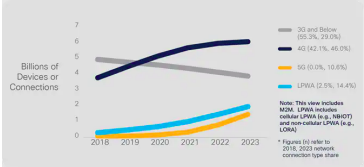

Figure 1.1: Wireless connections trend

1.1 Visible Light Communication

In recent years many technologies have been presented to solve the "spectrum crunch" problem, meanwhile Visible Light Communication (VLC) demonstrate a great capacity to complement the RF systems including the huge unregulated bandwidth, immunity to interference with RF technologies, free-of-charge operations, and several other benefits. Visible light is a portion of the electromagnetic spectrum that is visible to human eyes and falls between 430 and 770 nanometers of wavelength. VLC is a subset of optical wireless communication (OWC) that employs this part of the electromagnetic spectrum for wireless transmission, in the other words, VLC uses visible light as a carrier for data transmission and can be applied to many communication scenarios. For example, VLC can be used in electromagnetic waves restricted zones such as hospitals and airplanes, or it can be applicable in underwater communications where the seawater penetration is high [2]. Affordable and widespread applications of the LED in the automotive industry grab the attention of VLC standardization efforts and R&D studies in this market.

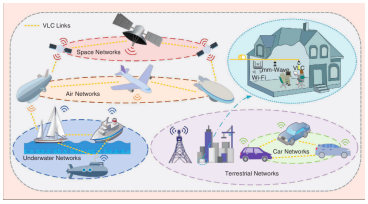

Figure 1.2: The applications of VLC in space, air, underwater, indoor, and car networks

The communication service of LED is based on high-speed Intensity Modulation (IM) that is transparent to human eyes without any adverse effects on illumination level. The principal element responsible for Direct Detection (DD) in the receiver side of the VLC system is the Photodetector (PD). PD including phototransistors and photodiodes collect the light radiation and transform it proportionally to electrical voltage or current signals. Thus, VLC employs Intensity Modulation and Direct Detection (IM/DD) for data transmission where the instantaneous radiated optical power is determined by the signal amplitude which is non-negative and real-valued. These constraints limit the choices of effective modulation schemes used in VLC systems. Single carrier modulation techniques such as Pulse Position Modulation (PPM) and On-Off Keying (OOK) were initially considered for low-rate data transmission in VLC studies while recently the sophisticated Orthogonal Frequency Division Multiplexing (OFDM) such as Direct Current biased Optical OFDM (DCO-OFDM) and Asymmetrically Clipped Optical OFDM (ACO-OFDM) have been

adopted. Alongside the drawbacks inherited from intensity modulation, the Line of Sight (LoS) restriction makes practical employment of VLC challenging. LoS is the most interesting scenario in various VLC systems where the optical lens concentrates the light on a narrow beam with minimal power consumption and a high power flux density on the photodiode. Moreover, LoS system does not suffer from multi-path distortions, and the noises from ambient light sources are substantially rejected with a narrow Field of View (FoV) at the receiver. However, the directionality may limit the communication range, and consequently, multiple VLC setups are needed to fully cover an area. In mobile communications, keeping the transmitter and the receiver in close alignment is the most challenging task, which has been dealt with by means of mobility management techniques. Future development of the VLC technology is subjected to increasing the robustness against noise and interference. The nature of the noise in VLC systems depends on the light flux hitting the PD. For instance, in outdoor applications, sunlight is the main source of noise while incandescent or fluorescent lamps create the major ambient noise indoors. Interference in VLC systems occurs when the signal from neighboring transmitters lands on the sensor. Although the interference and the noise can be from very different natures, however, they account for channel disturbances and degrade the performance of the VLC systems. In addition to the indicated Point-to-Point (P2P) challenges, VLC as a complementary technology needs to be integrated with the heterogeneous networks [3] [4]. Channel access, guaranteed time slot management, frame validation, association and disassociation, beacon management, and mobility management require further efforts on upper layers.

1.2 Vehicular Communications

In Intelligent Transportation system (ITS), Vehicular Communication (VC) include vehicles and other communication entities around it such as roadside infrastructures, networks, and the devices carried by individuals and pedestrians, setting up a reliable and scalable communication link between Vehicle to Vehicle (V2V), Vehicle to Infrastructure (V2I), and Vehicle to Pedestrian (V2P). Vehicle to Everything (V2X) enables the vehicle to communicate with its surroundings to disseminate and collect a variety of safety, infotainment, mobility, and environmental information in order to increase safety on the road and the driving experience. Safety applications supply drivers with information ranging from weather conditions, road construction, speed limits, and many other factors necessary to avoid accidents. Non-safety applications, on the other hand, include services related to the environment, maintenance, mobility infotainment, etc. The driver from its dashboard can access infotainment services such as multimedia, TV, messaging, navigation, calling, and many other applications available nowadays on smartphones. However, Quality of Service (QoS) and Quality of Experience (QoE) are essential issues in vehicular communication because of their high mobility and dynamic network topology. Car-Manufacturing companies such as Ford, Volvo, and BMW are adopting the available wireless technologies to provide safety and non-safety applications. DSRC and cellular networks are the most employed Radio Access Technologie (RAT) in V2X communications. The

Dedicated Short Range Communication (DSRC) was primarily deployed to ensure traffic efficiency and road safety through 3 Mbps bandwidth at 5.9 GHz in Europe. After launching the early version of LTE/4G in 2008, the first standard for Cellular V2X (C-V2X) was introduced in the Third Generation Partnership Project (3GPP) Release 14 and completed in September 2016. It uses an upgraded Device to Device (D2D) interface called PC5 to enable V2V links in high-density and high-speed scenarios. However, the significant Doppler shift due to high velocity degrades the performance of V2X radio access technologies. Moreover, excessive resource collision from the random resource allocation mechanism increase the packet loss and the packet delay in high-density scenarios. Finally, the lack of orthogonal resources in covered areas, as well as synchronized resources (infrastructures) in remote scenarios calls for an alternative paradigm to enhance the V2X performance [5].

1.3 Vehicular VLC

Vehicular Visible Light Communication (V2LC) represents one of the most attractive paradigms of V2X. The aim of V2LC like other VC mediums is to exchange information between generic vehicles and their surroundings in order to improve the safety and driving experience on the roads. Different from RF-based solutions (DSRC, C-V2X) that have congested licensed-band, complex structure, and high deployment cost, vehicular VLC is a less complex, unlicensed, low cost, reliable, low energy, efficient, secured, and interference-free solution. Widespread employment of LEDs in car lumps, traffic lights as well as control cameras and sensors in ITS, lends additional motivation for researchers and industries to invest in vehicular applications using VLC. Platooning is a popular application in Vehicular communications where autonomous vehicles are accessing each other's information and are grouped within close proximity. VLC can assist the safety message dissemination in multiplatoon [1] when the performance of the dominant RAT degrades due to congestion [6]. Directive features of LED (LoS propagation) provide highly accurate positioning of neighbors. Furthermore, Intel's scientists see excellent opportunities for VLC in automobile applications including adaptive cruise control, cooperative driving, collision avoidance, and even autonomous driving [5].

1: Multiplatoon is an enhanced version of platooning chain where the platoons follow one another

Vehicular applications of VLC technology remain potential in the presence of some critical issues such as an effective handover mechanism for efficient mobility management, Quality of Service (QoS) stability through VLC integration to the vehicular radio access technologies (C-V2X) as well as adaptive resource allocation and medium access process. As a matter of fact, to make VLC more operational in a real vehicular environment, an efficient design of Medium Access Control (MAC) protocol is required to ensure a seamless exchange of information in challenging V2X natures coming from high dynamicity, environmental disturbances, and co-channel interference.

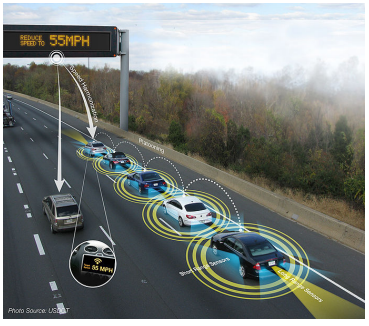

Figure 1.3: VLC platooning

1.4 Objectives and Contributions

Early studies on VLC technology have proven that it is highly applicable to vehicular communication. However, the current trend in VLC research is mainly restricted to the Physical aspects of LoS links such as noise mitigation and interference avoidance and new modulation techniques. The context of V2LC is highly dynamic rather than costly to implement. So the first challenge is to design and test an accurate model of an outdoor VLC channel. For this part, a channel model has been implemented which encounters two well-known signal attenuation: the sunlight shot noise and the climate fluctuation with atmosphere distortion index. This pragmatic channel model includes the Lambertian channel loss and statistical climate impairments that have been implemented on the open-source NS-3 simulating tool and tested for different outdoor illuminance ranges. [2] Under vibrant V2LC channel parameters including the front-end orientation, transmitter-receiver path loss, and climate conditions, the link performance is extremely time-variant, and having a precise evaluation of the channel quality requires a continuous sensing state along with the constant discovery of pilot messages. The pilot message periodicity has a massive impact on the link evaluation and MAC protocol efficiency. This parameter is discussed in the Link Adaptive Protocol (LAP) to find a compromise between the protocol overhead and the link performance in terms of goodput and outage probability. LAP is the 3-step MAC protocol developed originally in this thesis to make a quick connection when the VLC link is available, it adjusts the data rate based on the quality of the link, and moves to other links when the quality of the current link degrades.

2: Realistic simulation tools facilitate analyzing different channel factors and examination of new MAC algorithms.

Link quality in VLC is typically evaluated through Signal to Noise Ratio (SNR) and the corresponding Bit Error Rate (BER), ignoring any signal disturbances due to interference from other transmitters. The more accurate channel assessment is given by Signal to Interference and Noise Ratio (SINR) taking into account the normal distribution of interference and noise and the in-range variance of the disturbances. In contrast, the interference and noise distribution is depending on the dominant disturbance and are not always in the same range. The Interference based haNdover mechanism for VISIBle Light nEtworks (INVISIBLE) represents a new handover mechanism based on innovative link evaluation metrics called Interference to Noise Ratio (INR) and Interferer to Interference Ratio (IIR). In this handover mechanism, the dominant interferer has been selected as an Access Point (AP) candidate if its INR and IIR factors respect the thresholds. Eventually, among all the AP candidates the QoS requirement defines the handover host. This algorithm comes with an Adaptive Modulation Scheme (AMS) to further enhance the spectrum efficiency and prolong the connectivity. The performance of the invisible handover mechanism has been evaluated through extensive simulations based on the NS3 simulator tool and experimental validation in a small-scale version scenario in terms of handover rate, delivered traffic per handover, and handover delay ratio. The good match between the simulation and experiment results proves the faithful performance evaluation of the proposed handover and transmission mechanism.

As it has been mentioned earlier, one of the most interesting advantages of VLC in vehicular applications is the pre-existing infrastructure, which is apparently compatible with cellular V2X. To demonstrate the efficiency of

the VLC performance in V2X communication, a comprehensive study on V2LC has been carried out and compared to C-V2X, regarding the energy consumption, Packet Reception Ratio (PRR), and end-to-end latency. Based on the achieved results, the vertical handover mechanism has been implemented to guarantee the predefined 3GPP baseline for Cooperative Awareness Messages (CAM). The harmonical Cellular Vehicular VLC (CV2LC) network assures the safety message delivery at the lowest energy cost and lowest delay.

1.4.1 Manuscript outline

This manuscript is arranged into five chapters:
Chapter 1 introduces the general concepts of VLC, the advantages, the challenges as well as the potential applications including vehicular VLC. It is also including the motivations behind this thesis and the main contributions.
In Chapter 2 the related works have been narrated starting from a brief history of OWC to the most recent novelties in V2LC. It provides background knowledge for the general viewers as well.
Chapter 3 represents the first bunch of contributions of this work. It contains the realistic channel model realized on the open-source simulation tool, along with link adaptive protocol and its performance evaluation.
The interference-based horizontal handover mechanism has been presented in Chapter 4. This chapter includes an interesting discussion on the handover delay ratio in simulation and the testbed too.
In Chapter 5, a comprehensive comparison between two vehicular ad-hoc networks namely V2LC and C-V2X has been carried out. This chapter points out the major energy-consuming components of VLC and LTE transceivers based on a valid theoretical power model. Additionally, the Vehicular VLC shows a better performance in high-density scenarios in terms of latency and packet reception ratio. Based on these parameters, the CV2LC handover mechanism has been developed to guarantee the seamless dissemination of CAM messages at a relatively low price.
Finally, Chapter 6 is the outcomes synthesis of this thesis, discussion regarding the contributions and the future potential steps.
This thesis has been carried out in the "Institut national de recherche en sciences et technologies du numérique (INRIA) Lille - Nord Europe" under the supervision of Dr. Valeria Loscri. During this research, I have participated in multiple academic activities including:
• Enabling technologies for industrial Internet of things (21 July 2021 - 28 July 2021) summer school at the University of Pisa, Italy
• Vehicular Platooning (25 October 2021 - 9 November 2021) Online course
• Giving engaging scientific talks (28 October 2020 - 30 October 2020) Online course
• Français langue étrangère (FLE) - French language (07 February 2020 - 17 April 2020) Université de Lille - DEFI - bât. SUP SUAIO - Cité scientifique
• Ethique et intégrité scientifique - (27 Agust 2022) FUN MOOC, Université de Bordeaux

Some parts of this research have been published as follows:

• *Meysam Mayahi, Valeria Loscri, and Antonio Costanzo. 2021. Link adaptive protocol for V2LC. In Proceedings of the Workshop on Internet of Lights (IoL '21). Association for Computing Machinery, New York, NY, USA, 13–17. https://doi.org/10.1145/3469264.3469807*
• *M. Mayahi, V. Loscri and A. Costanzo, "INVISIBLE: Enhanced Handover technique for Vehicular Visible Light Networks," 2022 IEEE 95th Vehicular Technology Conference: (VTC2022-Spring), 2022, pp. 1-5, doi: 10.1109/VTC2022-Spring54318.2022.9860664.*
• *M. Mayahi, A. Costanzo, V. Loscri and A. M. Vegni, "An Interference to Noise Ratio Handover mechanism for Mobile Visible Light Communication Networks," 2022 13th International Symposium on Communication Systems, Networks and Digital Signal Processing (CSNDSP), 2022, pp. 457-462, doi: 10.1109/CSNDSP54353.2022.9907915.*

Related Works 2

The Growing number of mobile devices and their applications, enforces a huge amount of data exchange among mobile nodes and infrastructures, thereby, pushing the available RF technologies resources to their limit. VLC is a new paradigm that appeared to complement RF technologies in addressing the RF spectrum crunch. In this chapter first a brief summary of OWC is presented, then a more detailed VLC link and its characteristics are outlined. Later on, the interesting applications of VLC and their challenges will be discussed, and finally, the most innovative solutions to these challenges from recent academic literature are examined.

2.1 VLC

Optical communication is any kind of telecommunication that uses light as the transmission medium. Historically, optical wireless communication (OWC) originates in the form of beacon fires and smokes to convey a message in old cultures. In 1588, an army of 130 Spanish battleships known as the Spanish Armada set off from Flanders with the aim of invading England and overthrowing Queen Elizabeth I. When the fleet was spotted off the shore, a system of interlinking beacons was lit along the South Coast from Cornwall to London, to give warning of the arrival of the invading army. This rudimentary but effective system meant that English sea captain Sir Francis Drake and his men had time to prepare defenses and gather weapons. Drake's ships were able to stop the invasion and defeat the Spanish fleet before it could reach the English shore [1].

While after, the heliograph was the standard wireless solar telegraph between British and Australian armies until the 1960s. The heliograph was a semaphore system that reflects the sunlight by pivoting a mirror in a given order (*e.g.*, to generate the Morse code). In 1880, Alexander Graham Bell was able to modulate a voice message to a light signal and employs Free Space Optical (FSO) link to transmit it. Figure 2.2 shows the sketch of his Photophone including a vibrant mirror at the transmitter and crystalline selenium cells at the focal point of a parabolic receiver [8]. The recent advancement in OWC technology gained a higher pace after

1: https://www.atlasobscura.com/places/armada-beacon, Published on July 25, 2018

Figure 2.1: Armada Beacon Hove, England [7]

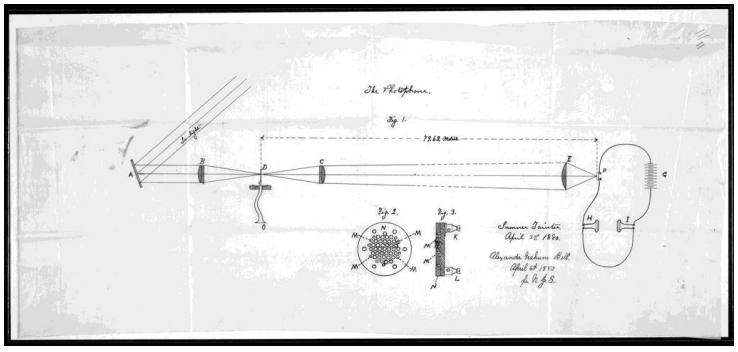

Figure 2.2: Photophone of A. G. Bell

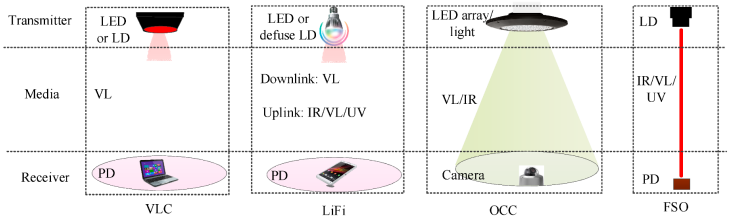

Figure 2.3: OWC technologies architecture

Table 2.1: Performance metrics in different OWC technologies

Metric	VLC	LiFi	OCC	FSO
Topology	Unidirectional/Bidirectional	Bidirectional	Unidirectional	Unidirectional/Bidirectional
Coverage	20 m	10 m	60 m	≤ 10,000 km
Mobility support	Low	High	Low	No
Distortion source	ambient light, atmospheric disturbance	ambient light	ambient light	atmospheric disturbance
Interference level	Low	Low	Zero	Low
Data rate	10 Gbps in LED and ≤ 100 Gbps in LD	10 Gbps in LED and ≤ 100 Gbps in LD	55 Mbps	40 Gbps
Security	High	High	High	High

the pioneering work of Bapst and Gfeller in 1979. They showed the extraordinary capacity of OWC which is promising hundred of terahertz of bandwidth. The four main OWC technologies, namely visible light communication (VLC), Light Fidelity (LiFi), Optical Camera Communication (OCC), and Free Space Optics have different characteristics [9], and use different infrastructures. VLC uses light emitting diode (LED) as the transmitter, a photodetector (PD) as a receiver, and visible light (VL) as a communication medium. LiFi is the optical equivalent of Wireless Fidelity (WiFi). In LiFi, the PDs are used as a receiver, and the LEDs or defused Laser Diode (LD) infrastructures are dual-used for co-located lighting and wireless communications [10]. It uses the VL for the uplink and the Infrared (IR) or VL for the downlink. The OCC uses an LED array as a transmitter and a camera or image sensor as a receiver. The communication medium of OCC is normally VL or IR, but Ultra Violate (UV) also can be used. FSO technology utilizes LD as a transmitter and PD as the receiver, while the communication medium is normally IR rather than UV and VL. The performance metrics of these technologies are represented in table 2.1 [9].

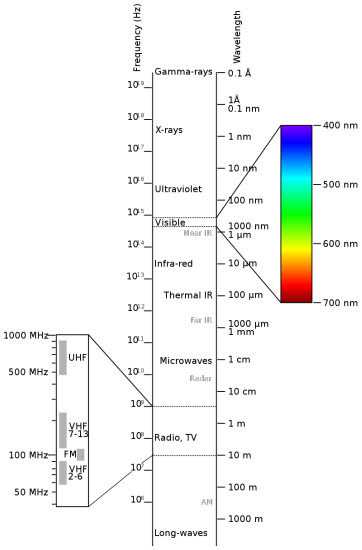

Figure 2.4: Electromagnetic spectrum and visible light

Nowadays, increasing the popularity of smartphones and their applications (nearly 300 billion mobile applications), the wireless data traffic exchanged among connected devices is growing exponentially. According to Cisco annual report [1] nearly two-thirds of the global population will have Internet access by 2023-5.3 billion internet users equal to 66% of the global population- 70% of them are through mobile connections. Globally, mobile data traffic in 2021 approximated 48.3 Exabytes per month which is 23 times the volume of the entire Global Internet in 2005 [11]. While the mobile data traffic demands continue to increase, the technical advancements and novel standards saturate the network spectral efficiency, and the concerns about the "RF spectrum crisis" becomes alarming [12]. Therefore, the acquisition competition on the limited RF spectrum increases the assignment price and induces security issues.

Recent complementary wireless transmission techniques have been explored in order to relieve the spectrum occupation. They can be divided in two main categories: spectrum sharing, and spectrum discovery. Spectrum sharing is relying on central resource management unit to re-use the spectrum resources when they are not used by the owner licensed owner, or to use it non-adjacent geographical cells simultaneously such as cognitive radio [13]. On the other hand, spectrum discovery is trying to find empty rooms in higher frequency bands for example terahertz and millimeter wave [14]. OWC is one of the promising emerging alternative

approaches which offers lots of advantages over RF transmission. As a subset of OWC, VLC is allowing the use of commercial LEDs for both illumination and data transfer operations. Owing to the widespread usage of such convenient illumination appliances, the interest in VLC technologies has multiplied in academia and industry. VLC uses an unregulated visible light spectrum between 380 nanometers and 780 nanometers with 670 Terahertz bandwidth for data transmission (see figure 2.4). With an unregulated huge band spectrum and the commercial LED, the implementation cost of VLC front-ends is low. In addition, VLC is free of any health concern as long as the eye safety regulations are respected [15]. Additionally, with the invention of precise PDs, VLC becomes a reliable candidate for medium-range data transmission that can contribute to addressing the RF shortage.

Figure 2.6 illustrates the major components of a generic VLC link. At the transmitter, the modulated digital information (bits, symbols) is transformed into the current signal and fed to the LED. LED converts the current signal to the information-carrier optical density. The optical signal may pass through an optical system in order to further shape the transmitted beam. For example, an optical amplifier lens concentrates or expands the beam. The optical signal is then transmitted over the optical wireless channel. A portion of the optical energy is absorbed by the objects in the surrounding, and the rest is reflected back in a diffuse or specular way. LoS and Non-LoS components of the transmitted signal get attenuated, fluctuated, and interfered in the OWC channel before arrival to the receiver. An optical filter can select a portion of interest from the received optical spectrum, and limit the interference from ambient lights [16]. The useful signal then can be amplified to be fed to the photodetector. At the photodetector, the optical signal is converted back to electrical current and post-processed to recover the information bits. In this process, the intensity Modulation and Direct Detection (IM/DD) should guarantee the real value and positive VLC signal. The most common single carrier intensity modulation techniques are listed in 2.5.

The difference between the LoS and Non-LoS scenarios is twofold:
- The LoS kink neglects the multi-path dispersion.
- • Having a wide Field of View (FoV), the receiver at Non-LoS scenario accounts for surrounding surfaces dispersion

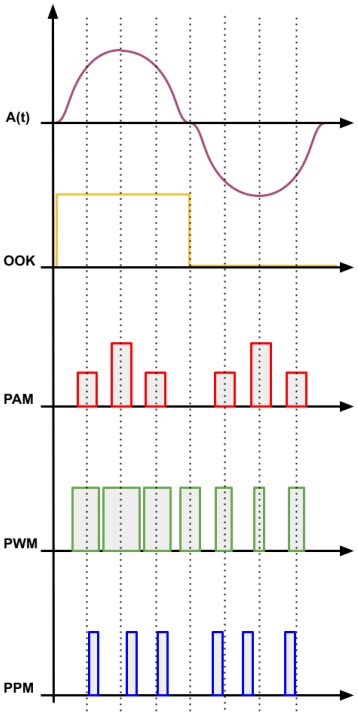

Figure 2.5: Single carrier intensity modulation techniques in VLC

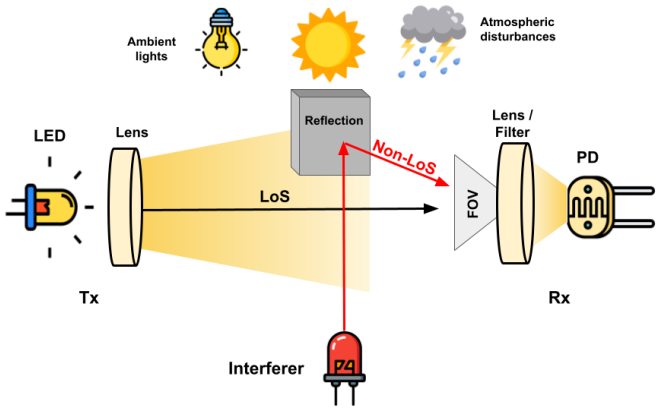

Figure 2.6: VLC transmission link including the major disturbance sources in outdoor and indoor applications. The optical wireless channel is affected by reflected interference.

At Non-LoS scenarios the receiver accounts for the dispersion from nearby surfaces

The sources of the distortions in VLC depend on the applying environment. For instance, in indoor applications, the major noise is coming from ambient lights such as fluorescent and incandescent lights, while sunlight is the primary noise concern in outdoor scenarios. The atmospheric fluctuation might be an important issue in outdoor applications depending on the weather condition. For example, fog is much more difficult to deal with, in comparison to rain and snow due to attenuation effects and discursive water particles in such climatic circumstances [17].
Based on the aforementioned advantages and characteristics, VLC has a high potential to be employed in many applications. The application domains of VLC include indoor wireless communication, underwater communication, vehicular communications, positioning, and Machine-to-Machine (M2M) communications [18].
LiFi: LiFi is a high-speed bidirectional visible light access point equivalent of WiFi. It can illuminate the living areas and offloads the data traffic from cellular networks simultaneously.
Underwater Communication, The propagation loss of the RF signal in the seawater is very high because of its conductivity. VLC has been used in the Un Tethered Remotely Operated Vehicle (UTROV) project for observatory maintenance deep in the oceans controlled from the ship on the sea level (See figure 2.7).
Healthcare, In hospitals, the areas where electromagnetic waves are prohibited (*e.g.*, where the MRI scanner is located) are likely to adopt VLC because it will not interfere with RF waves of traditional systems.
Signalboard An array of modulated LEDs is used in the form of signboards in order to send the broadcasting information.

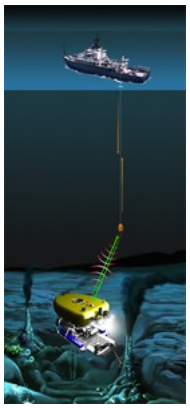

Figure 2.7: Underwater VLC in UTROV operation[18]

Positioning, Accurate coordinates of a receiver is feasible using multiple VLC transmitters even in noisy environment [19]. To carry out a precise positioning system using VLC, a receiver must pick up the signals from LEDs and calculate the distance from them. One algorithm for VLC positioning is to use Received Signal Strength (RSS) and count the Time of Arrival (ToA) in a synchronous way. Undoubtedly, VLC-based positioning applications going to be an important part of localization technologies in the near future [3].
Vehicular Communication, VLC can be used in vehicular communication owing to vehicle light and Road Side Unit (RSU) infrastructure. Vehicular VLC can support safety applications such as cooperative forward collision warnings, pre-crash sensing, emergency brake lights, lane change warnings, stop sign movement assistant, left turn assistant, traffic violation warning signal, and curve speed warnings. All of these safety applications, have some Quality of Service (QoS) requirements such as low latency, reliability and seamless connectivity [20].
Vehicular VLC is in the heart of this thesis and it deserves further explanations on its objectives, standards, mediums and challenges, therefore the following section is devoted to the details of V2LC.

2.2 V2LC

Vehicular communications enable a broad area of safety, environmental, and infotainment applications. The vehicular communication systems include vehicles and other communication entities around them such

as RSU, clouds, grids and fog networks, the Internet, pedestrian smart devices, etc. The objective of vehicular communications is to ensure road safety, prevent road accidents, reduce fuel consumption and carbon emission, save time and offer a higher level of driving comfort. To reach these aims, information is exchanged among vehicles and other communication entities. This type of communication is called as the vehicle to everything (V2X) communication and it includes vehicle-to-vehicle (V2V), vehicle-to-infrastructure (V2I), Vehicle-to-Network (V2N), vehicle-to-pedestrian (V2P), and Vehicle-to-Device (V2D) communication [21]. Figure 2.8 represent schematics of V2X scenarios.

Figure 2.8: Vehicle to everything communication scenarios [22]

Intelligent Transport System (ITS) uses different radio access technologies (RATs) to implement V2X communication. Here we discuss the popular RATs for V2V and V2I communications and after we give a summarized comparison in form of table 2.2.

DSRC, IEEE 802.11p: The primary radio access technology enabling V2X communication in a connected vehicle is DSRC. DSRC spectrum is locally allocated by national organizations, and standardized by the IEEE and the American Society for Testing and Materials International (ASTM) in the USA, the European Telecommunications Standards Institute (ETSI) and the European Committee for Standardization (CEN) in Europe, and the Association of Radio Industries and Businesses (ARIB) in Japan. To use the DSRC in the vehicular networks the IEEE 802.11p and Wireless Access in Vehicular Environments (WAVE) have been implemented as an amendment to IEEE 802.11 (IEEE 802.11a) standard in 2010 and revised in 2012 to facilitate V2V and V2I communication. The IEEE 802.11p includes DSRC based on ASTM E2213-03 standard, which specifies the Medium Access Control (MAC) sub-layer and the physical layer of the WAVE protocol stack. The IEEE 802.11p protocol is widely used in North America and Europe [23].

Cellular V2X: The first standard of C-V2X is the release 14 from 3GPP in September 2016. It is an updated version of the LTE based device to device (D2D) communication ProSe introduced in 3GPP Release 12 which focuses on V2V communication and later on by further enhancements to support V2I-based safety and non-safety service requirements. The D2D interface PC5 introduced in Release 12/13 was not suitable for V2X services and needs to be modified. Thus, to enable V2V communication and address the two main challenges of a vehicular network: high-speed (up to 250Kph) and high density (thousands of nodes), the current interface is introduced in Release 14 with changes at the link and system level. This new design is scalable for different bandwidths namely 10 MHz and 20 MHz [24]. The C-V2X technology introduced two modes of vehicular communication. **Mode-3** provides the vehicle to infrastructure (base station) communication while **Mode-4** allows the vehicles to communicate with each other directly [25]. Mode-4 uses the PC5 interface at 5.9 GHz while Mode-3 uses the traditional LTE interface. In addition, Mode-3 depends on centralized scheduling, however Mode-4 is completely distributed. The purpose of direct communication between the vehicles (*e.g.,* Mode-4) is to reduce the latency requirements, necessary in most of the time-critical ITS applications. The vehicles may switch between the desired modes dynamically. LTE has severe security vulnerabilities and other countermeasures that are discussed in detail in Chapter 5. 5G-New Radio (5G-NR) aims to provide higher data rates, lower latency, and multiple access communications among devices. The

Table 2.2: Vehicular radio access technologies, adapted from [5]

Feature	DSRC	WiFi	LTE-V2X	5G-NR-V2X	VLC
Standard	IEEE 802.11p	IEEE 802.11p	3GPP Rel 13/14	3GPP Rel 15/16	IEEE 802.15.7
Frequency band	5.86 - 5.92 GHz	2.4 GHz , 5.2 GHz	450 MHz - 4.99 GHz	700 MHz , 3.6 and 26 GHz	380 - 800 THz
Bandwidth	10 MHz	20MHz	10 MHz, 20 MHz	400 MHz	400 THz
Bit rate	3 - 27 Mbps	6 - 54 Mbps	≤ 1 Gbps	≤ 20 Gbps	11.67 kbps - 96 Mbps
Coverage range	≤ 1 km	≤ 500 meters	≤ 30 km	Ubiquitous	≤ 100 meters
Mobility management	≤ 60 kmph	Low	≤ 350 kmph	≤ 500 Kmph	Low
QoS support	EDCA [a]	EDCA	QCI and bearer selection	NA	NA
V2X support	V2V Ad hoc, V2I	V2V Ad hoc, V2I	V2X via D2D, V2I	V2V, V2I	V2V, V2I
Deployment	RSU	Hotspot, access point	evolved NodeB (mode 3), ue (mode 4)	NSA and SA mode	Illumination infrastructure
Market penetration	Low	High	High	Potentially high	Low
Multicast support	Broadcast	Broadcast	eMBMS	Unicast, Broadcast, multicast	Unicast, Broadcast
Latency	100 msec	50 msec	10-30 msec	≤ 1 msec	≃ 1 msec

[a] Enhance Distributed Channel Access

enhanced interoperability service in 5G-NR facilitates access to C-V2X technology too. The RATs performance in terms of security, infrastructure distribution, quality of service, and edge services have been significantly enhanced in 5G [26].

WiFi: The smart city developments drive WiFi deployments in mobile devices excessively. WiFi uses unlicensed Industry, Science, and Medical (ISM) bands which carry more traffic than the cellular networks in the licensed bands. WiFi is one of the complementary and low-cost RATs to provide ITS services. The protocol stack of WiFi (IEEE 802.11a/b/g/n/ac) is not optimized for vehicular mobility context, however, various amendments to the IEEE 802.11 standard are bringing advancements in WiFi, such as assisted roaming support by IEEE 802.11k, Fast Basic Service Set Transition (FT-BSS) for fast roaming via IEEE 802.11r, better network performance with IEEE 802.11v, protection of management frames by IEEE 802.11w, and better bandwidth, security, and services-on-demand by Hotspot 2.0 based on IEEE 802.11u. These advancements make WiFi a potential and competitive candidate to provide seamless and secure vehicular connectivity [5].

Vehicular VLC: Based on strict competition on traditional radio resources, the new technologies are more appealing to use alternative bands for vehicular communications. Today, visible light communication is of high interest to engineers and scientists. Unlike RF-based solutions (*e.g.*, C-V2X, and DSRC), VLC has a less complicated structure, an unlicensed band, and represents a secured, power efficient, and reliable complementary solution for vehicular RATs. VLC spectrum resides between 380 and 800THz (380-780nm) and uses a directional LED-based transmitter for full-duplex communications [27]. Table 2.2 summarized the main features of the above-mentioned RATs.

2.2.1 V2LC Challenges

The exploitation of VLC as a transmission medium opened new horizons in communication systems and potentially promised to solve many issues associated with the wide range of applications, such as last-mile connectivity, positioning, and underwater communications. Since the time it came into being, VLC physical metrics such as data rate, and communication range grabbed the majority of the academic attention, while the Medium Access Control (MAC) issues, including network formation and handover, have been partially ignored mainly because the

target application sector was for indoor environment[12].
Outdoor applications including Vehicular Communications (VC), have a great capacity to host VLC technology based on the already-existed infrastructures such as vehicles and road side units equipped with Light Emitting Diodes (LED) and cameras. However, V2LC has a number of challenges to be addressed:
Hardware limitation: Hardware limitation of V2LC transmitters and receivers (*e.g.,* nonlinearity of the electronic components) highly impact the achievable performance. Nonlinear transfer function, the limited bandwidth of the LEDs, and the limited dynamic range are some of the transmitter challenges in V2LC. On the receiver side, the "square law" property of the direct detection receiver and the noise induced by the hardware affect the communication[28].
Line of Sight, Propagation characteristics of the light and its directionality usually require an LoS link between the transmitter and the receiver in V2LC. Maintaining a stable LoS link under the dynamic mobility conditions of vehicular traffic is challenging in V2LC. In addition, in the outdoor environment, the light beams are not spatially bounded; when they are propagating, the reflected components cannot maintain sufficient energy for detection and reliable communication. Although an LoS link is preferred, initial research has shown that Non-LoS communication via ground reflections can be beneficial for V2LC. Nevertheless, this depends on the weather conditions and the ground surface material, as they impact the reflectivity of the ground. Regarding Non-LoS reflections, V2LC does not suffer from multi-path fading, because of the inherent spatial diversity resulting from the significantly shorter carrier wavelength of visible light waves compared to the detection area of typical receivers [29].

A square law device produces an output proportional to the square of some input. For example, in demodulating radio signals, a semiconductor diode can be used as a square law detector, providing an output current proportional to the square of the amplitude of the input voltage over some range of input amplitudes.

Outdoor Environment: Outdoor is a challenging environment for VLC. Atmospheric phenomena like fog, rain, snow, and other particles in the atmosphere, degrade the transmitted signal by absorbing and scattering the light waves. Similarly, dirt or dust around the lighting modules (or PDs) can hinder the signal. This will heavily influence the range and reliability of V2LC. The icing on the ground can cause stronger reflections too. Natural and artificial light sources impose a challenge for the system as well. Sunlight causes shot noise at the receiver, while outdoor LED-based light sources (*e.g.,* roadside illumination, advertisement boards) can cause interference [30].
Propagation Characteristics: VLC signals cannot penetrate through objects which are opaque to the human eye such as wood, metal, and plastic. As these materials are prevalent in our lives, the interaction of visible light wavelengths with those materials largely impacts the design decisions for VLC-based applications, including V2LC [28].
Directionality of Lighting Function: The directionality of V2LC signals has governed by the design of the transmitter lighting modules and the Field of View (FoV) of the receiving PD. As a primary purpose, lighting modules for indoor or outdoor illumination are designed to provide optimal illumination in a certain area. In the case of automobile lights, the directionality of the light beams impacts many other properties of V2LC. For instance, it results in a small collision domain and allows high spatial reuse of the modulation bandwidth for devices in close proximity, and at the same time reduces the covered area[28].
Mobility: In the linear channel, the geometry between the sender and

the receiver (*i.e.*, relative distance and orientation) and the corresponding hardware characteristics (*e.g.*, receiver's FoV and active collection area, transmitter's radiation pattern, etc) have the largest impact on the large-scale channel conditions [31]. The geometric parameters are mainly influenced by the vehicle's mobility, which, in turn, impacts the temporal characteristics of the channel. The optical channel, characterized by the Channel Impulse Response (CIR), does not change significantly if the transmitter-receiver pair move in the order of a wavelength. In the vehicular environment, however, typical displacements are orders of magnitude larger than the VLC wavelengths, making the V2LC channel highly dynamic [32].
Power Distribution: the most interesting property of V2LC is the imbalance of different lighting modules. For instance, as the headlamps and taillamps of a vehicle serve different purposes (*e.g.*, illumination or signaling), there are significant differences in their design. Therefore, the light emitted by the headlamps is much stronger than the one emitted by the taillamps. This is resulting in an asymmetric link between two vehicles communicating with these lighting modules. Moreover, the light distribution of the headlight is not uniform. The idea is to illuminate more areas towards the curbside in order not to glare oncoming vehicles. These properties should be carefully taken into consideration when designing Medium Access Control (MAC) protocols for V2LC [33].

In a nutshell, inter-vehicle communication at high relative speeds via V2LC may face the following key challenges: • resources management in high-density scenarios (random allocation of resources may result in excessive collisions), • • ensuring reliability for covered and uncovered communication. These issues need to be addressed in order to maintain the connectivity at a modest bitrate under the Line of Sight (LoS) constraints of VLC and rapid flexibility of VC, which in this study have been committed from the MAC layer perspective.

2.2.2 Previous Contributions

The early efforts on the VLC MAC layer back to 2003 in Japan where VLC Consortium sets basic protocols for VLC positioning and later on has been revised by IEEE 802.15.7 VLC Task Group to include Channel Sensing Multiple Access (CSMA) MAC protocol [3]. It is the same standard used by LiFi technology which supports indoor wireless networking systems including bi-directional multiuser communication [34]. Bi-directional VLC link was also adopted in [35], in order to implement the adaptive modulation control but in unfair uplink-downlink bandwidth. Essential differences between indoor and outdoor applications triggered prospective developments of the distinct models in VLC ad-hoc networks where infrastructure-less mobile nodes qualified to tackle network failures. However, the techniques used in this area were blindly drawn from RF networks such as aloha protocols [4][36]. In aloha, each node or station transmits a frame without trying to detect whether the transmission channel is idle or busy. If the channel is idle, then the frames will be successfully transmitted. If two frames attempt to occupy the channel simultaneously, collision of frames will occur and the frames will be discarded. These stations may choose to re-transmit the corrupted frames

repeatedly until successful transmission occurs. In pure aloha, the time of transmission is continuous. Whenever a station has an available frame, it sends the frame. If there is collision and the frame is destroyed, the sender waits for a random amount of time before re-transmitting it. Slotted aloha reduces the number of collisions and doubles the capacity of pure aloha. The shared channel is divided into a number of discrete time intervals called slots. A station can transmit only at the beginning of each slot. However,there can still be collisions if more than one station tries to transmit at the beginning of the same time slot.
J. Jagannath in [37] presents an opportunistic medium access control protocol to counteract exclusive challenges of VLC ad-hoc networks such as hidden node, deafness and blockage. A three-way handshake mechanism has been proposed to negotiate medium access starting by choosing the optimal transmission sector which is the direction that maximizes the utility function. Utility function defined as a probability of establishing a duplex communication link when some of neighbor nodes are affected by blockage or deafness. Since full-duplex communication is inherent to VLC, the utility function boosts the establishment of full-duplex communication links. Hidden node problem has been met by full-duplex transmission or busy tone and power control implementation. All these factors contribute to maximizing the throughput of visible-Light ad-hoc network (LANET). *J. Jagannath et al.* have further elaborated VL-MAC to include a cross-layer optimized routing protocol (VL-ROUTE) that interacts closely with medium access control layer in order to maximize the throughput of the network by taking into account the reliability of the route. Route Reliability Score (RRS) computed by each node in the network using just the information gathered from its immediate neighbors, estimates the probability of reaching a given sink via that node. The RRS value then integrated to the utility based three-way handshake process proposed in [37] to mitigate the deafness, blockage and increase the chance of establishing a full-duplex links[38]. Opportunistic MAC protocol designed for VLC and based on three-way handshake [39] are not able to follow the high dynamicity of a vehicular context. The performance of V2LC has been enhanced in atmospheric turbulence conditions by Aperture Averaging (AA) technique. AA uses a lens in front of PD to increase the collection area of the receiver so that the Signal to Noise Ratio (SNR) increases [40]. SNR is a well-known maximum received power indicator, with Gaussian noise distribution, even though overhearing the disturbances from other VLC transmitters offer less accurate performance evaluation. In [41], the maximum received power has been used to make a soft horizontal handover among Coordinated Multi-Point (CoMP), by adjusting the handover power margin and time-to-trigger parameters. The Received Signal Intensity (RSI) extension in [42] was inspired by the RF Received Signal Strength (RSS) concept, and exploited in the RSI-based handover technique for mobile VLC systems. Signal-to-interference and noise ratio (SINR) is used in [43] to manage vertical handover between Li-Fi and Wi-Fi and to reduce the handover rate through the concept of handover skipping. The SINR evaluates the communication link more precisely, especially when the noise and interference power levels are comparable. Consequently, the interference is modeled as a Gaussian random process too, with finite independent signal aggregation, where no individual signal dominates over the rest, [44].
At the same time, scenarios, where the disturbances are dominated by

one or multiple sources, are commonly present in VLC systems. When the power of individual interferer or accumulative interference is at least one order of magnitude larger than the noise, the system is interference dominant. In this case, INR ought to properly describe the interference distribution [45], which was inspected as a Quality of Service (QoS) constraints for handover management in hybrid RF/VLC indoor systems [46]. Post-Crash Notification as an example of safety messages has been disseminated through IEEE 802.11p assisted by VLC within the area of accident to prevent possible accumulation in platoon [6].

As the main challenge for the LoS requirement is mobility, the mobile receiver in VLC has to maintain a high-speed connection in an uninterrupted manner within the coverage area of a single access point (AP), as well as when it is moving across multiple transmitters [34]. The principal solution for switching the communication session from one AP to another is the handover mechanism. The handover procedures are generally pushed by the degradation of the quality of the current link, followed by the selection of a higher quality host link (if there is any), and finally executing the handover through exchanging control packets among the nodes that share the link [47]. The link quality evaluation is determined by the error probability ratio, which follows the distribution of the link disturbances such as noise and interference [45]. In the context of V2I communication, the street lights have served as access points and handover among them has been performed based on the coordinated multipoint algorithm, regardless of the vehicle velocity [48]. Handover techniques for V2X communication gained the major attention of this dissertation.

2.3 Conclusion

As the VLC is gaining more and more attention in academia and industry because of its capacity to complement RF technologies, new challenges raised when it is applied to outdoor applications. VC is one of the most interesting markets for VLC. V2LC guarantees fast data offloading in a reasonable cost. Meanwhile, mobility management and signal disturbances are the main issues against building a robust Vehicular Visible Light Communication. The most recent contributions to these challenges have been reviewed in this section, based on the historical developments of VLC. It is summed up with the most appropriate solution for node mobility in VLC outdoor environment.

Link Adaptive Protocol | 3

This chapter is dedicated to the fundamentals of the VLC channel model and the simulation module. A new ns-3 V2LC module is presented to simulate a real outdoor VLC channel. The channel model accounts for Lambertian path loss and climate distortion. It also proposes the Link Adaptive Protocol (LAP) where a single handshake association and fast handover algorithm prolongs the VLC connectivity. Under such a pragmatic channel model, the LAP aims to prolong the VLC connectivity as well as boost the transmission rate collaborative to the quality of the received signal represented in Signal to Noise Ratio (SNR). SNR represents a safe metric to allocate different modulation schemes once it surpasses the threshold. Detecting large enough SNR triggers the association in a single handshake mechanism to proceed in adaptive modulation transmission. LAP performance has been verified in terms of outage probability and goodput in addition to further analysis of protocol efficiency. Moreover, adaptive modulation has been suggested in order to increase the throughput. Simulation results show that LAP outperforms slotted-aloha in outage probability and goodput. It is also properly achieving a trade-off between pilot rate and protocol efficiency.

3.1 Channel Model

As Visible Light Communications (VLC) is growing up, it is not restricted anymore to the traditional indoor applications such as LiFi and positioning, but it finds new customers at outdoor vendors like underwater and vehicular applications. Similar to any other communication system, the propagating channel limits the performance of the VLC system. The extensive studies that have been discussed in the last chapter, address the main challenges in indoor applications such as data rate. Those research restricted the channel impairments to the path loss. Path loss is reversely related to the distance between the transmitter and the receiver according to the Lambertian channel gain (*i.e.*, H_{Lam}). On the other hand, the performance of the outdoor VLC channel model has two signal attenuation factors: Sunlight shot noise via Lambertian radiation pattern and climate fluctuation model with atmosphere distortion index. The key elements of a generic outdoor VLC system are shown in figure 3.1. A Light emitting diode (LED) represents the transmitter, which transfers the optical power in the free space, while the photodetector (PD) as a receiver, generates an electrical current proportional to the optical received power. This communication scheme employs intensity modulation and direct detection (IM/DD). Elimination of local oscillators and broad employment of LEDs, nowadays, provides cost-effective infrastructure for communication services[49]. Intensity modulation assures non-negative instant emitted optical signal *X(t)* between minimum and maximum signal power as: $u \leq X(t) \leq U$, with average transmit power (*i.e.*, P_t) equivalent to the expected value of the emitted optical power $E(X)$ [50].

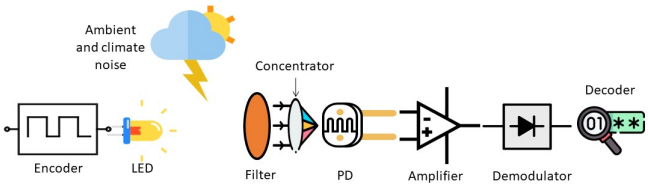

Figure 3.1: VLC front-end blocks

$$E(X) = P_t \tag{3.1}$$

Instant received optical signal can be modeled as 3.2:

$$Y(t) = rX(t) \otimes h(t) + N(t) \tag{3.2}$$

Here, r represents the photodetector responsivity, and $h(t)$ describes the outdoor optical channel impulse response (CIR), taking into account the Lambertian path loss h_{Lam} and statistical climate impairments h_{clm} model [51].
In 3.2, $N(t)$ stands for the Additive White Gaussian Noise (AWGN), and $\otimes$ is the convolution operator.
The average received power represented by 3.3:

$$P_r = h \cdot E(X) \tag{3.3}$$

Channel Gain

At the indoor line of sight (LoS) condition, the channel model is restricted to the Lambertian emission of order m, and formulated as 3.4:

$$h_{Lam} = \frac{(m+1)A}{2\pi d^2} \cos^m(\phi) T_s(\psi) g(\psi) \cos(\psi) \tag{3.4}$$

being m the order of Lambertian emission, it is calculated as 3.5:

$$m = -\ln(2)/\ln\left(\cos\left(\phi_{1/2}\right)\right) \tag{3.5}$$

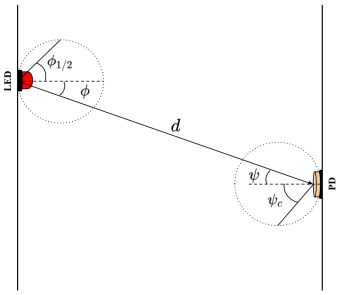

Figure 3.2: VLC front-end orientation

$\phi_{1/2}$ stands for the half-power semi-angle at the transmitter, the photodetector area is A, and d indicates the distance between the transmitter and the receiver. Based on figure 3.2, the angle of radiance and acceptance identified by ϕ and ψ respectively and $T_s(\psi)$ is optical filter gain. The concentration gain of the photodetector (*i.e.*, $g(\psi)$) ruled by 3.6 with n refractive index and ψ_c receiver field of view (FoV)[52].

$$g(\psi) = \begin{cases} \frac{n^2}{\sin^2 \psi_c} & , 0 \le \psi \le \psi_c \\ 0 & , \psi \ge \psi_c \end{cases} \tag{3.6}$$

Outdoor VLC channel on the other hands, suffers from additional climate distortion (*i.e.*, h_{clm}), statistically modeled as 3.7 with log-normal Probability Density Function (PDF) of climate distortion $f_{h_{clm}}$ and log-amplitude variance σ_L^2 determined through ray tracing analysis [43].

$$h = h_{Lam} \cdot h_{clm} \tag{3.7}$$

$$f_{h_{clm}}(h_{clm}) = \frac{\exp\left(\frac{(\ln(h_{clm})+2\sigma_L^2)^2}{8\sigma_L^2}\right)}{2h_{clm}\sqrt{2\pi\sigma_L^2}} \tag{3.8}$$

Noise model
The dominant part of the noise in outdoor applications is due to the daylight shot noise rather than other ambient interference sources like incandescent or fluorescent lamps.

Table 3.1: Outdoor illuminance range

Illuminance [Lux]	Example
0.002	Moonless night sky
$0.27 - 1$	Full moon on a clear night
3.4	Twilight
100	Dark overcast day
$300 - 500$	Sunrise/sunset on a clear day
$1,000$	Bright overcast day
$10,000 - 25,000$	Full daylight (not direct sun)
$32,000 - 130,000$	Direct sunlight

Encountering thermal noise as the other major noise source, the total noise variance (*i.e.*, σ_n^2) will be like 3.9:

$$\sigma_n^2 = \sigma_{shot}^2 + \sigma_{thermal}^2 \tag{3.9}$$

Shot noise variance and thermal noise variance derived from 3.10 and 3.11.

$$\sigma_{shot}^2 = 2qrB(P_r + I_2 P_{bg}) \tag{3.10}$$

$$\sigma_{thermal}^2 = 8\pi k T_k \eta A B^2 \left(\frac{I_2 g_m + 2\pi\Gamma\eta A I_3 B G}{g_m G}\right) \tag{3.11}$$

Background noise power (*i.e.*, P_{bg}) is estimated as 3.12:

$$P_{bg} = 0.0079 E_{det} T_0 A n^2 \tag{3.12}$$

Table 3.1 is associated with illuminance range (*i.e.*, E_{det}) of the ambient light [53], and table 3.2 contains the parameters used in the current model with their values.

3.2 Link Adaptive Protocol

The link adaptive protocol makes a quick connection when a VLC link is available, adjusts the data rate based on the quality of the link, and

Table 3.2: Main parameters

Parameter	Term	Value[unit]
Boltzmann constant	k	$1.3086e-23[J/K]$
Noise bandwidth factors	I_2 , I_3	0.562 , 0.868
Background power	P_{bg}	$0.533[mW]$
Open-loop voltage gain	G	10
FET transconductance	g_m	$30[mS]$
Fixed capacitance of PD	η	$112[pF/cm^2]$
Responsivity	r	$0.2[A/W]$
Electric charge	q	$1.60217e-19[C]$
Equivalent noise b.w	B	$3[MHz]$
Absolute temperature	T_k	$298[K]$
FET channel noise factor	Γ	1.5
Filter Transmission coef.	T_0	1
Refractive index	n	1.5
Number of LEDs		1
Input voltage		$4.5[V]$
Data packet size		$536[Bytes]$
Pilot size		$10[Bytes]$

moves to other links when the quality of the current link degrades. As shown in flowchart 3.3, the model includes 3 steps, naming: Scanning, Association, and Transmission.

Initially, the transmitter investigates the VLC environment by sending a tiny control message called pilot every T_p seconds. The receiver at the same time, estimates the SNR, by the received signal power during T_p based on 3.13.

$$SNR = \frac{(rP_t h)^2}{\sigma_n^2} \tag{3.13}$$

After each pilot window (*i.e.*, T_p), the maximum value of the SNR is derived, and once the maximum signal to noise ratio surpasses the threshold (*i.e.*, $Max\ SNR\ \geq \alpha$), the source of that signal will be nominated for the association, otherwise, the scanning phase relaunches. α initially set as the minimum SNR required to achieve a given quality of service(QoS) in terms of reliability (*i.e.*, BER).
In the association phase, the source sends an association request to the destination and waits for the association response on the same link. If the association has been accepted before the timeout, it passes to the transmission phase. If not, the scanning phase starts again. Finally, the transmission initiates and is maintained among different modulation schemes based on modulation table 3.3, unless the link quality factor E_b/N_0 drops below the threshold. Since then, the scanning step restarts.

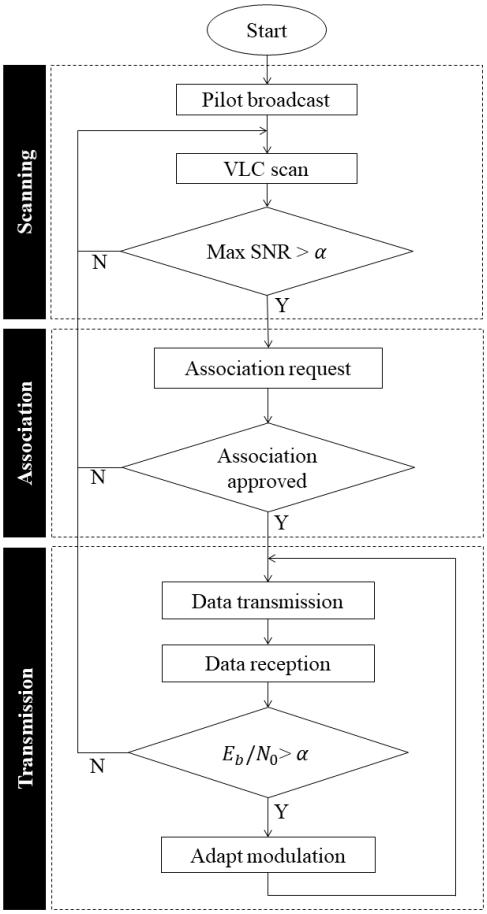

Figure 3.3: Link adaptive protocol flowchart

3.3 Simulation

As the majority of VLC research focused on the optimization of the physical medium, the cumbersome issue was to find a robust tool to evaluate the system performance in realistic situations. Current network simulators such as OMNeT++, ns2, and ns3 has limited evaluation support for VLC networks. This has motivated our work, to develop a VLC module within ns3 which offers an open-source network-level VLC simulator.
NS-3 is a discrete-event network simulator for Internet systems, targeted primarily for research and educational use. NS-3 is free, open-source software, licensed under the GNU GPLv2 license, and maintained by a worldwide community [54]. We extended the "ns3-V2LC" module from the VLC module proposed in [56]. The extension includes the patch to the most recent version of ns-3.33, as well as the integration to the SUMO mobility model. Simulation of Urban MObility (SUMO) is a free and open-source traffic simulation suite. It is available since 2001 and allows the modeling of inter-modal traffic systems - including road vehicles, public transport, and pedestrians. SUMO is a wealth of supporting tools that automate core tasks for the creation, execution and evaluation of traffic simulations, such as network import, route calculations, visualization and emission calculation. SUMO can be enhanced with custom models and provides various APIs to remotely control the simulation [33].

The motivations behind choosing ns3 to implement our system model are as follows:
- the number of ns3 users is increasing [55]
- It is open source and free
- It supports different libraries
- It can be integrated to the external software

The proposed module includes the VLC channel model with two types of channel impairments (*i.e.*, h_{Lam} and h_{clm}) as it is discussed earlier. The figure 3.4 represents the ns3-V2LC module structure.
NS3-V2LC includes 4 objects: • V2LC helpers, • V2LC channel, • performance model, and • mobility model.

V2LC Helper
the V2LC helper automatically implement the *vlc- helper*, *channel-helper*, and the *Net-Device helper* on the system. *vlc-helper* includes *vlc-NetDeviceTx* and *vlc-NetDeviceRx* that contains the main parameters of the VLC front-end such as transmitter optical power, angle of radiance, Lambertian order, concentration gain, FoV angle, etc. *channel-helper*, is derived from ns-3 point-to-point helper and connects the VLC channel to the Net-Device. On the other hand, *Net-Device helper* handles the connections between the node and the channel. It supports the link address and buffer-congestion control too.
V2LC channel
V2LC channel represents the optical characteristics of the outdoor vehicular VLC channel. The ns-3 point-to-point channel has been enhanced in [56] to include the Lambertian propagation model. The current channel includes the statistical model of climate turbulence based on the pdf of h_{clm} [51]. Moreover, it accounts for the delay, propagation loss, and sumo trace source.
Performance model
The link performance of different modulation schemes such as VPPM, PAM, OOK, and PSK is evaluated in terms of signal to noise ratio and the quality of service metric (*i.e.*, BER, and SER).

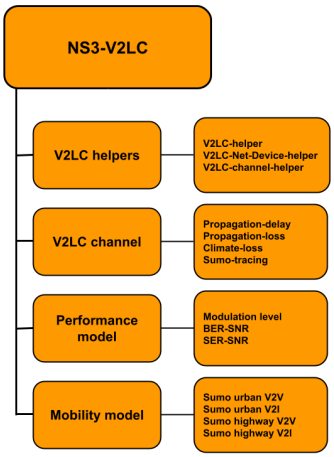

Figure 3.4: ns3-V2LC module structure

Mobility model
The *mobility model* parses the coordinates of the mobile nodes from SUMO in addition to the velocity vector and other mobility parameters in real-time. it includes urban and highway scenarios.

3.4 Performance Analysis

A generic scenario, shown in Figure 3.5, has been arranged in a way to include association, adaptive modulation and handover algorithms using NS3-V2LC module [50]. Mobile node1 rides for 20 meters, passing by node2 and node3, each of which is equipped with the VLC front-end of Figure 3.1. Simulation parameters are provided in Table 3.2.

Fixing the maximum error probability for safety applications equal to 10^{-5} we derive $\alpha = 11.5[dB]$ from Figure 3.6 and accordingly construct the modulation table 3.3 [57]. As a result, node1 associates with node2 as soon as SNR_{max} exceeds $11.5dB$ and goes to the transmission phase. Node1 starts transmission with the minimum modulation level (OOK) and as it is approaching node2, the modulation level upgrades based on modulation table 3.3. When node1 traverses node2, the received power from node2 starts to decrease, and consequently, the modulation level degrades relatively until the SNR drops below the threshold. Here node1 goes to the scanning phase where it finds the signal quality of node3 is

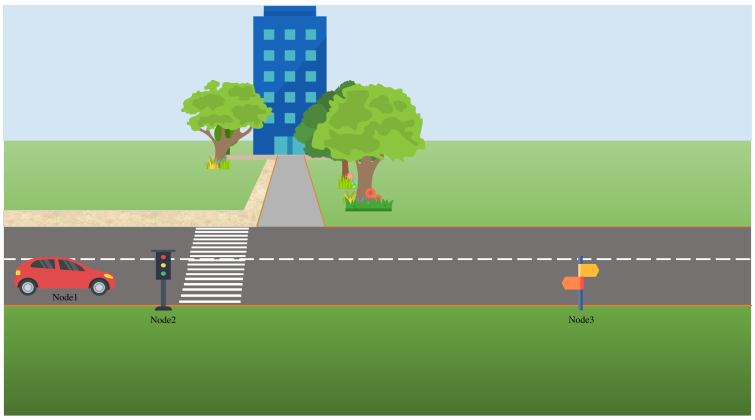

Figure 3.5: Generic V2LC scenario

Table 3.3: Modulation table

E_b/N_0 range	Modulation scheme	Relative bitrate
$11.5 - 15.0[dB]$	OOK	$150[Kbit/s]$
$15.0 - 19.0[dB]$	VPPM	$300[Kbit/s]$
$19.0 - 23.0[dB]$	16QAM	$500[Kbit/s]$
$23.0[dB] \leq$	16PSK	$700[Kbit/s]$

rising up to α. Instantly, node1 associates with node3 and repeats the previous process.

In order to evaluate the performance of the LAP, an analytical comparison with slotted aloha has been performed based on outage probability and the data rate. Additionally, the protocol efficiency has been examined as a function of pilot frequency f_P. Pilot frequency is the rate of broadcasting an exploring pilot message.
Outage probability is the Gaussian Q-function of SNR when it drops below the threshold [51] and can be modeled as follows (3.14):

$$P_{out} = Prob(SNR \leq \alpha) = \int_0^{h_{\min}} f(h)dh \tag{3.14}$$

Where $f(h)$ is the joint probability density function of the climate and path loss distortion, it is formed thereby (3.15) :

$$f(h) = \frac{1}{h_{Lam}} f_{h_{clm}} \left(\frac{h}{h_{Lam}} \right) \tag{3.15}$$

According to 3.4, minimum channel gain $h_{\min}$ is the channel gain at maximum transmission range $d_{\max}$ where α fulfills.

$$h_{\min} = \frac{(m+1)A}{2\pi d_{\max}^2} \cos^m(\phi) T_s(\psi) g(\psi) \cos(\psi) \tag{3.16}$$

Properly using (3.7) to (3.8), P_{out} is simplified as 3.17:

$$P_{out} = Q\left[-\frac{\ln\left(\frac{h_{\min}}{h_{Lam}}\right) + 2\sigma_L^2}{2\sigma_L} \right] = Q\left[-\frac{\ln\left(\frac{d^2}{d_{\max}^2}\right) + \sigma_L^2}{\sigma_L} \right] \tag{3.17}$$

Figure 3.7 represents the outage probability in respect of the relative distance between the front-end transmitter and the receiver. For the sake of comparison, the slotted aloha channel accessing model has been

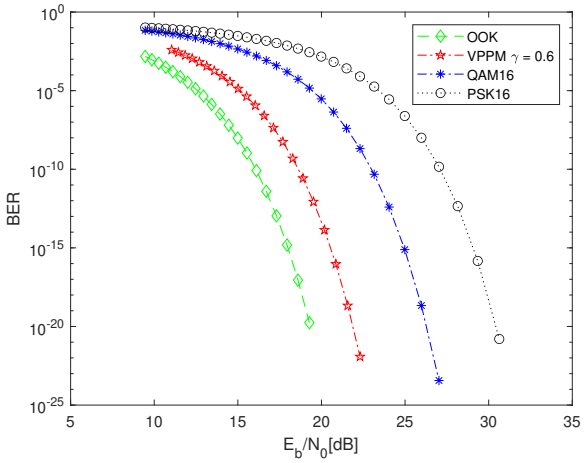

Figure 3.6: Bit error probability for different modulations

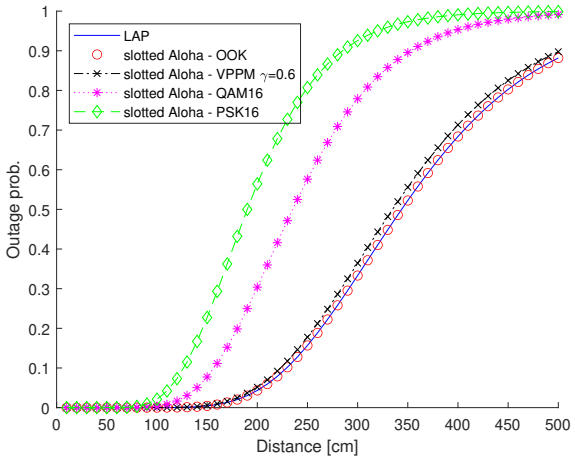

Figure 3.7: LAP outage probability comparing to slotted-aloha

implemented with different modulation schemes namely: on-off keying (OOK), Variable PPM (VPPM) with 0.6 duty cycle, Quadrature Amplitude Modulation (QAM) and phase shift keying with 16 modulation levels. Based on the figure 3.7 the link adaptive protocol (LAP) is outperforming the slotted aloha outage probability with VPPM, 16QAM, and 16PSK modulation schemes while it coincides with the performance of slotted-aloha with OOK modulation scheme. In the other words, the LAP adapts the transmission scheme to the best of channel quality such that when the distance between the transmitter and the receiver is high (*i.e.*, above 2.5 m), it uses the most robust modulation scheme (*i.e.*, OOK) for transmission in order to increase the coverage range in the charge of the data rate.
To assess the adaptive modulation algorithm, the goodput has been defined as the rate of delivered data to the application layer discarding all the overheads represented in 3.18, where ζ is the number of good packets received with payload p per transmission period T.

$$goodput = \frac{8 \cdot p \cdot \zeta}{T} \tag{3.18}$$

As it is visible in Figure 3.8, LAP goodput is improved proportionally to the signal quality while the goodput of slotted-aloha remains unchanged regardless of increasing the SNR albeit the more complicated modulation scheme results in higher goodput. It means, the LAP is capable to deliver

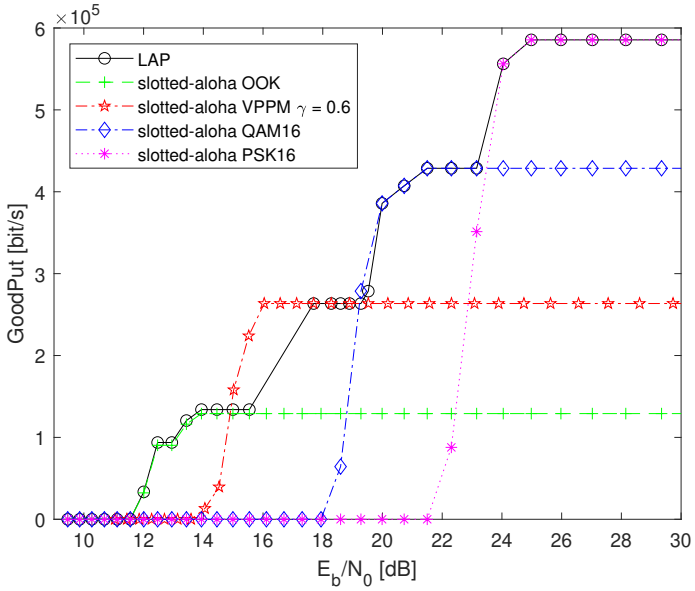

Figure 3.8: Achieved goodput of LAP and slotted-aloha

the maximum packets depending depending on the link quality (*i.e.*, E_b/N_0).

The goodput of the link adaptive protocol depends on the system's awareness of the received signal evolution. The earlier the signal alteration is detected, the faster the modulation adapts. A common technique to raise system awareness is exploring the VLC environment more often. The ideal case happened when the system is able to adapt the transmission criteria to the link condition continuously (*i.e.*, $f_P \rightarrow \infty$).

Figures 3.9 and 3.10 represent the effects of pilot frequency augmentation on the goodput when SNR increases, compared to the ideal case with different velocities. According to these figures when the pilot frequency increases, the LAP curves get closer to the ideal case meaning that it adapts faster to the link condition. Moreover, the adaptation sensitivity depends on the velocity of the mobile device too. At higher speeds, the adaptation sensitivity is higher which requires higher pilot frequency to keep the same performance as the lower speed.

The very direct benefit of rapid adaptation to the channel condition is the enhancement of the throughput, which is obvious in figure 3.11.
However, increasing the pilot rate (*i.e.*, f_P)imposes more overhead on the network according to to figure 3.12 which in consequence, reduces the protocol efficiency according to 3.19, and is shown in figure 3.13.

$$\eta_p = \frac{\text{delivered traffic}}{\text{delivered traffic + overhead}} \tag{3.19}$$

Increasing the inquiry messages (*i.e.*, pilot), enhance the Channel State Information (CSI) and as a result increase the throughput

Increasing pilot frequency imposes more overhead to the system which reduces the protocol efficiency

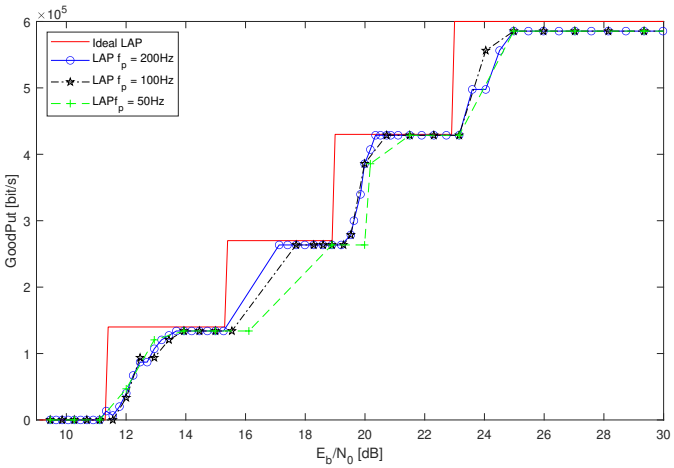

Figure 3.9: Adaptation sensitivity at 10 mps

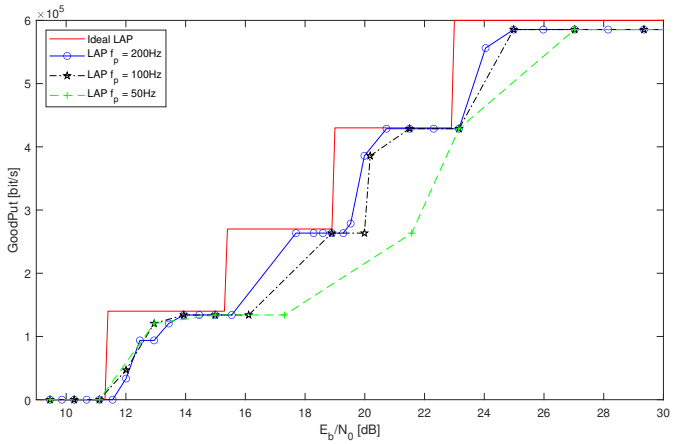

Figure 3.10: Adaptation sensitivity at 20 mps

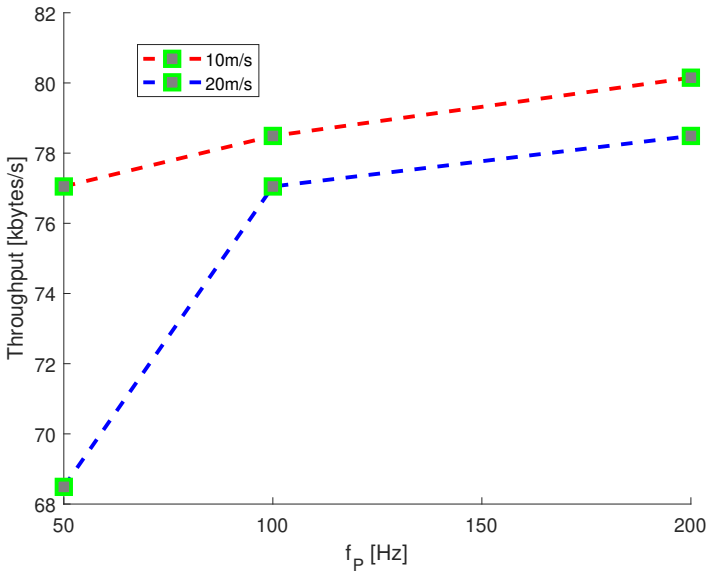

Figure 3.11: Throughput vs. pilot frequency

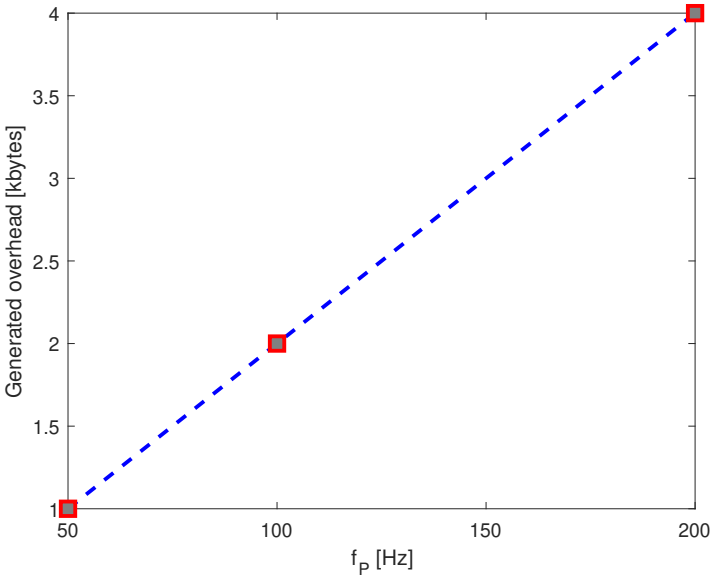

Figure 3.12: Control traffic increase with pilot frequency

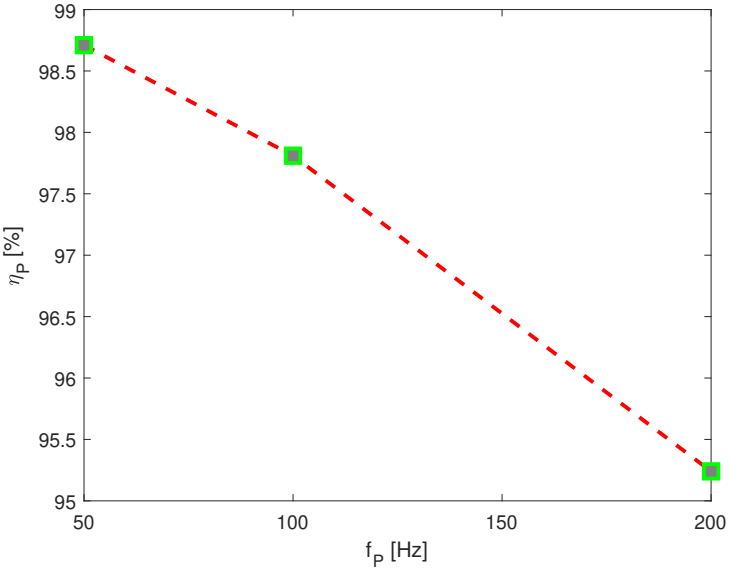

Figure 3.13: Protocol efficiency degrades as the pilot rate increases

3.5 Conclusion

This chapter addresses the challenges raised in VLC outdoor applications in terms of connectivity and throughput by means of Link Adaptive Protocol. A new ns3-based module has been proposed to implement the channel model. The frequent scanning, tactile association, and flexible transmission assure lower outage probability and high goodput in comparison to slotted-aloha. Last but not least, a trade-off between protocol efficiency and pilot frequency has been investigated. Based on our findings, higher investigation rate is beneficial for the throughput, however, it reduces the system efficiency.

Interference-Based Handover Mechanism

4

The wide use of light emitting diode (LED) in cars and roadside units is encouraging the exploitation of the Visible Light Communication (VLC) paradigm in vehicular applications. However, real scenarios are characterized by poor Signal-to-Noise Ratio (SNR) conditions and, heavy interference among devices in the same area, which make effective handover operations critical for properly supporting mobility. A novel approach called Interference based haNdover mechanism for VISIBle Light nEtworks (INVISIBLE) to perform handover in Vehicular Visible Light Networks, based on the evaluation of Interference to Noise Ratio (INR) and Interferer to Interference (IIR) Ratio, is proposed in this chapter, in place of the conventional approaches based on SNR evaluation. Our approach has been numerically validated, taking into account the Adaptive Modulation Scheme (AMS) and a VLC device moving at different speeds. Furthermore, a comparison with the SNR-based approach has been provided. Simulation results show how the INR-based handover mechanism outperforms SNR-based handover in terms of handover rate, the average delivered data per handover and handover delay ratio. Moreover, an experimental validation was carried out through a software-defined approach, considering a small-scale scenario and low-power LEDs. A perfect results alignment between simulation and measurement shows how the suggested INR-based mechanism overcomes classical SNR-based handover for all performance parameters evaluated in this study.

4.1 V2LC Handover

The growing number of mobile devices and their applications enforce a huge amount of data exchange, pushing radio frequency-based wireless technologies to their resources limit. New paradigms, such as visible light communication (VLC), are appeared to complement RF technologies in addressing the spectrum crunch. VLC exploits pre-existing infrastructures like Light Emitting Diodes (LEDs), in order to provide not only illumination but also to transfer data. Plenty of indoor and outdoor VLC applications have emerged in the last decade, including LiFi, localization, and underwater communications. Intrinsic security due to limited penetration depth and a huge bandwidth of totally free spectrum are the other key factors behind the growing interest in VLC [3] [58] [34] [59].

Vehicular Visible Light communication (V2LC) represents one of the most attractive outdoor applications of this paradigm. The aim of V-VLC is to enhance the safety and driving experience by exchanging information between a generic vehicle and its surrounding (*e.g.*, Vehicle-to-Vehicle V2V, Vehicle-to-Infrastructure V2I) using car lamps, traffic lights, control cameras and so on. However, like the other outdoor VLC techniques, advances in V-VLC are slower compared to indoor VLC, mainly due to environmental issues (e.g., sunlight noise, weather conditions, and

higher mobility) [5].
In absence of ambient disturbances, VLC link quality depends on the distance between the transmitter and the receiver and their orientation in addition to the front-end configuration (*i.e.*, field of view FOV of the receiver, area of the photodiode PD and radiation pattern). If the relative movement between the transmitter and the receiver is in the order of the signal wavelength, the quality of the optical channel represented by the channel impulse response (CIR) does not change significantly, therefore it has a minor impact on the temporal characteristics of the channel [60]. In vehicular communication, however, the transmitter-receiver motion is several orders of magnitude larger than the optical wavelength, which makes the V-VLC channel unstable[61]. Directional and line of sight (LoS) necessities of the VLC channel, further complicate the mobility management in the V-VLC context [47]. A principal solution for mobility management is handover, where the Mobile Entity (ME) has to switch its communication session to another Access Point (AP) in the same network (horizontal handover) or to another technology (vertical handover). An effective handover is important as well to meet the quality of service (QoS) requisites (e.g., reliability, delay).
The handover procedure is generally carried out in three steps: decision, target-AP/technology selection, and execution. In the handover decision, the ME decides to switch from the current AP to another candidate according to the quality of the link [62]. If there are multiple candidates, the ME has to select one of them, and finally, handover execution takes place via exchanging control packets between the ME and the candidate AP.
By reference to the previous works in the context of V-VLC, handover is generally based on the link quality which is evaluated by the signal-to-noise ratio (SNR), mainly considering in the analysis, the presence of Gaussian noise (*i.e.*, shot noise and thermal noise) [45].
In the dynamic soft handover algorithm, the coordinated multipoint (CoMP) is implemented according to the rate of change in the maximum received power to adjust handover parameters such as handover margin and the time-to-trigger [48]. However, the evaluation of the system by observing only the SNR and ignoring any disturbances from other transmitters does not provide an accurate performance evaluation [62].
Signal-to-interference and noise ratio (SINR) is also employed in handover decisions, since it provides higher precision compared to SNR, especially when noise and interference power levels are in the same order of magnitude. In this case, the interference is modeled as a Gaussian random process too, considering the accumulation of many independent signals where no individual signal dominates over the others [44].
Handover skipping could reduce the handover rate in hybrid LiFi-WiFi networks by implementing Reference Signal Received Power (RSRP) for vertical handover and SINR for horizontal handover [41].
Nevertheless, a dominant interferer is present in many real scenarios. In this case, a more accurate way to describe the interference distribution is by utilizing the interference to noise ratio (INR) [45].

In the next section, we employ the INR as the main metric for handover procedures. We consider both Gaussian interference distribution, and dominant interferer distribution, but we select which of them is applied, on the basis of interferer-to-interference ratio (IIR). Moreover, target

AP selection is made based on the QoS requirements of the vehicular application. In order to achieve further improvement in overall system performance, the adaptive modulation scheme (AMS), dynamically switching between On-Off Keying (OOK) and Phase Shift Keying (PSK) Modulation with a different order (4-8-16 PSK), has been implemented.

4.2 System model

As illustrated in figure 4.1, we consider a V2LC architecture, composed of street lights, acting as APs and randomly distributed along the direction of the road with a linear distribution density ρ_l, defined as the number of APs per kilometer. Each AP has a maximum transmission range d_{max}, which depends on the VLC front-end configuration and the optical channel, whose transfer function (h) is characterised by the Lambertian emission (h_{lam}) and the climate loss (h_{clm}) (see equation 4.1).

$$h = h_{lam} h_{clm} \tag{4.1}$$

The climate loss is statistically related to the variance of the amplitude and modeled by the ray tracing analysis [43]. Under LoS constraint, the channel model is restricted to the Lambertian model [51]:

$$h_{Lam} = \frac{(m+1)A}{2\pi d^2} \cos^m(\phi) T_s(\psi) g(\psi) \cos(\psi) \tag{4.2}$$

Where m is the order of Lambertian emission, A is the area of the photodiode PD, d is the distance between the ME and the AP. ϕ and ψ are the angles of radiance and acceptance respectively, and the optical filter gain is represented by T_s. g is photodetector concentrator gain. The main loss in the outdoor applications of VLC is due to daylight shot noise and thermal noise which are assumed to be Gaussian distributed with respective variances σ^2_{shot} and $\sigma^2_{thermal}$. Given independent noise sources, the central limit theorem is applied to find the variance of the aggregate noise current (*i.e.*, σ^2_n) as 4.3

$$\sigma^2_n = \sigma^2_{shot} + \sigma^2_{thermal} \tag{4.3}$$

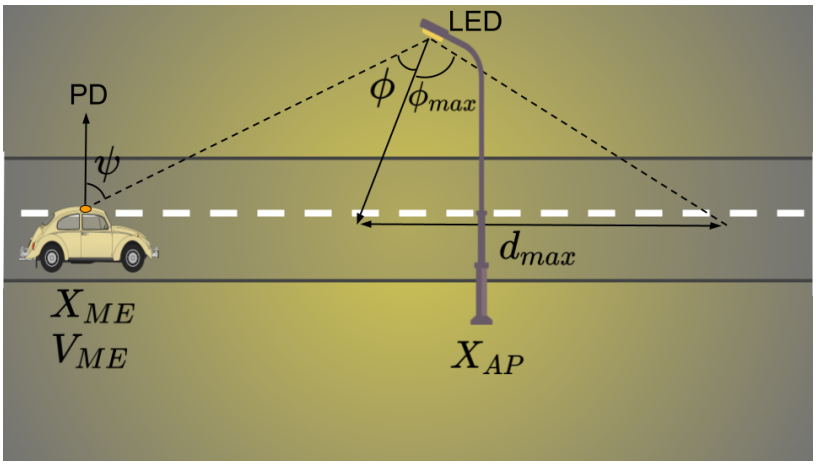

Figure 4.1: Handover Scenario

The SNR provides an accurate optical link evaluation when the system is Gaussian noise dominant.

$$SNR = \frac{(r \cdot P_r)^2}{\sigma_n^2}, \tag{4.4}$$

In (4.4), r represents the PD responsivity and P_r stands for the average received optical power. In an interference-dominant network, where the sensor is affected by the neighboring transmitters, an accurate performance analysis requires the evaluation of the interference and the noise jointly.
System interference is frequently modeled as a Gaussian random process since it is assumed no individual signal dominates [44]. In such scenarios the variance of the aggregate interference current (*i.e.* σ_I^2 $[A^2]$) is used to define signal-to-interference ratio (SIR) evaluation of the link between the transmitter and the receiver *i.e.* 4.5,

$$SIR = \frac{(r \cdot P_{r)^2}}{\sigma_I^2}, \tag{4.5}$$

Performance evaluation of the Tx-Rx link when the disturbances from both noise and interference are in the same order of magnitude is feasible through $SINR$ (*i.e.*, 4.6)

$$SINR = \frac{(r \cdot P_r)^2}{\sigma_I^2 + \sigma_n^2}, \tag{4.6}$$

These assumptions are not precise when the dominant interferer is present. In such scenarios, the interference is properly modeled by the distribution of the dominant interferer [45]. In order to determine if a dominant interferer is present, one can define the interferer to interference ratio as 4.7

$$IIR = \max_i \left(\frac{P_{r,i}}{\Sigma_{i \neq s} P_{r,i}} \right), \tag{4.7}$$

where the useful signal s is not included within the interferers i. Lower IIR values fit well with the Gaussian distribution[45], while high values of IIR exclude this hypothesis. In fact, if IIR is greater than β, we consider that the interference distribution follows the dominant interferer. β statistically defines the minimum IIR the system can be detected. Once this aspect has been determined (interference dominated or not), one can rely on the appropriate metric in order to evaluate the quality of the link. In our system, the total interference to noise ratio INR_t is calculated as 4.8:

$$INR_t = \sum_{i \neq s} INR_i, \tag{4.8}$$

where the INR_i is the interference to noise ratio of the i^{th} interferer.
Link performance evaluation depends on the QoS required by the application. One of the essential QoS requirements is the reliability described as the BER-SNR curve. Fixing the maximum error probability for vehicular safety applications equal to $10e-3$, the minimum required signal to noise ratio (α) is shown in table 4.1 [57]. If the system was recognized as interference dominated (*i.e.* $INR_t \geq 10$), then it is possible to search for the dominant interferer using IIR. Dominant interferer could be

α	Modulation scheme	Relative bitrate	d_{max}
11.14$[dB]$	OOK	100$[Kbit/s]$	12.5$[m]$
11.3$[dB]$	4PSK	150$[Kbit/s]$	12.0$[m]$
18.4$[dB]$	8PSK	200$[Kbit/s]$	8.0$[m]$
20.6$[dB]$	16PSK	250$[Kbit/s]$	6.5$[m]$

Table 4.1: Modulation table

represented as a Handover (HO) candidate if 4.9 holds.

$$INR_i = \frac{(rP_{r,i})^2}{\sigma_n^2} \geq \alpha \tag{4.9}$$

In order to increase the lifetime of the link, the vehicle should avoid unnecessary handovers [63]. Skipping unnecessary handovers will reduce the handover rate. The handover is unnecessary if the sojourn time t_s is shorter than connection lifetime T_c which is the other important QoS requirement for lots of applications. Sojourn time is defined as the time estimated for the ME to be served by a given AP (4.10):

$$t_s = \frac{d_{max} + (X_{ME} - X_{AP})}{V_{ME}} \tag{4.10}$$

where X and V are the position and the velocity vectors respectively. Putting these conditions together, the dominant interferer will be candidate as an AP if $INR_i \geq \alpha$ and $t_s \geq T_c$. This process will be successively reapplied if there are multiple dominant interferers.

Algorithm 1 Interference-based handover

Require: $s, \alpha, \beta, T_c, t_i$
  $INR_t = \Sigma_{i \neq s} INR_i$
  while $INR_t \geq 10$ **do**
    $IIR = \max_i \left(\frac{P_{rx,i}}{\Sigma_{i \neq s} P_{rx,i}} \right)$
    if $IIR \geq \beta$ **then**
      $INR_i = \frac{(rP_{rx,i})^2}{\sigma_n^2}$
      if $INR_i \geq \alpha$ **then**
        $t_s = \frac{d_{max} + (X_{ME} - X_{AP})}{V_{ME}}$
        if $t_s \geq T_c$ **then**
          $T_c = t_s$
          $s = i$
        end if
      end if
    end if
    $INR_t = INR_t - INR_i$
  end while

  if null **then**
    backoff t_i
  end if

The adaptive modulation scheme (AMS) is employed according to algorithm 2 on top of the handover mechanism (Algorithm 1) in order to obtain a proper trade-off between the throughput and the communication robustness. Switching between different modulations is based on the modulation parameters described in table 4.1.

Algorithm 2 Adaptive Modulation Scheme

Require: s, α
  while $SNR \geq \alpha$ **do**
    adapt the modulation
    Transmit
    Receive
    $SNR = \frac{(rP_{rx})^2}{\sigma_n^2}$
  end while
  call handover

4.3 Simulation Analysis

In this section, we compare the INVISIBLE handover mechanism with the SNR-based handover as a benchmark scheme described in algorithm 3. For the sake of fairness, we applied the AMS on top of both handover mechanisms using the NS3 simulation tool [56]. The main simulation parameters are shown in table 4.2.

Algorithm 3 SNR-based handover

Require: s, α, T_c, t_i
  $SNR = \max_{i \neq s} \left(\frac{(rP_{r,i})^2}{\sigma_n^2} \right)$
  if $SNR \geq \alpha$ **then**
    $t_s = \frac{d_{max} + (X_{ME} - X_{AP})}{V_{ME}}$
    if $t_s \geq T_c$ **then**
      $T_c = t_s$
      $s = i$
    end if
  end if

  if null **then**
    backoff t_i
  end if

The HO rate of the proposed handover mechanism is illustrated in figure 4.2 with two speeds and compared to the SNR-based handover algorithm. Considering the same AP density, the higher the speed, the shorter the average sojourn time and therefore, the higher the handover rate (4.11):

$$HO_{rate} = \frac{1}{t_s} \times 60 \; [1/min] \tag{4.11}$$

At the same speed, when the AP density increases, the SNR-based handover rate increases almost linearly. As the AP density increases the distance between the ME and the AP decreases and since the d_{max} is fixed, the handover rate increases accordingly. On the other hand, the INR-based handover rate increases in sparse AP density and is almost constant in dense AP distribution. The INR-based handover algorithm, in fact, always selects the AP which provides the largest t_s. The largest sojourn time is when the distance between the ME and the AP is less than d_{max} and it is represented by the farthest AP which stands at most d_{max} meter from the ME.

Parameter	Term	Value[unit]
Responsivity	r	$0.2[A/W]$
Minimum Transmission time	T_c	$200[Milliseconds]$
Sampling Time	t_i	$100[Milliseconds]$
Minimum IIR	β	0.5
Half power semi-angle	ϕ_{max}	35°[degree]
Linear AP density	ρ_l	$20 - 200\ [Km^{-1}]$
INR-based HO frame size		$39[Bytes]$
SNR-based HO frame size		$28[Bytes]$
Number of LEDs		10
Input power		$1.0[W]$
Number of simulations		30
Duration of each simulation		$100[s]$
Rounds of each simulation		10

Table 4.2: Main parameters

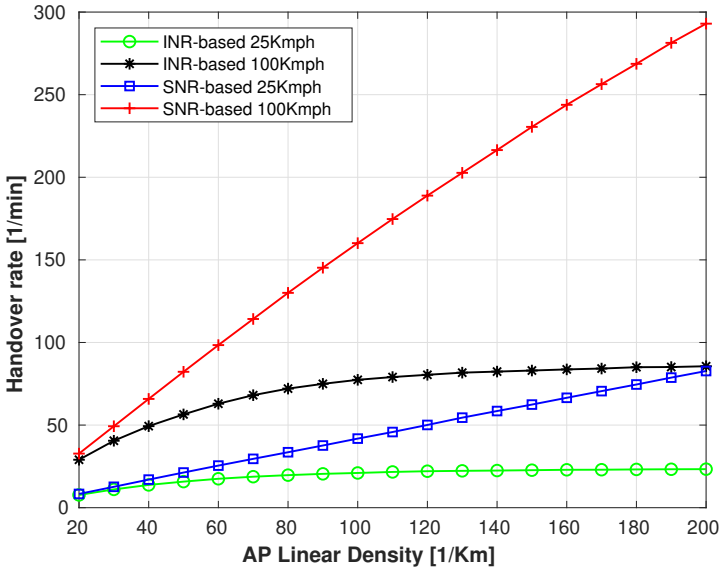

Figure 4.2: Handover rate vs AP linear density with different speeds of the mobile entity.

In figure 4.3, we assess the impact of the AP density on the average delivered data per handover, considering the slow speed of the vehicles, equal to 25 Kmph and a rapid gait equal to 100 Kmph. The average delivered data per handover is the total amount of delivered data over the total number of handovers.
Since in the proposed mechanism, the transmission takes place only under good coverage of a given AP (based on QoS requirement), as the speed increases, the sojourn time decreases, reducing the useful time to transmit and deliver data. In a given velocity, with sparse AP distribution (low AP density), the amount of delivered data per handover is higher, not because we delivered more data (because we delivered almost the same amount of data when we are connected to a given AP) but because the total number of handover is less in both schemes.
As the AP density grows, both the amount of delivered data and the number of handover increase, but the number of handovers grows faster than the amount of delivered data, therefore the overall ratio goes down.
On the other side, an interference-based handover mechanism delivers almost the same amount of data by much lower number of handovers. In the other words, signal-based handover mechanism performs many

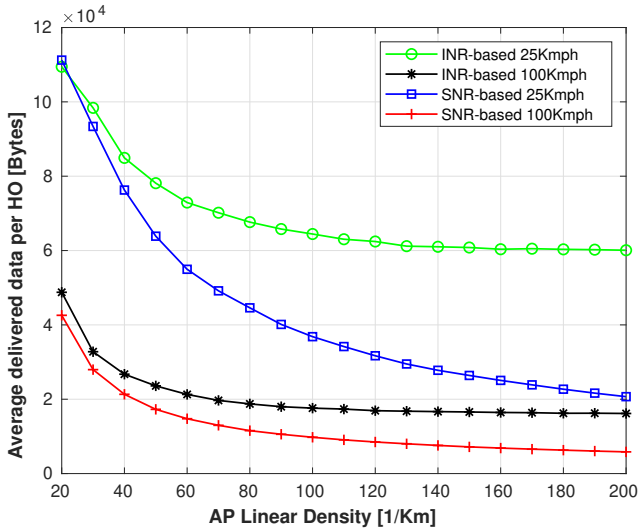

Figure 4.3: Average delivered data per handover vs AP linear density with different speeds of mobile nodes.

unnecessary handovers which degrade its performance compared to the interference-based mechanism.

Handover delay is a vital parameter to assess the time efficiency of performing a handover [47]. Regarding the handover delay, the time efficiency of a given handover mechanism is defined as the time required for performing the handover(HO_{delay}) to the whole connection time offered by that handover (t_s)[62] *i.e.*,

$$HO_{delay\ ratio} = \frac{\overline{HO_{delay}}}{\overline{t_s}} \times 100, \tag{4.12}$$

$$\overline{HO_{delay}} = \overline{t_{HO\ req}} + \overline{t_{HO\ res}}\ , \tag{4.13}$$

with $\overline{t_{HO\ req}}$ and $\overline{t_{HO\ res}}$ defined as the time necessary to • make an handover request and •• provide an handover response, respectively. Assuming the same frame size used for handover request and handover response (*i.e.*, $t_{HO\ req} = t_{HO\ res}$) included in the MAC frame format specified by IEEE standard for short-range wireless optical communication using VLC 802.15.7 [64], the reserved bits in the control frame of Figure 4.4 is used to specify the velocity of the mobile node, as well as d_{max} of each LED rather than the number of interferers N for the INR-based mechanism. The required time to perform a handover is the handover frame size (*i.e.*, $HO_{frame\ size}$ [bits]) over the bitrate at both the transmitter and the receiver (*i.e.*, $\frac{1}{R_b(M)} = \frac{1}{R_{b,tx}(M)} + \frac{1}{R_{b,rx}(M)}$). Given the modulation scheme M ($M \in \{OOK, 4PSK, 8PSK, 16PSK\}$) and $R_{b,tx}(M) = R_{b,rx}(M)$ the handover request time is simplified through eq. (4.14),

$$t_{HO\ req}(M) = \frac{2\ HO_{frame\ size}}{R_{b,tx}(M)} \tag{4.14}$$

The average handover time is calculated as follows:

$$\overline{t_{HO\ req}} = \frac{\sum_M \left(t_{HO\ req}(M) \cdot HO_{rate}(M)\right)}{HO_{rate}}, \tag{4.15}$$

where $HO_{rate}(M)$ is the handover rate on the modulation scheme M.

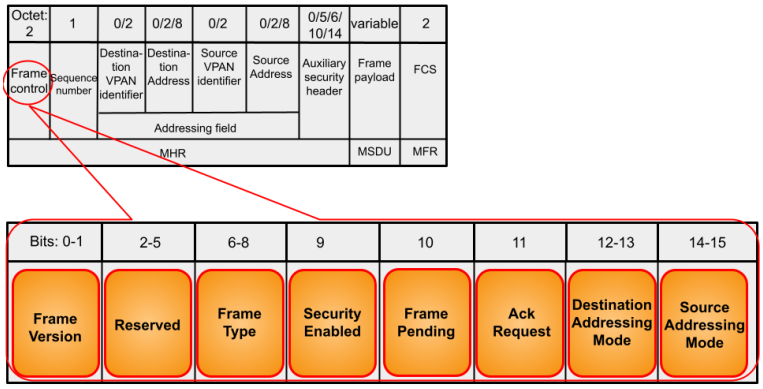

Figure 4.4: General MAC frame 802.15.7 and the modified control field.

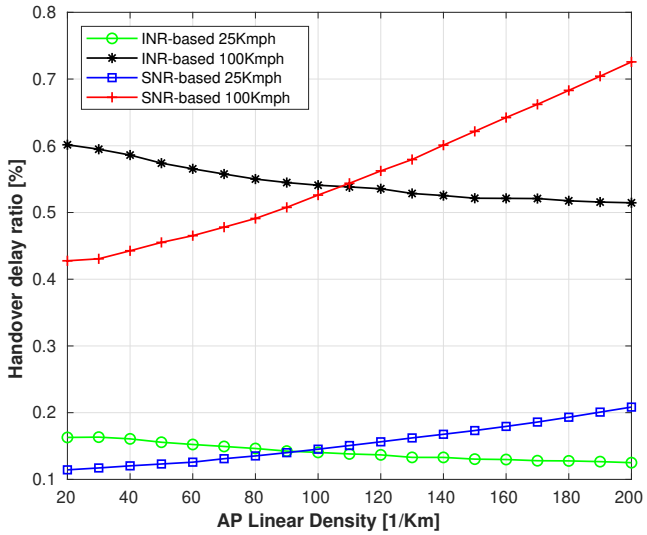

Figure 4.5: Handover delay ratio

The evolution of the handover delay ratio compared to the AP density, for 25Kmph and 100Kmph, is shown in figure 4.5. For different speeds, the average sojourn time $\overline{t_s}$ is different while the average handover delays $\overline{t_{HO}}$ is constant. The higher the speed the lower the sojourn time and as a consequence the higher the HO delay ratio. This ratio weakly increases in the interference-based handover mechanism, however in the SNR-based handover scheme this ratio shows faster progress. For low AP density, the performance of the signal-based HO is better because the HO frame size of SNR based is shorter than the interference-based handover frame size while both schemes perform the same number of handovers. When the AP density increases, the interference-based handover substantially outperforms the SNR-based handover, as it compensates for the higher overhead with a lower handover rate.

4.4 Small-scale Implementation

In this section, we implement in smaller scales the INR-based handover mechanism and compare it to the benchmark scenario (SNR-based). To verify how much the simulation results are close to the real scenarios we repeated the same procedures however downscaling the distances and

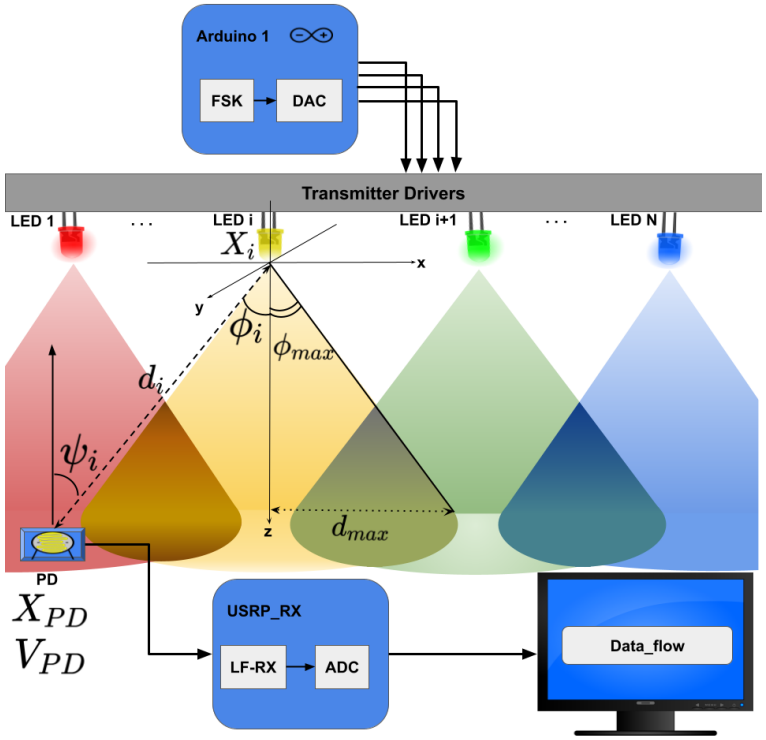

Figure 4.6: Proposed VLC network architecture.

the velocities to match our working environment. The communication system is evaluated at 0.15 mps and 0.3 mps velocities for different parameters *i.e.*, handover rate, delivered data per handover, and handover delay ratio, through an extensive simulated campaign. Experimental validation was carried out through a software-defined approach, considering a small-scale scenario and low-power Light Emitting Diodes (LEDs). A perfect results alignment between simulation and measurement shows how the suggested INR-based mechanism overcomes classical SNR-based handover for all performance parameters evaluated in this study.

The mobile node (PD) in Figure 4.6 is crossing multiple VLC coverage areas while moving along $x - axis$. The quality of the link degrades as it moves away from a fixed AP (LED i) due to the path loss and the front-end orientation. In order to maintain the connectivity link with a predefined Quality of Service (QoS) level, the receiver PD may assess the link quality frequently (*i.e.* every t_i seconds) and modify the transmission parameters, if required . The INR-based algorithm (1) evaluates the link performance based on the prominent component of the disturbances. To this end, it starts with a INR calculation to determine if the system is noise-dominant or interference-dominant. In order to consider the system interference dominant, the interference power must be 10 times bigger than the noise power. In case $INR < 10$, the noise and the interference power are comparable, and we treat them equally as noise.

At the interference dominant system, there could be single or multiple dominant interferers. The IIR is able to identify the dominant interferer if the IIR value is bigger than a threshold β, which is the minimum amount of IIR the system can detect and it is experimentally selected according to the node density(ρ_l). The interferers with $IIR \leq \beta$ are not dominant and are considered as noise. The dominant interferer i with $IIR \geq \beta$ will

be nominated for handover if it satisfies the QoS requirements of safety applications, expressed in terms of reliability and stability.
A reliable link has $SNR_i \geq \alpha$ [dB], where α is the minimum SNR level required for safety applications at maximum error probability, equal to 10^{-3} [57].
In order to increase the lifetime of a single link, the mobile node should avoid unnecessary handovers [63]. Skipping unstable VLC sessions will increase the connection time *i.e.*, t_s [s], estimated as 4.10. Setting the minimum required connection time equal to T_c [s], the dominant interferer i will be candidate as AP if $INR_i \geq \alpha$ and $t_s \geq T_c$. This process will be successively reapplied in case of multiple dominant interferers. Finally, the dominant interferer i with the maximum connection time is returned to adaptive modulation scheme, as explained in Algorithm 2.

On top of the handover mechanism, an Adaptive Modulation Scheme (AMS) protocol triggers different modulation schemes based on Table 4.3, in order to obtain a proper compromise between the data rate and the communication robustness. The relative bitrates are appropriately selected at the simulator to cope with the testbed limited components. After co-channel interference mitigation among different LEDs using frequency division multiplexing [19], the proper modulation scheme is used for transmission, while the low SNR_i amount requires a handover decision.

α [dB]	Modulation scheme (M)	Relative bitrate [kbps]	d_{max} [cm]
11.14	OOK	100	20
11.3	4PSK	150	16
18.4	8PSK	200	12
20.6	16PSK	250	8.5

Table 4.3: Modulation table

4.5 Experimental Validation

The proposed INR-based protocol for transmission and handover has been implemented in NS3 simulator [50] as well as a real small-scale scenario for proper experimental validation. In particular, we compare simulated and experimental protocol performance in terms of • handover rate, namely the number of successful handovers per minute, •• average delivered data per handover, namely the total delivered data over the total number of handover, and • • • handover delay ratio, namely the ratio between the time required for performing the handover and total connection time.

In practice, we used an array of commercial low-power LEDs as APs, in order to build a small-scale setup. Each optical transmitter is connected to a dedicated output port of an Arduino 1 in order to control and drive separately each LED. A simple receiver consisting of a low-cost PD and other passive elements is used for delivering the data to the signal process unity, mainly composed of a USRP 2920 and a Low-Frequency daughterboard. The distance between the ceiling of the APs setup and the plane of the mobile receiver is constant, while the number of LEDs and the distance between them is properly modified to allow performance evaluation for different linear node densities.

Table 4.4: Main parameters

Parameter	Value[unit]
Responsivity, r	0.2 [A/W]
Area of PD , A	1.3 [cm^2]
Minimum Transmission time, T_c	200 [ms]
Sampling Time, t_i	100 [ms]
Half power semi-angle, ϕ_{max}	35°
Linear AP density, ρ_l	[1, 10] [m^{-1}]
Minimum IIR, β	0.3
INR-based HO frame size	39 [Bytes]
SNR-based HO frame size	28 [Bytes]
Number of LEDs	5
Number of PDs	4
Input electrical power	1.0 [W]
Number of simulations	30
Duration of each simulation	100 [s]
Rounds of each simulation	10

As a benchmark, we model the SNR-based handover mechanism with the same parameters, and we compared both mechanisms in simulation and experimental tests. In the SNR-based case, the handover decision is based on the maximum received power and the connection time, while, for the sake of fairness, we applied the ADM on top of both handover mechanisms. Table 4.4 shows the main system parameters used in the simulation and experimental tests.

Assuming the testbed scenarios of Figure 4.7, different configurations of LEDs represent different nodes' linear densities while feeding the signal to the USRP at different time intervals manipulates different speeds. As the mobile node moves along the coverage area of a given AP, the SNR metric is used to measure the link QoS and allocate the modulation scheme for the next transmission bursts, whereas the interference is mitigated based on the frequency shift keying. When the error probability increases as a result of the degradation of the link quality, the INR-based handover nominates an alternative AP with the highest connection time. On the other hand, the SNR-based algorithm is suggesting the link with the highest received power that lasts at least T_c seconds, otherwise it backs off the scanning for t_s seconds.

In Figure 4.8, we compare the handover rate (*i.e.*, HO_{rate} $[min^{-1}]$) obtained with the INR-based and the SNR-based handover schemes, for different speeds. It can be shown that the handover rate has a reverse relationship with the average connection time $\overline{t_s}$ $[s]$ as follows 4.11

Regarding the excellent matching between the simulation and the testbed results, it is admitted that at the same speed as the AP density increases, the SNR-based handover rate increases linearly. According to equation (4.10) and (4.11), going from lower to higher ρ_l, the distance between node PD (Rx) and node i (Tx) is decreasing. Since d_{max} and V_{PD} are fixed, the average connection time declines accordingly, and as a result the handover rate increases. On the other side, the INR-based handover rate increases in the sparse AP deployment and saturates in the dense AP distribution. At the dense AP installation ($X_{PD} - X_i \leq d_{max}$) the longest t_s is determined by the farthest AP which stands at most d_{max} meter far from the mobile node. Higher velocity corresponds to a lower connection

Figure 4.7: Testbed configurations for performance evaluation, considering different

time and hence higher handover rate.

In Figure 4.9, we assess the impact of the node density on the average delivered data per handover at speed 0.3 mps and 0.15 mps. In both medium access schemes, the transmission is carried out when the front-end device is well covered by the AP (*i.e.*, $SNR \geq \alpha$). Giving t_s the available time for transmission, at rapid gait (*i.e.*, 0.3 mps) the connection time is shorter than the one of lower speed (*i.e.*, 0.15 mps) providing bigger portion of time for transmissions in different bitrate according to Table 4.3. As a result, the average delivered data is larger for the higher speed than the lower one. It is also obvious from Figure 4.9 that the INR-based mechanism always transmits more data per access point than the SNR-based scenario, that is not because of higher data rate obtained with our proposed scheme (*i.e.*, the transmission scheme is the same at both proposed scheme and the benchmark), but because the INR-based mechanism makes much less handovers for the same AP distribution. As the ρ_l increases the average delivered data decreases in both schemes with a slight incline for the INR-based scheme.

The evolution of the handover delay ratio compared to AP density for different velocities is depicted in Figure 4.10 based on the delay ratio model explained in section 4.3. At higher velocities, the connection time is lower resulting in a less efficient handover delay ratio. For a given velocity, at the low-density scenarios the SNR-based performs better due to the shorter handover frame size. As the node density increases, the number of SNR-based handovers grows linearly. Simultaneously, the dense AP deployment boosts the received power at the front-end device which in return applies higher modulation levels and increases the bitrate, although the handover rate progresses faster than the bitrate,

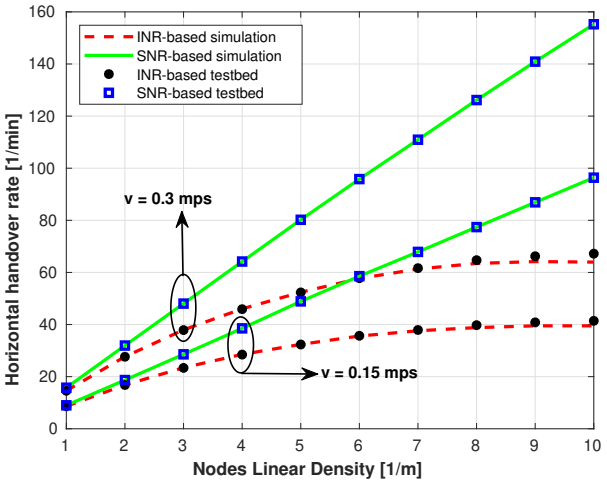

Figure 4.8: Handover rate versus node density.

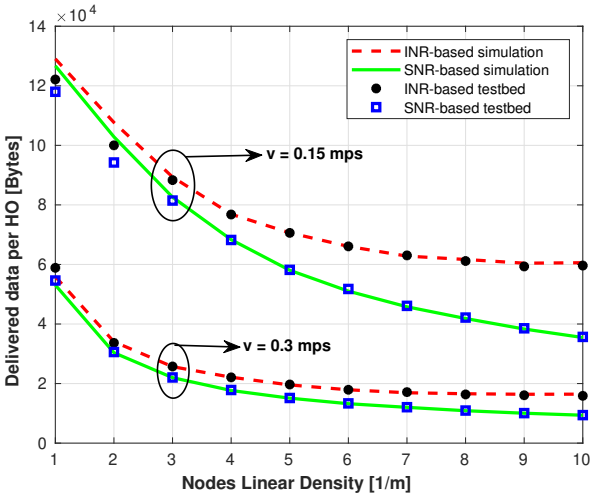

Figure 4.9: Delivered data per handover versus node density.

leading to $\frac{HO_{rate}}{R_b} \geq 1$. That is why the SNR-based handover delay ratio is monotonically increasing. On the other side, the interference-based handover mechanism substantially outperforms the SNR-based handover by recovering the higher overhead with the lower HO_{rate}. The ratio $\frac{HO_{rate}}{R_b}$ in INR-based scheme is less than unity because the HO_{rate} reaches the saturation level at the high density, while the R_b continues increasing leading to decreasing delay ratio.

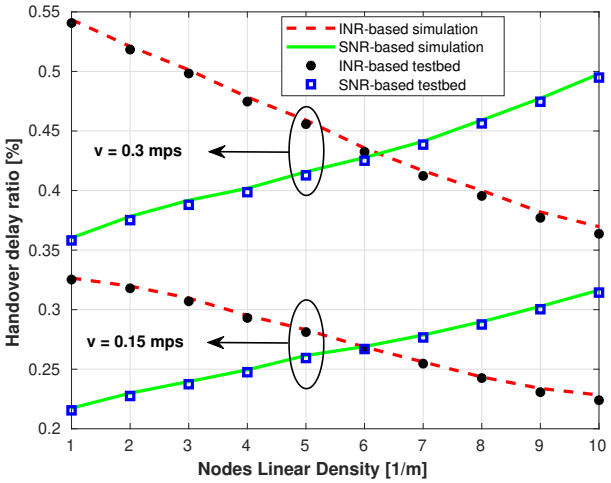

Figure 4.10: Handover delay ratio versus node density.

4.6 Conclusion

An Enhanced Handover Technique for Vehicular Visible Light Communication Networks INVISIBLE, based on Interference to noise ratio and Interferer-to-Interference ratio, has been proposed and validated through simulations, using the software NS3 and the experimental tests. A comparison between our technique and the conventional technique based on SNR has been provided in terms of handover rate, average delivered data per handover and handover delay ratio.
The results in both simulation and experimental tests show how the proposed technique avoids useless handovers, and by consequence, considerably improves the average delivered data per handover and reduces the amount of overhead information in the network. At the same time, our technique shows a significantly reduced handover delay ratio, in comparison with the SNR-based technique, in dense scenarios. Since the latter aspect is frequent in vehicular network architectures with a high number of users, this handover policy could be easily applied in most realistic scenarios.

Cellular Vehicular Visible Light Communication

5

In this chapter, the cooperation of Visible Light Communication (VLC) and the long-term evolution (LTE) cellular network in vehicular communication is discussed. The advantages of V2LC over C-V2X have been studied in detail to clarify the motivation for using VLC over cellular networks in vehicular communication. The metrics that have been considered in this study are energy efficiency, latency, and packet reception ratio. Moreover, a new power consumption model has been defined in this chapter to measure the power efficiency of each technology. Finally, we propose a Cellular Vehicular VLC (CV2LC) protocol for adaptive vertical handover between VLC and LTE in vehicular scenarios. This protocol meets the 3GPP baseline for Cooperative Awareness Messages (CAM) safety massages in different traffic densities.

Vehicle to everything (V2X) applications are supported by radio access technology (RAT) standards such as IEEE 802.11p (*i.e.*, DSRC or ITS-G5) and Cellular V2X (*i.e.*, LTE-V2X). LTE-V2X is an LTE (long-term evolution) adaptation for vehicular scenarios standardized by 3GPP, under released 14 and 15. It is based on the PC5 or sideline LTE radio interface. It supports distributed V2V and V2I communications, using Mode 3 and Mode 4 respectively, which do not require cellular infrastructure support, so it is interesting for ubiquitous ad-hoc networks. LTE however, faces strict challenges in handling aperiodic messages of different sizes due to the sensing-based Semi-Persistent Scheduling (SPS) scheme and these challenges can not be resolved by different configurations of LTE. SPS scheme causes further issues in vehicular communication such as:

1. **High traffic and power consumption** LTE-based Cellular Vehicle-To-Everything (C-V2X) allows vehicles to communicate with each other directly without the need for infrastructure and is expected to be a critical enabler for connected and autonomous vehicles. V2X communication-based safety applications are built on the periodic broadcast of basic safety messages with vehicle state information. Vehicles use this information to identify collision threats and take appropriate countermeasures. As the vehicle density increases, these broadcasts can congest the communication channel resulting in increased packet loss, fundamentally impacting the ability to identify threats without delay. To address this issue, it is important to incorporate a congestion control mechanism. Congestion management scheme based on rate and power control has proved to be effective for DSRC [65].
2. **Mobility Management (MM)** in Long-Term Evolution (LTE) networks is a vital process to keep an individual User Equipment (UE) connected while moving within the network coverage area. MM Entity (MME) is the LTE component responsible for tracking and paging procedures and controlling the corresponding signaling between the UE and its serving cell, which is necessary for data-packet exchange. Because of the massive increase in the density of mobile UEs, MME is burdened by the high volume signaling load, especially because most of that load comes from Tracking

LTE-V2X and C-V2X have been used interchangeably in this study

Area Update (TAU) and Paging messages, which are essential to exchange UE-specific information with the network. To achieve cost-efficient resource provisioning, many solutions have been proposed for TAU and Paging management to optimize not only UE experience (*i.e.*, battery power consumption) but also network resources (*i.e.*, bandwidth). [66].

On the other hand, vehicular VLC has less overhead in terms of channel access regulation and signaling, owing to short-range and point-to-point link style [56]. Therefore, vehicular traffic may be handled jointly through these two technologies. This chapter compares LTE and VLC performances in vehicular communication. A new power model has been suggested to measure energy efficiency at the transmitter and the receiver, in addition to the packet reception ratio, and latency metrics. The two technologies are united through a vertical handover mechanism called CV2LC. Vertical handover guarantees a seamless transition from one technology to another.

5.1 C-V2X

C-V2X (LTE-V2X) operates with 10 MHz and 20 MHz channels. It uses a time-frequency resource structure similar to the one which has been used in LTE. Time is structured in 1ms sub-frames that contain 14 OFDM symbols. The frequency bandwidth is divided into Resource Blocks (RB) of 180 kHz each. Each RB is made of 12 OFDM sub-carriers of 15 kHz. Adjacent RBs of the same sub-frame are organized into sub-channel. Data information is encapsulated in a Transport Block (TB), which is transmitted in a Physical Sidelink Shared Channel (PSSCH) and may occupy one or multiple sub-channels depending on the Modulation and Coding Scheme (MCS), and the number of RBs per sub-channel. Control information is encapsulated into Sidelink Control Information (SCI) and transmitted over the Physical Sidelink Control Channel (PSCCH) and occupies 2 RBs. An SCI contains information to decode TB such as MCS, TB length, and the time stamp of the next TB. TB and its associated SCI are transmitted on the same sub-frame as demonstrated in 5.1.

LTE-V2X works in Mode 3 and Mode 4. In Mode 3, the sub-channels between vehicles are assigned by the cellular base station. In Mode 4, vehicles autonomously select their sub-channels based on common sets

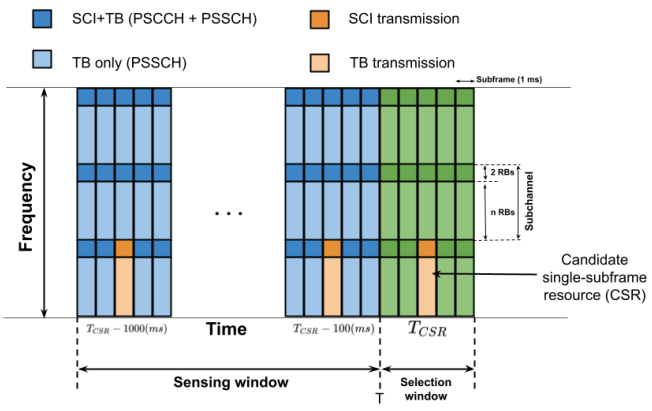

Figure 5.1: LTE-V2X resource structure

of parameters such as the number of sub-channels and the number of RBs per sub-channels. These parameters are configurable by users or operators when vehicles are covered by the cellular network. In LTE-V2X Mode 4, vehicles use the sensing-based Semi-Persistent Scheduling (SPS) defined in ITS Release 14 to autonomously sense, identify and select the unoccupied sub-channels. For this aim, SPS transmits Resource Reservation Interval (RRI) within SCI to inform the neighboring vehicles when they will utilize the reserved sub-channels for their next transmission [67, 68]. A vehicle that uses a given sub-channel to transmit its current TB (and its associated SCI) at time t will use the RRI to notify nearby vehicles that it plans to use the same sub-channel for its next transmission at t+RRI. The RRI is then used to prevent other vehicles from utilizing the same sub-channel(s). The RRI can be configured equal to 20 ms, 50 ms, 100 ms, or any multiple of 100 ms. The 3GPP standard does not fix a value of the RRI and its configuration is up to UE implementation. The configuration of the RRI has an important impact on the operation of the sensing-based SPS scheme. Its value should be adapted as much as possible to the characteristics of the messages that vehicles must transmit. Vehicles use the selected sub-channel(s) for a number of consecutive Reselection Counter transmissions. The reselection counter is randomly selected between 5 and 15 for RRI = 100 ms (or any multiple of 100 ms). The reselection Counter is decremented by 1 after each transmission, and a new value must be selected every time a vehicle needs to reserve new sub-channel(s). New sub-channel(s) must be reserved if at least one of the following conditions is satisfied:

- New sub-channel(s) must be reserved with probability$(1 - P)$ if the Reselection Counter reaches 0. P can be configured between 0 and 0.8. Increasing P augments the probability to maintain selected sub-channel(s) for longer periods of time. This provides a more stable sensing environment. However, increasing P also augments the probability of persistent packet collisions between two vehicles that select the same sub-channel(s). If a vehicle does not maintain the current reservation when Reselection Counter reaches 0, it notifies other nodes by setting the RRI in the SCI equal to 0.
- New sub-channel(s) must be reserved if the new packet or TB does not fit in the reserved sub-channel(s).
- New sub-channel(s) must be reserved if the current reservation cannot satisfy the latency deadline of a new packet. This happens if the time until the next reserved sub-channel(s) is higher than the latency deadline of the new packet.

The process to select and reserve new sub-channel(s) is referred to as re-selections. To select new sub-channel(s) at time T, the ego vehicle executes the following three steps of the sensing-based SPS scheme:

- Step 1. The ego vehicle identifies first the Candidate Single Sub-frame Resources (CSR) within the Selection Window. The Selection Window (Figure 5.1) is the time period between T and the latency deadline of the incoming packet (equal or lower than 100 ms). A CSR is a group of adjacent sub-channels within the same sub-frame where the new SCI+TB to be transmitted fits.
- Step 2. The ego vehicle excludes the identified CSRs that it estimates will be used by other vehicles. To this aim, the ego vehicle senses the transmissions from other vehicles during the so-called Sensing

Window. The Sensing Window is the time period that includes the last 1000 sub-frames before T (Figure 5.1). A CSR is excluded if the two following conditions are met:

1. the ego vehicle has received an SCI from another vehicle indicating that it will utilize this CSR in the current Selection Window or at the same time as the ego vehicle will need it to transmit any of its following Reselection Counter transmissions
2. the ego vehicle excludes a CSR if its average Reference Signal Received Power (RSRP) measured over the TB associated to the corresponding SCI is higher than a given threshold. The RSRP threshold is a configurable parameter.

The ego vehicle builds a list L1 with all the CSRs that have not been excluded. L 1 must include at least 20% of all CSRs in the Selection Window. Otherwise, Step 2 is iteratively executed increasing the RSRP threshold by 3 dB at each iteration until the 20% target is met.

- Step 3. The ego vehicle builds a list L2 with the CSRs included in L1 that has the lowest average Received Signal Strength Indicator (RSSI) over all its RBs. This RSSI value is averaged over all the previous $T_{CSR} - T_{IPI} \cdot j$ sub-frames where $T_{IPI} = 100$ ms. The total number of CSRs in L2 must be equal to 20% of all CSRs in the Selection Window. The ego vehicle randomly selects a CSR from L2 to transmit its new packet, and it maintains the selection for its next Reselection Counter transmissions.

Semi-persistent scheduling has severe impacts on LTE-V2X performance. The sensing window increase, and obliged the receiver to detect the signaling for a longer time, which in consequence increases the power consumption for signaling messages. Moreover, the re-selection period increases the Packet Inter-Reception (PIR). PIR is the time between two successful receptions of regularly transmitted messages [69].

5.2 LTE Power Consumption

The energy efficiency of communication networks is progressively attracting the research communities due to the exploding wireless technologies. The energy efficiency is usually evaluated in an extensive measurements regime using small-scale or actual devices which increases the total cost of projects and requires further expertise for implementation. In addition, new energy-saving methods and optimization techniques proposed in academia, require a comprehensive power model considering all the major energy-consuming components and their performance during different phases of transmission, reception, and ideal states. Nokia proposed a power model which considers only radio resource configuration mode for 3GPP but it does not take into account different data rate power control at the transmitter [70]. The chip manufacturers have detailed models based on their development platforms, however, they are confidential. Launching LTE opened new horizons to empirical models. A precise model based on the LTE USB dongle has been proposed in [70] which is robust and transferable. This model describes an LTE user equipment (UE) radio modem which is depending on power levels and data rates.

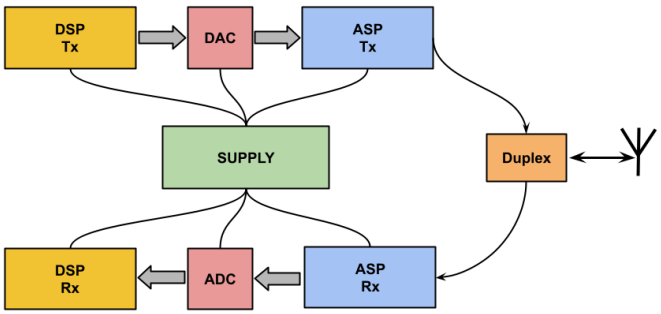

Figure 5.2: LTE power consumption model

The current theoretical power model is based on the major power components of LTE and VLC systems.
LTE Figure 5.2 shows the LTE physical layer components and the UE model parameters. The envisioned UE model depends on the received (Rx) and the transmitter (Tx) power levels, Uplink (UL) and Downlink (DL) data rate, and Radio Resource Configuration (RRC) mode.
Transmitter DSP In the LTE transmitter, the main task of digital signal processing is to turbo-encode user data with Forward Error Correction codes. Turbo encoding relies on convolutional encoding and generates a bit stream with a given code rate. The Turbo encoding complexity scales linearly with the amount of data to encode which is set by the Transport Block Size (TBS) *e.g.*, the UL data rate, but is independent of the UL Tx power [71].

DAC & ADC Digital to analog converter, converts the digitally processed signals to the analog waveform at the transmitter. On the other hand, the analog waveform at the receiver is digitized by the analog-to-digital converter.

Transmitter ASP Generally, the analog signal processing at the transmitter (ASP Tx) will not depend on the uplink (UL) data rate, but when the modulation format is changed, the Peak-to-Average Power Ratio (PAPR) is affected. This involves the Power Amplifier (PA), and adjusts its performance to comply with the transmission emission requirements in [72], such as the Adjacent Channel Leakage Ratio (ACLR), and this may affect the power consumption. The ASP Tx will obviously depend on the UL Tx power. A single PA only has one output power level where it achieves its maximum energy efficiency, and therefore researchers develop methods to increase the efficiency at other output power levels. These include the use of multiple PAs [73], supply voltage and bias switching, and the envelope tracking concept [74].

Receiver ASP The receiver analog signal processing power consumption is expected to be independent of the downlink (DL) data rate, but it will depend on the DL Rx power level. The reason is that the RF contains gain controls and low noise amplifiers, which are used to obtain a certain signal level at the ADC. If the DL received power level is high, the gain in the aforementioned circuits can be reduced, and they may be powered

off in order to reduce power consumption.

Receiver DSP The majority of the complexity at the receiver digital signal processing, *e.g.*, channel estimation and equalization, is independent of the DL data rate. To decode the received user data, the UE applies turbo decoding, which is an iterative algorithm and the most complex computational task in the digital baseband. To support the high data rates of LTE, a parallel turbo decoder architecture is required. The complexity and thus the power consumption scales linearly with the DL data rate [75].

UE LTE Power Model

Based on the review of the six physical components of the LTE UE device, the model is defined as 5.1:

$$P_{Total} = P_{Tx} + P_{Rx} \tag{5.1}$$

where P_{Total} is the total power consumption. The P_{Tx} is the transmitter power consumption derived from 5.2 and P_{Rx} is the receiver one computed as 5.3.

$$P_{Tx} = P_{DSP,Tx} + P_{ASP,Tx} + P_{DAC} \tag{5.2}$$

$$P_{Tx} = P_{DSP,Rx} + P_{ASP,Rx} + P_{ADC} \tag{5.3}$$

The ADC and DAC power consumption is represented by the offset b and the slope k of the ADC/DAC circuit design which is further scaled with the operating bandwidth B.

$$P_{DAC/ADC} = B \cdot k_{DAC/ADC} + b_{DAC/ADC} \tag{5.4}$$

The digital signal processing unit power consumption is defined as 5.5 and it is assumed identical for the transmitter and the receiver [76].

$$P_{DSP} = P_{leak} \cdot P_{dynamic} \tag{5.5}$$

where $P_{dynamic}$ represents the power dissipation at the dynamic charging and discharging of the Complementary Metal Oxide Semiconductors (CMOS) inherent capacitors, and P_{leak} denotes the leakage power dissipated due to reverse leakage of the employed CMOS switches.

$$P_{leak} = \eta_{leak} \cdot P_{dynamic,ref} \tag{5.6}$$

where η_{leak} stands for the leakage power ratio which is measured in Giga operations per second per watt (GOPS/W), and $P_{dynamic,ref}$ refers to the dynamic power at the reference bandwidth B_{ref} $[Hz]$

$$P_{dynamic} = \frac{O_C \cdot B}{\eta_{CMOS} \cdot B_{ref}} \tag{5.7}$$

The O_C represents the digital computational complexity function at the reference bandwidth B_{ref} which is scaled linearly with the operating bandwidth value (B). η_{CMOS} is the intrinsic CMOS power-efficiency

factor.

The analog unit includes different elements of a transmitter and the receiver such as carrier generation, modulator, mixer, low noise amplifier (LNA), variable gain amplifier (VGA), filter, buffer, and Power Amplifier (PA). Direct conversion transceiver is a popular architecture for LTE-UE (see Figure 5.3) [77]. Direct conversion means that an RF signal is directly down-converted to a Base-band (BB) signal or vice versa without any Intermediate Frequency (IF) stages, and therefore it is also referred to as zero IF architecture. The direct conversion architecture has many attractive features. The direct-conversion receiver has no IF, and thus the expensive IF passive filter (SAW filter) can be eliminated, and then the cost and size of the overall transceiver are reduced. The channel filtering of the direct-conversion receiver is implemented in the analog baseband by means of an active low-pass filter. In a direct conversion receiver, the function of the duplexer band pass filter (BPF) is to suppress the leakage power of the transmission and other out-of-receiver band interference. The received signal after pre-selecting the duplexer is amplified by an LNA, and it is further filtered by an RF filter. The filtered RF signal is then directly down-converted into In-phase and Quadrature baseband (BB) signals by an I/Q down converter which is also called a quadrature demodulator. The BB signals in the I and Q channels are synchronously amplified, but their 90° phase offset will be kept unchanged as possible. In the direct conversion receiver, the overall receiver gain is obtained from the analog baseband block when the receiver operates at its high gain mode. There exists a low pass channel filter in each of the I and Q channels. Unlike the superheterodyne receiver, channel selectivity mainly depends on the stop-band rejection of the low-pass filter without any passive band-pass filter assistance. The amplified and filtered BB analog signals in the I and Q channels are converted into digital signals by analog-to-digital converters (ADC), and the digital signals pass through digital filters to further suppress nearby interferers and enhance the channel selectivity.
Compared with the receiver, the direct-conversion transmitter has fewer issues, and it is relatively easy to be implemented. The I and Q BB signals coming from the transmitter DAC converters first pass through low-pass filters to make the adjacent channel and alternate channel emission levels further suppressed and to eliminate aliasing products. The filtered and amplitude attenuated I and Q BB signals both are directly up-converted to RF signals, and then they are added together by an I/Q modulator. The composite RF signal is amplified all the way up to the RF power amplifier (PA).

The power consumption of the transmitter ASP can be modeled as 5.8, considering only the aggressive power consumer components of the direct conversion transmitter:

$$P_{ASP,Tx} = P_{IQ\ modulator} + P_{Clock} + P_{VCO} \tag{5.8}$$

in 5.8, P_{VCO} is nominal power consumption at voltage-controlled oscillator, $P_{IQ\ modulator}$ is the in-phase and quadrature modulators power consumption, and P_{Clock} is the power needed for clock generation and buffering in [mW]. On the other hand, the power consumption of the

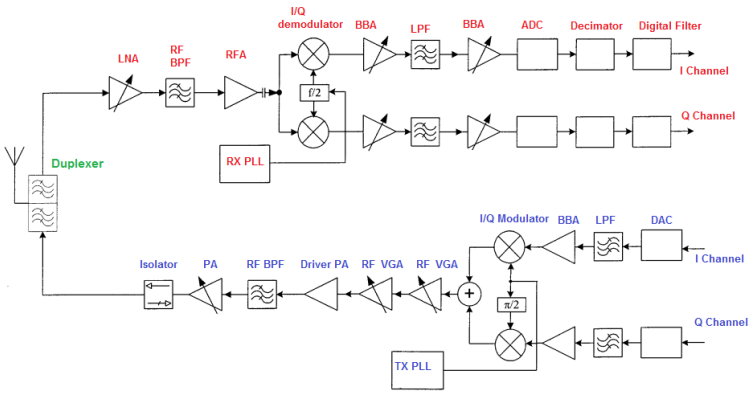

Figure 5.3: Direct Conversion Transceiver Radio Architecture

receiver ASP is derived from 5.9:

$$P_{ASP,Rx} = P_{LNA} + P_{attenuator} + P_{mixer} + P_{Clock} \tag{5.9}$$

where P_{LNA} stands for low-noise amplifier power consumption, $P_{attenuator}$ is the power lost in the main variable attenuator, and P_{mixer} is the dual mixer power.

5.3 VLC Power Consumption

A similar power consumption model is presented based on the VLC system block diagram of Figure 5.4, where the front-end blocks are divided into digital and analog components according to the place of DAC and ADC converters in the transmitter and the receiver sides respectively [78]. This model accounts for the most significant power consumer VLC components, specifically:

- At the transmitter side the signals are processed digitally using **Digital Signal Processing** and then converted to an analog waveform by digital to analog converter **DAC**.
- **Transmitter Amplifier** amplifies and biases the analog signal to fit the linear region of LED transfer characteristic.
- **LED** transforms the electrical signal to visible light and then passed it to the optical wireless channel.
- At the receiver side, the **PD** is used as a passive element to convert the optical signal back to a current signal. When a bias is applied to the photodiode, the current output can be controlled to provide thresholding, linear response, or nonlinear response.
- The trans-impedance amplifier **TIA** alters the current to a voltage signal.
- The analog voltage waveform is digitized by the analog to digital converter **ADC** and eventually delivered to **DSP** for further processing.

Analogue power consumption: The analog power consumption at the transmitter part of this model can be decomposed to the power consumption at the transmitter amplifier and the power consumption of the LEDs, as 5.10:

$$P_{ASP,Tx} = P_{Tx\ Amp.} + n \cdot P_{LED} \tag{5.10}$$

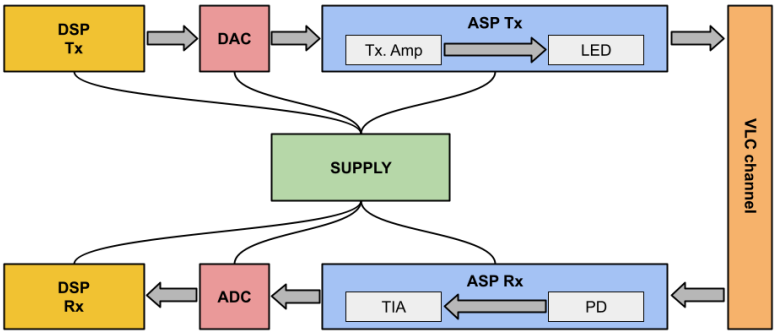

Figure 5.4: VLC power blocks

The LED's power consumption (*i.e.*, P_{LED} is determined by the DC bias level and the total number of the deployed LEDs (*i.e.*, n). In the same way, the analog power consumption at the receiver part is decomposed to the PD power consumption and the trans-impedance amplifier power consumption, as 5.11:

$$P_{ASP,Rx} = m \cdot P_{PD} + P_{TIA} \tag{5.11}$$

where m is the number of photodiodes and bounded trans-impedance amplifiers.
Digital power consumption: Due to the similarity in the digital processing techniques between RF and VLC, the same power consumption model is adopted in this study [78, 79].

5.4 Energy Efficiency

To model the energy consumption during one transmission time interval (TTI), one can relay on the conversion of the power to energy in different states as 5.12, 5.13 and 5.14:

$$E_{TTI} = E_{Tx} + E_{Rx} \tag{5.12}$$

$$E_{Tx} = P_{Ts} \cdot D_s + P_{Ti} \cdot D_i + P_{Tt} \cdot D_t \tag{5.13}$$

$$E_{Rx} = P_{Rs} \cdot D_s + P_{Ri} \cdot D_i + P_{Rr} \cdot D_r \tag{5.14}$$

where D_x is the time spent in state x, and p_x is power consumed in state x.
s: sensing, i: idle, t: transmission, r: reception

The energy consumption at the transmitter and the receiver can be re-formed as 5.15 and 5.16

$$E_{Tx} = E_{TBB} + E_{TRF} \ , \ E_{TBB} = a \cdot R_b \cdot D \ , \ E_{TRF} = b \cdot P_t \cdot D \tag{5.15}$$

$$E_{Rx} = E_{RBB} + E_{RRF} \ , \ E_{RBB} = c \cdot R_b \cdot D \ , \ E_{RRF} = p_{RRF} \cdot R_b \cdot D \tag{5.16}$$

a, b, c are coefficients that depend on the technology.

Energy Efficiency Finally, energy efficiency is formalized as the ratio of delivered data in a given throughput to the energy consumption in one TTI.

$$EE = R_b \cdot Z/E_{TTI} \ [bit/Joule] \tag{5.17}$$

The equivalent power-related version of 5.17 is derived as 5.18

$$EE = \frac{Z/D}{k_1 + k_2 \, P_t/R_b} \tag{5.18}$$

k_1, k_2 coefficients that depend on the technology.

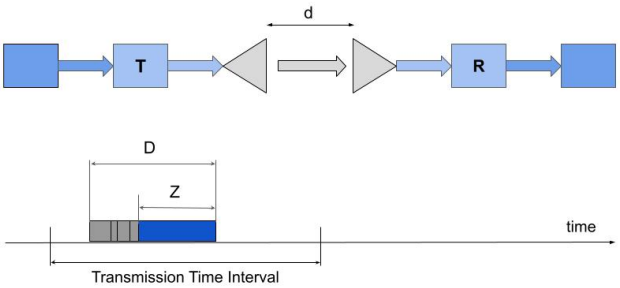

Figure 5.5: Point-to-point transmission model

5.4.1 Performance analysis: VLC vs. LTE

In this section, we compare the energy efficiency of the LTE radio access technology for vehicular communications with the V2LC model. The energy efficiency model defined in section 5.2 has been implemented in the ns3-V2LC module for visible light communication vehicular applications, and the Multi-Stack VANET framework for ns-3 (ms-van3t) for LTE-V2X compliant application [80]. Figure 5.6 demonstrate a SUMO environment where the yellow cars represent the mobile nodes. Mobile nodes are generating Cooperative Awareness Message (CAM) based on

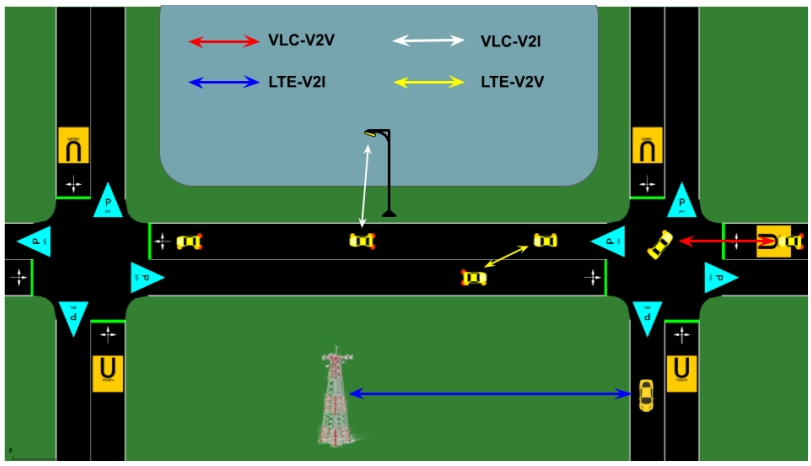

Figure 5.6: V2X communication possible links

Header	Signer_Info
	Generation_Time
	ITS-AID for CAM
CAM Information	ITS-Station Type
	Last Geographic Position
	Speed
	Driving Direction
	Longitudinal Acceleration
	Curvature
	Vehicle Length
	Vehicle Width
	Steering Angle
	Lane Number
	...
	Vehicle Role
	Lights
	Trajectory
	Emergency
	Police
	Fire Service
	Road Works
	Dangerous Goods
	Safety Car
	...
Signature	ECDSA Signature of this Message
Certificate	According Certificate for Signature Verification

Figure 5.7: CAM Structure

the empirical model proposed in [81]. This model has derived from ETSI ITS communication architecture. The format of the CAM message is coming in Figure 5.7. According to ETSI ITS regulations, vehicle should generate a new CAM if any of the following conditions are triggered:

- The distance between the current position of the vehicle and the position mentioned in the previous CAM exceeds 4 m.
- The absolute difference between the current velocity and the velocity included in the previous CAM exceeds 0.5 m/s.
- The absolute difference between the current heading of the vehicle and the heading included in its previous CAM exceeds 4°.
- The time elapsed since the last CAM was generated is equal to or higher than 1 s.

These generation rules are applicable regardless of the access technology.

Most of the basic awareness traffic in C-V2X is encapsulated either in broadcast cooperative awareness message (CAM) specified by the European Telecommunications Standards Institute (ETSI), or in Broadcast Basic Safety Message (BSM) specified by the Society of Automotive Engineers (SAE). These messages contain basic information about the position, speed, or direction of the transmitting vehicle. In LTE-V2I, CAMs are generated and broadcasted by the vehicle through a given wireless interface (ITS-G5) while the V2V communication employs PC5 or sidelink to share CAMs among cars [82]. The on-board C-V2X units -a small scale base station (Femto) used in cars- use more power-efficient dedicated components compared to large base stations (macro and micro), the downscaling factor defined in [76] is used to reduce the power on smaller base station due to less constraining space and different hardware implementation. The reason is twofold: • The amount of blockers, a small

base station has to face is smaller, leading to more relaxed linearity specs, and hence less power is needed. •• Smaller base stations can work from a lower supply voltage, further reducing their consumption. All RF components' powers are downscaled based on the constraining space and different hardware implementations of smaller cells. Scaling of RF power with input parameters is done as follows. All RF sub-components have a scaling exponent of 1 with respect to the number of antennas and time-domain duty cycling. For carrier and clock generation sub-components, scaling exponents have the value zero. For the other RF sub-components, the scaling exponent is 1 with respect to frequency-domain duty-cycling, assuming a scalable implementation. Technology scaling is used for analog, too, based on a scaling factor as a function of the selected CMOS technology compared to the reference tech = 65 nm case. 5.19 is an empirical rule from the designer's experience, not a physical law:

$$Downscaling\ factor = Power(65\ nm)\left(1 + \frac{tech/65 - 1}{2}\right) \tag{5.19}$$

Femtocells are the smallest unit in the LTE system hierarchy which suits the C-V2X ranges (10-1000m) [83]. The downscale factor for LTE-femtocell is 12. The power amplifier behavior can not be captured by a single reference power number and scaling rules. Hence, the PA model is represented by a table containing measurements of output power versus consumed power. Measured points differ in requested output power and in the tuning of the 1 dB compression point. The power model picks up the point with minimal power consumption that is satisfying the output power and linearity constraints. The maximum total output power for femtocells is 20 dBm, and its minimum power consumption is 650 mW. Table 5.1 represents the power consumption of the analogue components in LTE on-board unit. In order to simulate the MAC performance of the LTE-V2X the following scenario is assumed: n eNBs are uniformly distributed such that the Tx-Rx distance will meet the LTE rel.14 requirements in terms of Packet Reception Ratio(PRR) equal to 95%. In fact, in order to concentrate on the MAC performance we cancel the performance degradation of the physical layer (propagation loss and shadowing effect) [84] following the WINNER+B1 channel model by the 3GPP [24]. The B1 channel model for the 5.9 GHz band is calculated as follows:

• LOS for 30 $m < d < d'_{BP}$

$$PL(dB) = 22.7 \cdot \log_{10}(d) + 27.0 + 20.0 \cdot \log_{10}(f_c) \tag{5.20}$$

• for $d'_{BP} < d < 5\ Km$

$$PL(dB) = 40.0 \cdot \log_{10}(d) + 9 - 16.2 \cdot \log_{10}(h_{BS}) - 16.2 \cdot \log_{10}\left(h_{MS} + 3.8 \cdot \log_{10}(f_c)\right) \tag{5.21}$$

• NLOS

$$PL(dB) = (44.9 - 6.65 \cdot \log_{10}(h_{BS})) \cdot \log_{10}(d) + 5.83 \cdot \log_{10}(h_{BS}) + 15.38 + 23 \cdot \log_{10}(f_c) \tag{5.22}$$

The effective breakpoint distance d'_{BP} is calculated by:

$$d'_{BP} = 4 \cdot h'_{BS} \cdot h'_{MS} \cdot f_c / c \tag{5.23}$$

where the effective antenna height $h'_{BS} = h_{BS} - 1\ m$ and $h'_{MS} = h_{MS} - 1\ m$ and $c = 3 \cdot 10^8\ m/s$ [69]
Based on [24] the antenna height is set to $h_{BS} = h_{MS} = 1.5\ m$ for V2V communications and $h_{BS} = 5\ m\ ,\ h_{MS} = 1.5\ m$ for V2I communications.

Analogue Item	Power Consumption [mW]
IQ Modulator	1000
VCO	170
Clock	990
LNA	300
Attenuator	10
Dual Mixer	1000
PA	650

Table 5.1: LTE Analogue Major component's Power

Similarly, table 5.2 shows the power consumption of the VLC components used in the proposed energy model. The street light poles have been used as VLC infrastructure based on global lighting design guidance [85]. In this design, the pole height is 8-10 m and the spacing between two light poles should be roughly 2.5-3 times the height of the pole. This regulation let us to uniformly distribute the light poles with 25-meter spacing in highway scenarios and 23 meters in urban scenarios. The vehicle velocity is defined according to the federal highway administration of US government since the urban scenario follows the Manhattan mobility scenarios. Following this regulation, the speed in the urban areas is changed between 45 to 72 and on highways is set between 90 and 105 kilometers per hour [86].

OOk single carrier modulation has been used for its low complexity and robustness. The computational complexity factor O_C for OOK modulation is set to 505.15 GOPS at 20 MHz reference bandwidth B_{ref}. According to [78], CMOS power efficiency is $3.6e + 4$ GOPS/W, while the leakage ratio was 24.3 in 2020. Additionally, 2 different transmission methods have been proposed naming: regular transmission, and adaptive transmission.
Regular Transmission, strictly follows the ETSI (TS 102 637-2) specifications [87] where CAMs are generated and transmitted regardless of the availability of the access technology.
Adaptive Transmission on the other hand, disseminates CAMs based on ETSI ITS regulation under good coverage of the access technology.
The two transmission methods have been attempted and compared using SNR-based and INR-based handover mechanisms that are presented in earlier chapters. Receiver energy efficiency $[Kbits/Joule]$ digitizes the amount of data received per unit of energy consumed at the receiver and it is calculated in 5.18. This metric is compared to the traffic density vector in figure 5.8 for VLC technologies in various scenarios. Traffic density describes the average number of vehicles per unit of road length (in

Analogue Item	Power Consumption [mW]
LEDs	2000
DAC	1400
ADC	770
TIA	90
TA	345

Table 5.2: VLC analog power specification

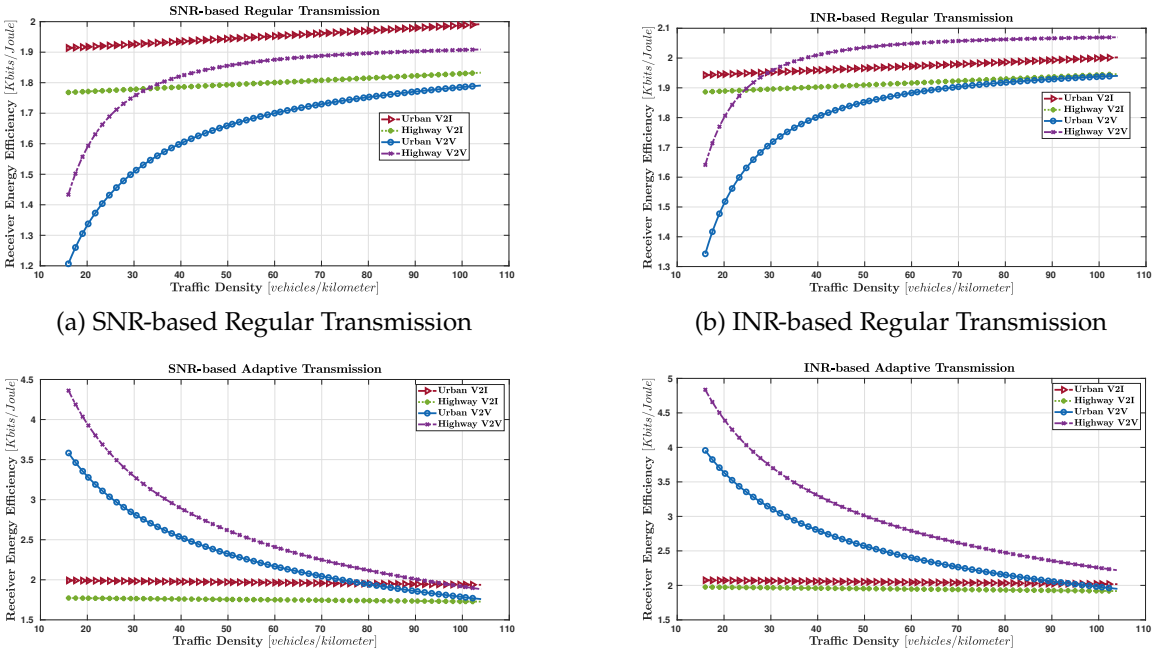

(a) SNR-based Regular Transmission

(b) INR-based Regular Transmission

(c) SNR-based Adaptive Transmission

(d) INR-based Adaptive Transmission

Figure 5.8: Receiver Energy Efficiency VLC

[*vehicles per kilometer*]) per day [88]. In figure 5.8 the receiver energy efficiency for the SNR-based handover mechanism has been presented under continuous transmission/reception. In the V2I scenarios, receiver energy efficiency is steady because the data traffic flow and the power consumption do not change with increasing the traffic density. The data traffic flow is constant because the transmission period (equal to simulation time), as well as the number of received packets, is stable. Moreover, the receiver energy efficiency increase in the V2V scenario according to figure 5.8a. In V2V cases the CAM dissemination rate increased as a consequence of more received packets when the traffic density increased. As a result, the receiver receives more and more data per unit of energy. In figure 5.8b, the same metric has been examined for INR-based regular transmission. The receiver efficiency in energy consumption is similar to the SNR-based performance using the same transmission method and in both cases, the receiver can not receives more than 2.1-kilobits per joule. The performance of the adaptive transmission in terms of receiver energy efficiency is higher than the regular transmission for SNR-based and INR-based handover mechanisms according to figures 5.8c and 5.8d. The difference is that in the V2V scenarios the reception period (*i.e.*, T) is lower in a low traffic density and it increased to be equal regular transmission period in high traffic density. Finally, the INR-based adaptive transmission is outperforming the other 3 schemes in receiver energy efficiency by means of restricting the working time of the most energy-consuming components to the connection interval.

In figure 5.9 the LTE-V2X receiver energy efficiency in respect of traffic density is presented. Compared to the VLC technology, the LTE receiver, collect more information per unit of energy (*e.g.*, $Joule$). In vehicular to vehicular scenarios, the performance is slightly enhanced in dense scenarios because the receiver is receiving more and more bits per unit

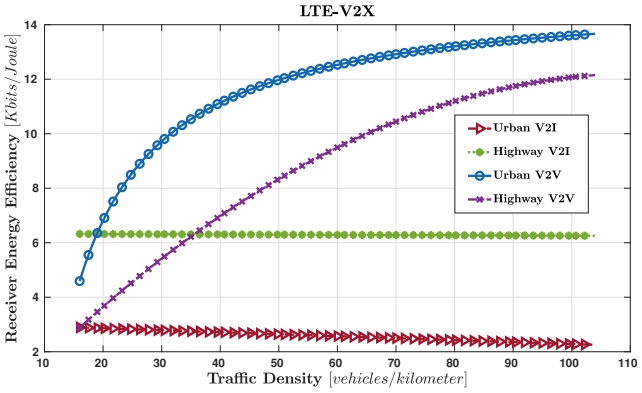

Figure 5.9: Receiver Energy Efficiency C-V2X

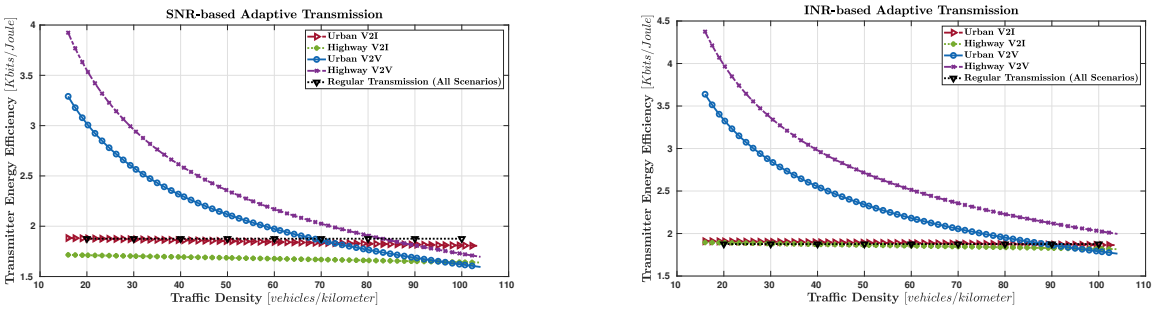

(a) SNR-based (b) INR-based

Figure 5.10: Transmitter Energy Efficiency VLC

of energy, where in the best case it reaches up to 15 Kbits per Joule in high-density V2V. For vehicular to infrastructure scenarios, the receiver energy efficiency is sustained with increasing the number of vehicles due to the central dissemination of CAM messages which are fixed per car.

At the transmitter side of VLC, the energy consumption efficiency is constant in regular transmission schemes no matter what is the scenario, because the transmitter is disseminating CAM messages as long as the light is open. As figure 5.10 shows, the V2I scenarios are less sensitive to the traffic density in the urban areas as well as highways in both SNR-based and INR-based horizontal handover schemes. It is interesting to observe that the performance of the SNR-based handover mechanism in highway V2I is even lower than the benchmark (regular transmission). As a matter of fact, the signaling overhead in a vibrant scenario like a highway prevents the SNR-based mechanism from transmitting the CAM messages despite being exposed to a potential VLC infrastructure all the time. The V2V communication energy efficiency is degrading by increasing the traffic density. In SNR-based for example, as the number of surrounding nodes is increased, the signaling overhead increases and as a result, the amount of energy that should be spent to disseminate the CAM massage is spent for signaling. Conversely, in the INR-based algorithm, the EE_{Tx} performance is improving with traffic density augmentation owing to the lower number of handovers and overhead in general. The black dash-line shows the transmitter's energy efficiency when it follows the regular transmission method. It is obvious that the energy consumption in this method is not efficient and it represents the baseline for any energy optimization technique.

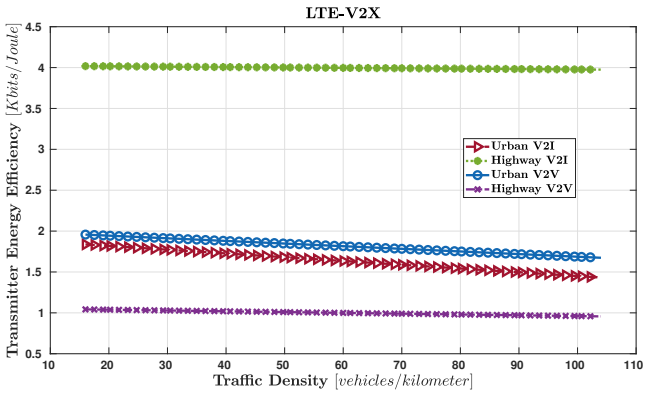

Figure 5.11: Transmitter Energy Efficiency LTE-V2X

The energy efficiency is less reliant on the traffic density in the LTE-V2X transmitter. The LTE-V2X transmitters are very harsh in energy consumption such that they can not transmit more than a few kilo bites per Joule of energy. Figure 5.11 shows the LTE transmitter energy efficiency in different scenarios. The best C-V2X can do in terms of transmitter energy efficiency is at highway V2I scenario.

Packet reception ratio (PRR) is defined as the number of correctly received packets to the total transmitted packets and represented through (5.24).

$$PRR = \frac{Received\ Packets}{Transmitted\ Packets} \tag{5.24}$$

Packet accounts are delivered if the number of erroneous bits (symbol) is less than the coding threshold. Since we do not use any channel coding scheme (FEC, ARQ, etc), a packet is correctly received when all the packet's bits(symbols) are correctly detected. Assuming OOK modulation scheme [50] has been used then the Packet Error Ratio is defined as 5.25:

$$PER = 1 - (1 - BER)^m \tag{5.25}$$

Where m is the packet size in bits and BER is the bit error rate for the OOK modulation scheme defined as 5.26 [45]:

$$BER_{OOK} = 0.5\, Q(SNR_o) \tag{5.26}$$

in 5.26 Q is the tail probability of the standard normal distribution and SNR_o is the optical signal to noise ratio defined as 3.13

In figure 5.12a the PRR of SNR-based with the regular transmission is gradually improved for all scenarios but with a different slope, as the urban and highway V2V is highly dependent on the traffic density such that, the higher traffic density decreases the distance among vehicles and so increase the received power of the VLC signal. In that case, the SNR is increased and the packets are more likely received successfully. On the other hand, in the vehicular to infrastructure (V2I) VLC, the density of the infrastructures (street light poles) is constant and they are arranged in a way to provide sufficient illumination as a primary purpose along the streets and the roads based on street lighting standards [89] and the VLC connectivity as a secondary purpose. The PRR for V2I scenarios remains almost constant when the number of mobile devices increases, since the distribution of the infrastructure does not change and as a

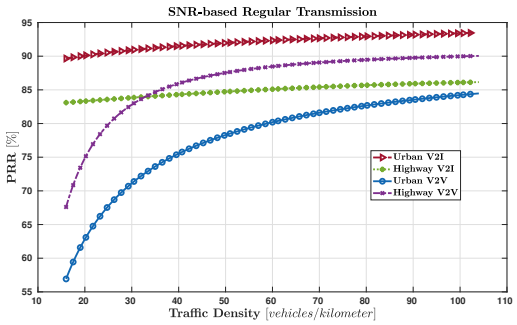

(a) SNR-based Regular Transmission

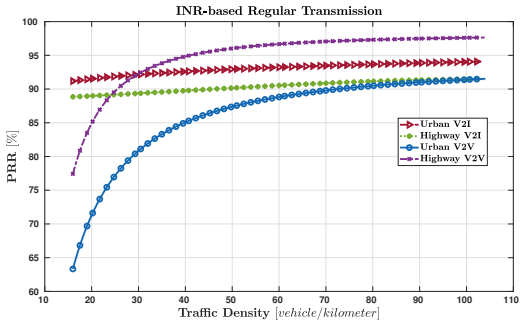

(b) INR-based Regular Transmission

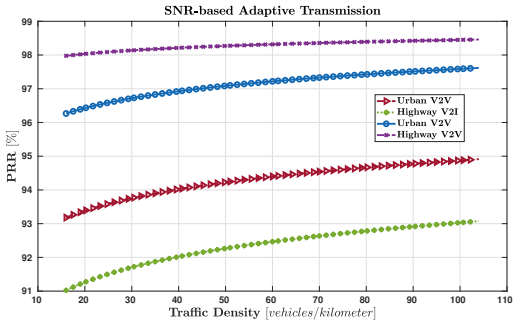

(c) SNR-based Adaptive Transmission

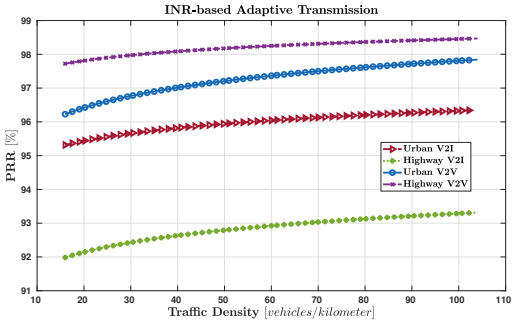

(d) INR-based Adaptive Transmission

Figure 5.12: Packet Reception Ratio

result, the covered area of the infrastructure is constant. According to [89], spacing among highway lighting infrastructures is higher than urban infrastructures which explains why the urban V2I PRR curve is upper than highway V2I 5.12a. Figure 5.12b pictures the INR-based packet reception ratio when the transmission is regular. The PRR has been enhanced a little bit for all scenarios because the INR-based handover mechanism is designed to connect the most durable access point and so reducing the possibility of disconnection. Similarly, the vehicular-to-vehicular packet delivery ratio is much more responsive to the traffic density increment compared to the vehicular-to-infrastructure one. In the adaptive transmission case (figures 5.12a and 5.12b) the performance is nearly comparable with a slight preference in INR-based regular transmission V2I cases. For adaptive transmission schemes, the PRR is much higher than the regular transmission schemes because in adaptive transmission schemes the transmitter actually transmits only when the link quality indicator (SNR in SNR-based and INR in INR-based) is above the threshold which gives a higher probability of successful transmission. More precisely, the augmentation in the PRR metric of adaptive transmission is due to the reduction of uncertain transmission.

Figure 5.13 demonstrates the packet reception ratio at the mobile nodes that are transmitting CAM packets using cellular long-term evolution Mode 3 and Mode 4. 4 curves show 4 different scenarios similar to vehicular VLC scenarios. The LTE-V2I has the best PRR performance in urban and highway scenarios regardless of the traffic density, owing to the wide coverage and reliable resource allocation strategy of LTE. In the next world, the packet reception ratio of V2V is smaller, due to the lower coverage range of onboard modules in the vehicles compared

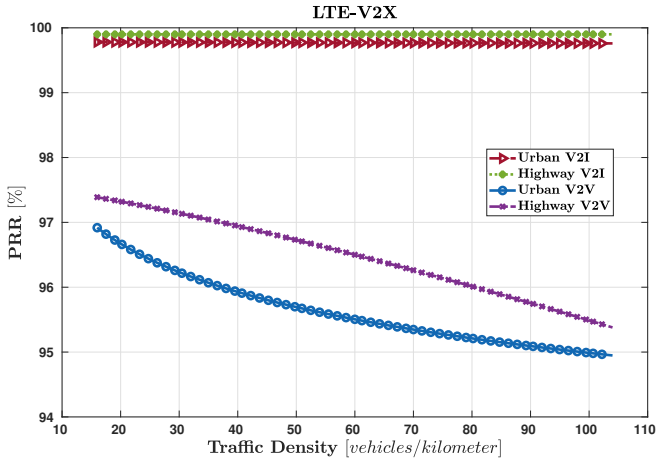

Figure 5.13: PRR C-V2X

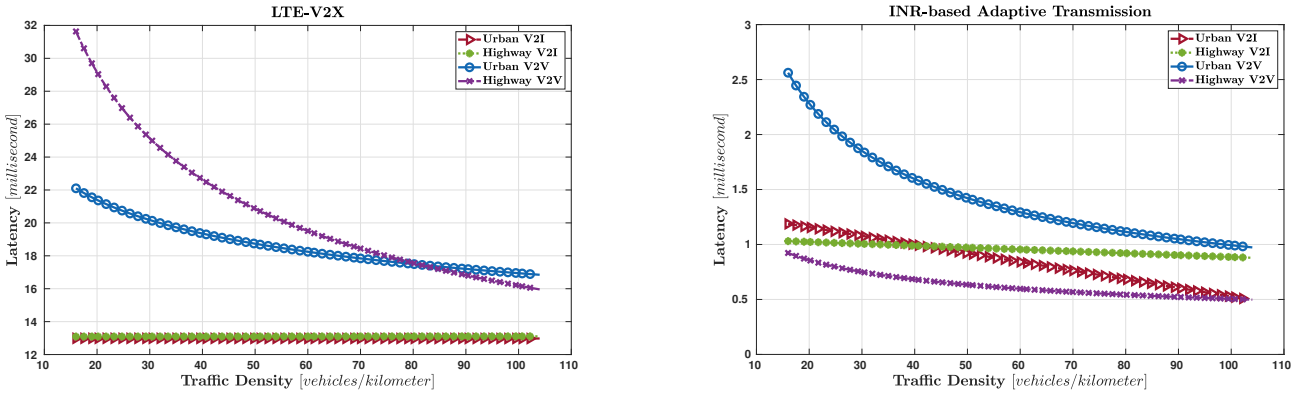

(a) LTE-V2X (b) VLC

Figure 5.14: Latency

to the eNB station at V2I scenarios. PRR is decreased by increasing the number of vehicles in V2V urban and highway scenarios. In cellular V2V, each vehicle has to manage its own communication session in a distributed way, it gives higher chance to an individual mobile node to find a free channel for transmission at lower density while in the higher traffic density the completion to acquire RF resource for transmission is stronger and decrease the chance of finding a free channel, so the PRR decreases.

Vehicular applications have some requirements in terms of latency. In [90] latency has been defined as the maximum time span during which vehicular traffic may be successfully delivered to the target vehicle. In our application, latency is the time delay from the CAM generated, until the successful delivery to the destination.
In Figure 5.14 the latency of LTE-V2X and VLC is compared in multiple scenarios. Generally, the latency in LTE-V2X is much longer than the end-to-end latency in VLC. In LTE-V2V scenarios, increasing the traffic density decreases the distance among communicating vehicles which reduces the latency by its part. However, the latency in V2I scenarios does not change significantly in dense traffic in both technologies, since the average distance between the cars and the infrastructure is constant. This distance is much lower in VLC technology (the coverage range of

VLC technology is lower than LTE-V2X) which makes communication faster.

5.5 CV2LC

In this section, a new vertical handover mechanism called Cellular Vehicular Visible Light Communication (CV2LC) has been proposed. Owing to the multiple advantages that have been discussed in the earlier section, CV2LC prefers VLC technologies for CAM dissemination. VLC works as a complement to cellular LTE-V2X technology, but in this model VLC is the primary transmission option and LTE radio technology is the second option for data transmission. The main trigger for vertical handover is reliability. Such that when the PER degrades below the threshold, CV2LC switches to LTE to maintain an acceptable packet reception ratio (PRR). Moreover, the energy consumption and the delay performance of these handover mechanisms give a good compromise between ad hoc VLC and LTE.

5.6 represents the scenario where the mobile nodes rely on VLC technology to transmit their CAMs. The INR-based handover mechanism guarantees seamless horizontal handover inside VLC coverage. When the performance of the VLC link degrades, CAMs are sent through LTE radio access technology. Figure 5.15 shows CV2LC module implemented on ns-3 simulation tools.

As in the previous case, CAMs are generated on the mobile nodes based on the ETSI ITS model, then they are disseminated through the VLC link if optical SNR is above the threshold (*i.e.*, SNR_o), otherwise the CAM is sent via LTE network. It assumed that the mobile node is already has been registered in the LTE network according to the RRC procedure. When the mobile node does not have any active ink, the CAM generation is prevented. A heterogeneous LTE-VLC network has been simulated at vehicular applications for V2V and V2I communications in urban and highway scenarios. The CV2LC performance is evaluated in terms of PRR, latency, transmitter EE, and receiver EE.

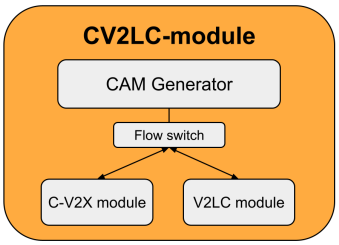

Figure 5.15: Transitions between V2LC and C-V2X modes are carried out in the flow switch based on each module's feedback

5.5.1 Simulation Results

The packet reception ratio is presented in figure 5.16 in respect of the traffic density, and it is visible that the 95% 3GPP baseline is always respected because the reliability (represented in PER) is the triggering metric for CV2LC protocol. When the PER degrades below the given threshold (10e-3), the mobile node use INR-based to select an alternative VLC link to send CAM and if it fails, the LTE is the last option. PRR is slightly increasing in V2V communication when the traffic increases, however PRR in vehicular to infrastructure is almost constant. The CV2LC performance in V2I is higher than V2V and Highway V2I has the best PRR. Due to the fact that VLC does not fulfill the 3GPP requirement in terms of PRR, in the highway V2I, CV2LC totally relies on C-V2X for CAM transmission.

The energy efficiency at the receiver at CV2LC has been improved compared to the ad hoc V2LC especially in high traffic density according

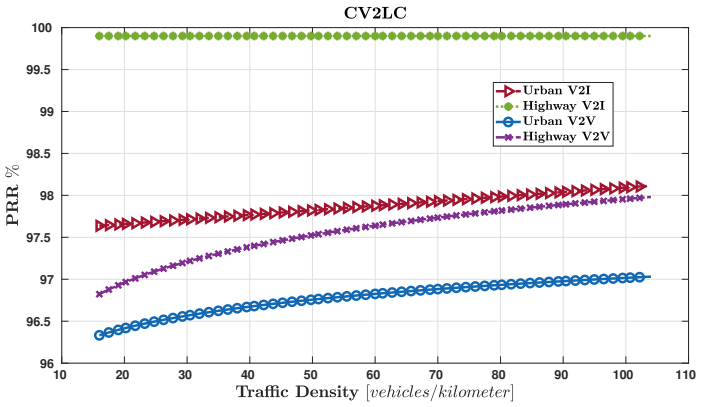

Figure 5.16: Packet Reception Ratio in different scenarios of cellular vehicular VLC

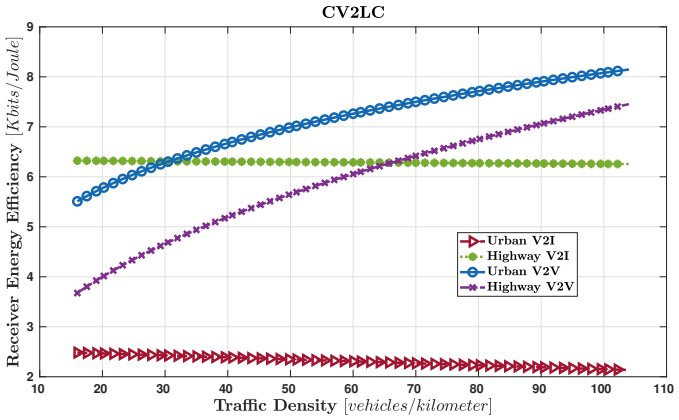

Figure 5.17: Receiver energy efficiency in different scenarios of cellular vehicular VLC

to figure 5.17. In this figure, when the traffic density is growing, it has a positive effect on the V2V receiver EE, while it is less effective in V2I scenarios. Moreover, the receiver in urban V2V has the highest performance, and the lowest performance is happen in the urban V2V environment. The receiver energy efficiency in highway V2I is equivalent to the C-V2I curve at the same condition. It means, the CV2LC is mostly using LTE in highway V2I.

Figure 5.18 shows the energy efficiency at the transmitter part in relation to the traffic density. Compared to the C-V2X, the transmitter energy efficiency is improved in urban V2I, urban V2V, and highway V2V, and it is identical to C-V2I in highways. In the sparse traffic density, the CV2LC uses the energy more efficiently at the transmitter to send CAMs to other mobile nodes, and as the traffic density increases, the transmitter energy efficiency decreases. In V2I communication, the energy efficiency at the transmitter is steady but it is higher than ad hoc C-V2X and V2LC.

The latency of CV2LC has been shown in figure 5.19 when the traffic density grows in different scenarios. The CV2LC latency is improved by one order of magnitude compared to ad hoc C-V2X in vehicular-to-vehicular communication. In the urban V2I scenario, the latency is decreased significantly, while in highway V2I, CV2LC and CV2X are identical.

Figure 5.20 demonstrates the comparison of the above metrics in ad hoc and heterogeneous vehicular networks. The PRR, latency, and energy efficiency at the transmitter and the receiver of the two ad hoc V2X

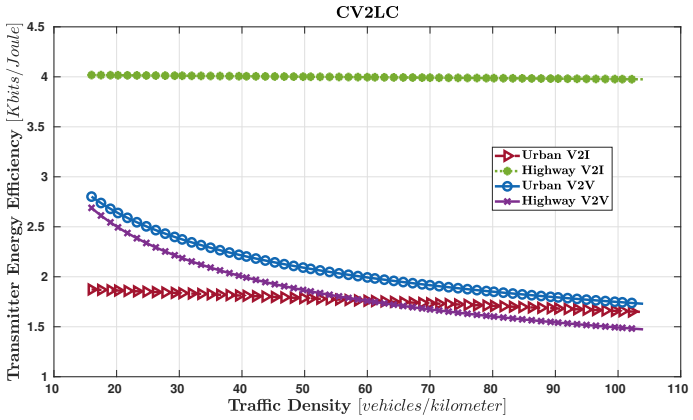

Figure 5.18: Transmitter energy efficiency in different scenarios of cellular vehicular VLC

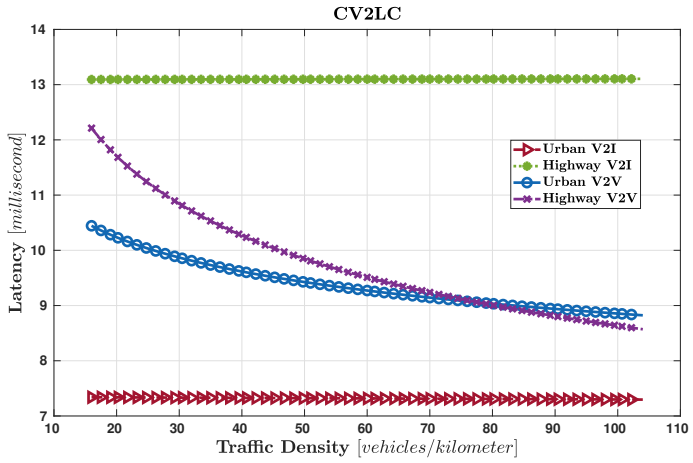

Figure 5.19: Latency in different scenarios of cellular vehicular VLC

network naming: C-V2X and V2LC have been compared with a heterogeneous CV2LC network. For each metric, 4 different scenarios have been analyzed in 2 extreme traffic densities (*i.e.*, high density and low density). In general 8 cases have been analyzed to compare the performances in PRR, latency, transmitter EE, and receiver EE. The horizontal axis contains the scenario cases including urban V2I high density, urban V2V high density, highway V2I high density, highway V2V high density, urban V2I low density, urban V2V low density, highway V2I low density, and highway V2V low density. On the other side, the vertical axis stands for the range of represented metrics.

HD: High Density (Traffic Density = 100 vehicles/kilometer)
LD: Low Density (Traffic Density = 20 vehicles/kilometer)

For instance, in figure 5.20a the PRR of CV2LC is always above the 95 percent while the V2LC is below this range in 2 cases: highway V2I high density and highway V2I low density. Specifically, in these two cases the CV2LC use only the LTE network to disseminate its CAMs, so the PRR of CV2LC is equal to C-V2X in these cases. In the other scenarios, the performance of CV2LC is lower than C-V2LC in terms of PRR, just because when both networks (VLC and LTE) are available, CV2LC chooses VLC for CAM transmission which in return has a lower PRR than C-V2X.

the 3GPP threshold for CAM reception rate

The latency performance of CV2LC is compared with the other two standalone networks (C-V2X and V2LC) in figure 5.20b. The latency of the CV2LC is considerably decreased in comparison with LTE, while it is bigger than VLC latency. The difference in latency is due to the different channel access regulations in V2LC and LTE. As it was discussed in

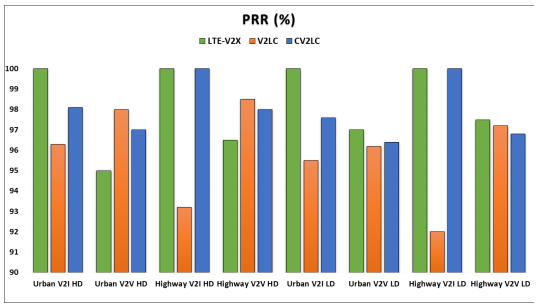

(a) Packet Reception Ratio [%]

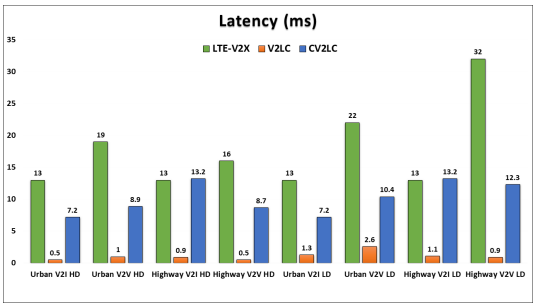

(b) Latency [ms]

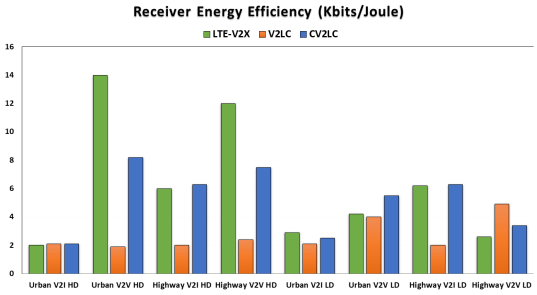

(c) Receiver Energy efficiency [Kbits/Joule]

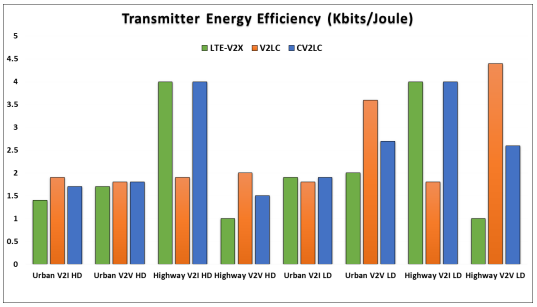

(d) Transmitter Energy efficiency [Kbits/Joule]

Figure 5.20: Performance comparison of LTE-V2x, V2LC, and CV2LC

previous sections, the SPS resource selection in LTE increases the delivery time while the point-to-point VLC links are liberated from channel access complexity. Moreover, CV2LC finds a good compromise between two channel access although it was not optimized for strict delay traffic.
The energy efficiency at the receiver of CV2LC is larger than VLC in most of the scenarios, and also larger than C-V2X in low-density scenarios except urban V2I according to figure 5.20c. Generally, CV2LC is less efficient in low density due to using of LTE technology in sparse scenarios and spending much more time in the listening phase. On the other hand, in high density, the CV2LC energy efficiency is slightly improved, but the C-V2X is more efficient this time because it receives more data per joule in dense V2V compared to dispersed V2V.
At first look at figure 5.20d, it is understandable that the energy efficiency at the transmitter is lower than the receiver, especially in C-V2X. Moreover, the VLC technology is more efficient than LTE in all scenarios apart from highway V2I. Accordingly, the CV2LC algorithm is more stable in energy consumption in the transition from low density to high density.

5.6 Conclusion

This chapter was dedicated to the vertical handover mechanism. In our case, The VLC has been chosen as a primary technology to transmit cooperative awareness messages in vehicular scenarios. In addition to VLC, LTE is supporting CAM dissemination when VLC is unavailable. Vertical handover is a frequent technique to keep a mobile node connected by switching a connection link from one technology to another. The selection of using VLC rather than LTE was motivated by packet reception

ratio, latency, and energy consumption. A new theoretical power model has been suggested in this chapter to analyze the energy efficiency of the transmitter and the receiver. Finally, the CV2LC handover algorithm was implemented in the ns-3 simulator with supplementary performance assessment tools.

Conclusions and Future Vision 6

The current study aimed to establish a stable VLC link between mobile nodes. The main challenges in maintaining a good QoS in the vehicular visible light network was mobility management and line of sight. We proposed different techniques to deal with these challenges. A realistic channel model based on the outdoor environment was presented and implemented in the ns3 simulator. Two different handover mechanisms and adaptive modulation schemes have been proposed to prolong the connection time of V2LC networks. The findings of this study have been verified through mathematical models, simulations, and experimentation.

6.1 Conclusions

Chapter 1 represented a summary of the thesis contents, including the definition of VLC and vehicular communication technologies, challenges, contributions, and the supplementary activities during the 3 years of Ph.D. In Chapter 2, a short history of VLC is presented. In addition to a detailed explanation of different technologies used in vehicular communications. The up-to-date state of the art was listed in this chapter according to the perspective of this thesis. Chapter 3 included the first bunch of contributions to this thesis. First of all, we defined a channel model for outdoor VLC including Lambertian emission and climate distortion models. For the more, link adaptive protocol has been suggested to scan the available VLC links and get associated to, for higher spectrum efficiency, upgrades the modulation level according to the link quality. This algorithm was performed in the ns3-V2LC networks module which includes a realistic channel model, sumo mobility, and LAP protocol. We assessed the performance of the V2LC network via multiple metrics in comparison with slotted-aloha, including outage probability, and goodput. Finally, we did an interesting analysis of the relation between pilot rate and protocol efficiency. Interference based haNdover mechanism for VISIBle Light nEtworks (INVISIBLE) was proposed in Chapter 4. It utilizes INR and IIR metrics instead of a conventional signal-based metric to assess the link quality. According to our study, normal Gaussian distribution is not a precise model in dominant interference systems. Therefore, INR defined the system dominant disturbances and IIR nominate the dominant interferer to proceed with the channel access procedure. When the dominant interferer verified, the distribution closely matches the distribution of the dominant interferer, while in noise dominant system the distribution is assumed Gaussian. Following INVISIBLE in presence of multiple interferer, the QoS requirement forces to pick the candidate access point which has the longest connection time. This model has been validated in ns3 simulator as well as a software-defined approach. The practical part in a small scale was composed of low power LEDs, low-cost PD, Arduino 1 as the LED driver, and USRP. The results showed an excellent alignment between simulation and real device experiment in terms of handover rate, delivered traffic per handover, and

handover delay ratio. The final contribution of this thesis was presented in Chapter 5, which includes a vertical handover mechanism called CV2LC. Initially, we proposed a theoretical model for power consumption for the VLC and LTE networks, then we compared their performances in terms of energy efficiency, PRR, and latency. Last but not least, CV2LC uses VLC to transmit CAM and switches to LTE when VLC does not meet the reliability requirement. In terms of validation the CV2LC, represents a more stable performance in different scenarios in comparison to C-V2X and V2LC stand-alone.

6.2 Future Vision

The CV2LC mechanism proposed in Chapter 5 was optimised for safety application traffics which should comply with a certain PRR threshold. More efficient vertical HO may integrate several application traffic types including safety and non-safety traffic. Considering various data traffic types, QoS requirement could be different. For instance, multimedia traffic requires larger bandwidth compared to voice call traffic, with different latency red lines.

Although, in this thesis we attempted to include all the important components in the power model, but experiments are necessary to achieve a more precise power model. Including real device implementation in future works will enhance the accuracy of the current model and validate it for other research activities.

Eventually, adaptive coding schemes could increase the robustness of the VLC in outdoor environments and prolong the coverage range. Integrating different coding rates into the adaptive modulation scheme is the highest priority of future work. Adaptive modulation and coding scheme (AMC) will increase the throughput and spectrum efficiency.

Special Terms

Numbers
3GPP Third Generation Partnership Project. 3
5G-NR 5G-New Radio. 11

A
AA Aperture Averaging. 15
ACLR Adjacent Channel Leakage Ratio. 49
ACO-OFDM Asymmetrically Clipped Optical OFDM. 1
ADC Analog to Digital Converter. 49
AMS Adaptive Modulation Scheme. 4
AP Access Point. 4
ARIB Association of Radio Industries and Businesses. 11
ARQ Automatic repeat request. 60
ASP Analog signal Processing. 49
ASTM American Society for Testing and Materials International. 11
AWGN Additive White Gaussian Noise. 18

B
BB Base-band. 51
BER Bit Error Rate. 4, 60
BPF band pass filter. 51
BSM Basic Safety Message. 55

C
CAGR Compound Annual Growth Rate. 1
CAM Cooperative Awareness Messages. 5, 45
CEN European Committee for Standardization. 11
CIR Channel Impulse Response. 14
CMOS Complementary Metal Oxide Semiconductors. 50
CoMP Coordinated Multi-Point. 15
CSI Channel State Information. 25
CSMA Channel Sensing Multiple Access. 14
CSR Candidate Single Sub-frame Resources. 47
CV2LC Cellular Vehicular VLC. 5, 45, 70
C-V2X Cellular V2X. 3

D
D2D Device to Device. 3
DAC Digital to Analog Converter. 49
DCO-OFDM Direct Current biased Optical OFDM. 1
DD Direct Detection. 1
DL Downlink. 49
DSP Digital Signal Processing. 49
DSRC Dedicated Short Range Communication. 2, 3

E
eNB evolved NodeB. 12
ETSI European Telecommunications Standards Institute. 11

F

FEC forward error correction. 60
FLE Français langue étrangère. 5
FoV Field of View. 2
FSO Free Space Optical. 7
FT-BSS Fast Basic Service Set Transition. 12

G
Gbps Gigs bits per second. 8
GHz Giga Hertz. 11
GOPS Giga operations per second. 57
GOPS/W Giga operations per second per watt. 50

H
HO Handover. 33, 70

I
I/Q In-phase and Quadrature. 51
IF Intermediate Frequency. 51
IIR Interferer to Interference Ratio. 4
IM Intensity Modulation. 1
IM/DD Intensity Modulation and Direct Detection. 1
INR Interference to Noise Ratio. 4
INRIA Institut national de recherche en sciences et technologies du numérique. 5
INVISIBLE Interference based haNdover mechanism for VISIBle Light nEtworks. 4, 29, 34, 69
IR Infrared. 8
ISM Industry, Science, and Medical. 12
ITS Intelligent Transportation system. 2

K
Kmph Kilometer per hours. 12

L
LANET visible-Light ad-hoc network. 15
LAP Link Adaptive Protocol. 4, 17
LD Laser Diode. 8
LED Light Emitting Diode. 1
LiFi Light Fidelity. 8
LNA low noise amplifier. 51
LoS Line of Sight. 2

M
M2M Machine-to-Machine. 1, 10
MAC Medium Access Control. 3
Mbps Mega bits per second. 12
MCS Modulation and Coding Scheme. 46
ME Mobile Entity. 30
MHz Mega Hertz. 11
MM Mobility Management. 45
MME MM Entity. 45
msec millisecond. 12

N
NS-3 Network Simulator Version 3. 4

O
OCC Optical Camera Communication. 8

OFDM Orthogonal Frequency Division Multiplexing. 1, 46
OOK On-Off Keying. 1, 22
OWC Optical Wireless Communication. 5

P
P2P Point-to-Point. 2
PA Power Amplifier. 49, 51
PAM Pulse Amplitude Modulation. 22
PAPR Peak-to-Average Power Ratio. 49
PD Photodetector. 1
PDF Probability Density Function. 19
PIR Packet Inter-Reception. 48
PPM Pulse Position Modulation. 1
ProSe Proximity Services. 11
PRR Packet Reception Ratio. 5, 70
PSCCH Physical Sidelink Control Channel. 46
PSK Pulse Shift Keying. 22
PSSCH Physical Sidelink Shared Channel. 46

Q
QAM Quadrature Amplitude Modulation. 24
QoE Quality of Experience. 2
QoS Quality of Service. 2, 69, 70

R
R&D Research and development. 1
RAT Radio Access Technologie. 2
RB Resource Blocks. 46
RF Radio Frequency. 1, 7–10, 14–16, 29, 49, 51, 53, 56, 62
RRC Radio Resource Configuration. 49
RRI Resource Reservation Interval. 47
RSI Received Signal Intensity. 15
RSRP Reference Signal Received Power. 30
RSS Received Signal Strength. 10, 15
RSSI Received Signal Strength Indicator. 48
RSU Road Side Unit. 10, 11

S
SAE Society of Automotive Engineers. 55
SCI Sidelink Control Information. 46
SINR Signal to Interference and Noise Ratio. 4
SNR Signal to Noise Ratio. 4, 17
SPS Semi-Persistent Scheduling. 45
SUMO Simulation of Urban MObility. 21

T
TAU Tracking Area Update. 45, 46
TB Transport Block. 46
TBS Transport Block Size. 49
THz Tera Hertz. 12
TIA trans-impedance amplifier. 52
ToA Time of Arrival. 10
TTI transmission time interval. 53

U

UE User Equipment. 45, 47
UL Uplink. 49
USRP Universal Software Radio Peripheral. 40
UTROV Un Tethered Remotely Operated Vehicle. 10
UV Ultra Violate. 8

V
V2D Vehicle-to-Device. 11
V2I Vehicle to Infrastructure. 2, 16
V2LC Vehicular Visible Light Communication. 3, 16
V2N Vehicle-to-Network. 11
V2P Vehicle to Pedestrian. 2
V2V Vehicle to Vehicle. 2
V2X Vehicle to Everything. 2
VANET Vehicular ad hoc Networks. 54
VC Vehicular Communication. 2, 16
VGA variable gain amplifier. 51
VLC Visible Light Communication. ix, xi, xii, 1, 16, 45, 46, 49, 52–54, 57–60, 62, 63, 65, 66, 69
VPPM Variable PPM. 22, 24

W
WAVE Wireless Access in Vehicular Environments. 11
WiFi Wireless Fidelity. 8, 12

Bibliography

Here are the references in citation order.

[1] *Cisco Annual Internet Report (2018-2023) white paper*. https://www.cisco.com/c/en/us/solutions/collateral/executive-perspectives/annual-internet-report/white-paper-c11-741490.html. Updated: March 9, 2020 (cited on pages 1, 8).

[2] Nan Chi et al. 'Visible Light Communication in 6G: Advances, Challenges, and Prospects'. In: *IEEE Vehicular Technology Magazine* 15.4 (2020), pp. 93–102. DOI: 10.1109/MVT.2020.3017153 (cited on page 1).

[3] Luiz Eduardo Mendes Matheus et al. 'Visible Light Communication: Concepts, Applications and Challenges'. In: *IEEE Communications Surveys & Tutorials* 21.4 (2019), pp. 3204–3237. DOI: 10.1109/COMST.2019.2913348 (cited on pages 2, 10, 14, 29).

[4] Alin-Mihai Căilean and Mihai Dimian. 'Current Challenges for Visible Light Communications Usage in Vehicle Applications: A Survey'. In: *IEEE Communications Surveys Tutorials* 19.4 (2017), pp. 2681–2703. DOI: 10.1109/COMST.2017.2706940 (cited on pages 2, 14).

[5] Pranav Kumar Singh, Sunit Kumar Nandi, and Sukumar Nandi. 'A tutorial survey on vehicular communication state of the art, and future research directions'. In: *Vehicular Communications* 18 (2019), p. 100164. DOI: https://doi.org/10.1016/j.vehcom.2019.100164 (cited on pages 3, 12, 30).

[6] Seyhan Ucar, Sinem Coleri Ergen, and Oznur Ozkasap. 'Visible light communication assisted safety message dissemination in multiplatoon'. In: *2017 IEEE International Black Sea Conference on Communications and Networking (BlackSeaCom)*. 2017, pp. 1–5. DOI: 10.1109/BlackSeaCom.2017.8277704 (cited on pages 3, 16).

[7] *Armada Beacon (1588) Great Britain*. https://www.geograph.org.uk/photo/3223640. taken in 2012 by Paul Gillett, near to Portslade-by-Sea, Brighton And Hove, Great Britain (cited on page 7).

[8] A. G. Bell. 'Selenium and the Photophone'. In: *Nature* 569 (1880), pp. 500–5030 (cited on page 7).

[9] Mostafa Zaman Chowdhury et al. 'The Role of Optical Wireless Communication Technologies in 5G/6G and IoT Solutions: Prospects, Directions, and Challenges'. In: *Applied Sciences* 9.20 (2019). DOI: 10.3390/app9204367 (cited on page 8).

[10] Ton Koonen. 'Indoor Optical Wireless Systems: Technology, Trends, and Applications'. In: *Journal of Lightwave Technology* 36.8 (2018), pp. 1459–1467. DOI: 10.1109/JLT.2017.2787614 (cited on page 8).

[11] *Highlights of Cisco's Internet Traffic Report and Forecast*. https://techblog.comsoc.org/2021/12/29/highlights-of-ciscos-internet-traffic-forecast/. Posted on December 29, 2021 by Alan Weissberger (cited on page 8).

[12] Svilen Dimitrov and Harald Haas. *Principles of LED Light Communications: Towards Networked Li-Fi*. Mar. 2015 (cited on pages 8, 13).

[13] Beibei Wang and K.J. Ray Liu. 'Advances in cognitive radio networks: A survey'. In: *IEEE Journal of Selected Topics in Signal Processing* 5.1 (2011), pp. 5–23. DOI: 10.1109/JSTSP.2010.2093210 (cited on page 8).

[14] Maris Bauer and Fabian Friederich. 'Terahertz and Millimeter Wave Sensing and Applications'. In: *Sensors* 22.24 (Dec. 2022), p. 9693. DOI: 10.3390/s22249693 (cited on page 8).

[15] BSI British Standards Std. 'Photobiological safety of lamps and lamp systems'. In: *EN 62471* 20 (2008) (cited on page 9).

[16] B. Alexander Stephen. *Optical Communication Receiver Design*. 1997 (cited on page 9).

[17] Christoph F. Mecklenbrauker et al. 'Vehicular Channel Characterization and Its Implications for Wireless System Design and Performance'. In: *Proceedings of the IEEE* 99.7 (2011), pp. 1189–1212. DOI: 10.1109/JPROC.2010.2101990 (cited on page 10).

[18] Latif Ullah Khan. 'Visible light communication: Applications, architecture, standardization and research challenges'. In: *Digital Communications and Networks* 3.2 (2017), pp. 78–88. DOI: https://doi.org/10.1016/j.dcan.2016.07.004 (cited on page 10).

[19] Antonio Costanzo and Valeria Loscri. 'Visible Light Indoor Positioning in a Noise-aware Environment'. In: *2019 IEEE Wireless Communications and Networking Conference (WCNC)*. 2019, pp. 1–6. DOI: 10.1109/WCNC.2019.8885607 (cited on pages 10, 39).

[20] Deok-Rae Kim et al. 'Outdoor Visible Light Communication for inter- vehicle communication using Controller Area Network'. In: *2012 Fourth International Conference on Communications and Electronics (ICCE)*. 2012, pp. 31–34. DOI: 10.1109/CCE.2012.6315865 (cited on page 10).

[21] Christian Weiß. 'V2X communication in Europe – From research projects towards standardization and field testing of vehicle communication technology'. In: *Computer Networks* 55.14 (2011). Deploying vehicle-2-x communication, pp. 3103–3119. DOI: https://doi.org/10.1016/j.comnet.2011.03.016 (cited on page 11).

[22] *C-V2X Scenario Simulations and Validation*. https://www.allion.com/automotive/cv2x-validation/. Updated: 2017 (cited on page 11).

[23] Yunxin (Jeff) Li. 'An Overview of the DSRC/WAVE Technology'. In: *Quality, Reliability, Security and Robustness in Heterogeneous Networks*. Ed. by Xi Zhang and Daji Qiao. Berlin, Heidelberg: Springer Berlin Heidelberg, 2012, pp. 544–558 (cited on page 11).

[24] 3GPP. *Study on LTE-based V2X services*. ETSI TR 36 885. Sophia Antipolis Cedex, FRANCE: ETSI(European Telecommunications Standards Institute, Sept. 2016 (cited on pages 11, 56, 57).

[25] M. Nadeem Ahangar et al. 'A Survey of Autonomous Vehicles: Enabling Communication Technologies and Challenges'. In: *Sensors* 21.3 (2021). DOI: 10.3390/s21030706 (cited on page 11).

[26] Massimo Condoluci et al. '5G V2X System-Level Architecture of 5GCAR Project'. In: *Future Internet* 11.10 (2019). DOI: 10.3390/fi11100217 (cited on page 12).

[27] Shareh Lewin. 'LEDs bring new light to car-to-car communication'. In: *IEEE Spectrum* (2014) (cited on page 12).

[28] Agon Memedi and Falko Dressler. 'Vehicular visible light communications: A survey'. In: *IEEE Communications Surveys & Tutorials* 23.1 (2020), pp. 161–181 (cited on page 13).

[29] Claas Tebruegge, Agon Memedi, and Falko Dressler. 'Empirical characterization of the NLOS component for vehicular visible light communication'. In: *2019 IEEE Vehicular Networking Conference (VNC)*. IEEE. 2019, pp. 1–4 (cited on page 13).

[30] Gurinder Singh, Anand Srivastava, and Vivek Ashok Bohara. 'Impact of Weather Conditions and Interference on the Performance of VLC based V2V Communication'. In: *2019 21st International Conference on Transparent Optical Networks (ICTON)*. 2019, pp. 1–4. DOI: 10.1109/ICTON.2019.8840164 (cited on page 13).

[31] R.J. Green and Mark Leeson. 'The optical wireless channel'. In: *Advanced Optical Wireless Communication Systems* (Jan. 2012), pp. 240–272. DOI: 10.1017/CBO9780511979187.010 (cited on page 14).

[32] Ai-Ling Chen et al. 'Time variation in vehicle-to-vehicle visible light communication channels'. In: *2016 IEEE Vehicular Networking Conference (VNC)*. 2016, pp. 1–8. DOI: 10.1109/VNC.2016.7835926 (cited on page 14).

[33] Agon Memedi et al. 'Impact of Vehicle Type and Headlight Characteristics on Vehicular VLC Performance'. In: *2018 IEEE Vehicular Networking Conference (VNC)*. 2018, pp. 1–8. DOI: 10.1109/VNC.2018.8628444 (cited on pages 14, 21).

[34] Harald Haas et al. 'What is LiFi?' In: *Journal of Lightwave Technology* 34.6 (2016), pp. 1533–1544. DOI: 10.1109/JLT.2015.2510021 (cited on pages 14, 16, 29).

[35] Antonio Costanzo, Valeria Loscri, and Mauro Biagi. 'Adaptive Modulation Control for Visible Light Communication Systems'. In: *Journal of Lightwave Technology* 39.9 (2021), pp. 2780–2789. DOI: 10.1109/JLT.2021.3056177 (cited on page 14).

[36] Nan Cen et al. 'LANET: Visible-light ad hoc networks'. In: *Ad Hoc Networks* 84 (2019), pp. 107–123. DOI: https://doi.org/10.1016/j.adhoc.2018.04.009 (cited on page 14).

[37] J. Jagannath and T. Melodia. 'An Opportunistic Medium Access Control Protocol for Visible Light Ad Hoc Networks'. In: *2018 International Conference on Computing, Networking and Communications (ICNC)*. 2018, pp. 609–614 (cited on page 15).

[38] Jithin Jagannath and Tommaso Melodia. 'VL-ROUTE: A Cross-Layer Routing Protocol for Visible Light Ad Hoc Network'. In: June 2019, pp. 1–9. DOI: 10.1109/WoWMoM.2019.8793030 (cited on page 15).

[39] Jithin Jagannath and Tommaso Melodia. 'An Opportunistic Medium Access Control Protocol for Visible Light Ad Hoc Networks'. In: *2018 International Conference on Computing, Networking and Communications (ICNC)*. 2018, pp. 609–614. DOI: 10.1109/ICCNC.2018.8390277 (cited on page 15).

[40] Elizabeth Eso et al. 'Performance of Vehicular Visible Light Communications under the Effects of Atmospheric Turbulence with Aperture Averaging'. In: *Sensors* 21.8 (2021). DOI: 10.3390/s21082751 (cited on page 15).

[41] Xiping Wu et al. 'Smart Handover for Hybrid LiFi and WiFi Networks'. In: *IEEE Transactions on Wireless Communications* 19.12 (2020), pp. 8211–8219. DOI: 10.1109/TWC.2020.3020160 (cited on pages 15, 30).

[42] Anna Maria Vegni and Thomas D. C. Little. 'Handover in VLC systems with cooperating mobile devices'. In: *2012 International Conference on Computing, Networking and Communications (ICNC)*. 2012, pp. 126–130. DOI: 10.1109/ICCNC.2012.6167395 (cited on page 15).

[43] Mehdi Karbalayghareh et al. 'Channel Modelling and Performance Limits of Vehicular Visible Light Communication Systems'. In: *IEEE Transactions on Vehicular Technology* 69.7 (2020), pp. 6891–6901. DOI: 10.1109/TVT.2020.2993294 (cited on pages 15, 19, 31).

[44] Moe Z. Win, Pedro C. Pinto, and Lawrence A. Shepp. 'A Mathematical Theory of Network Interference and Its Applications'. In: *Proceedings of the IEEE* 97.2 (2009), pp. 205–230. DOI: 10.1109/JPROC.2008.2008764 (cited on pages 15, 30, 32).

[45] Michael Rahaim and Thomas D.C. Little. 'Optical interference analysis in Visible Light Communication networks'. In: *2015 IEEE International Conference on Communication Workshop (ICCW)*. 2015, pp. 1410–1415. DOI: 10.1109/ICCW.2015.7247376 (cited on pages 16, 30, 32, 60).

[46] Marwan Hammouda et al. 'Link Selection in Hybrid RF/VLC Systems Under Statistical Queueing Constraints'. In: *IEEE Transactions on Wireless Communications* 17.4 (2018), pp. 2738–2754. DOI: 10.1109/TWC.2018.2802937 (cited on page 16).

[47] Quang-Hien Dang and Myungsik Yoo. 'Handover Procedure and Algorithm in Vehicle to Infrastructure Visible Light Communication'. In: *IEEE Access* 5 (2017), pp. 26466–26475. DOI: 10.1109/ACCESS.2017.2771199 (cited on pages 16, 30, 36).

[48] M. Selim Demir, Hossien B. Eldeeb, and Murat Uysal. 'CoMP-Based Dynamic Handover for Vehicular VLC Networks'. In: *IEEE Communications Letters* 24.9 (2020), pp. 2024–2028. DOI: 10.1109/LCOMM.2020.2994416 (cited on pages 16, 30).

[49] Jian Dang, Liang Wu, and Zaichen Zhang. *OFDM Systems for Optical Communication with Intensity Modulation and Direct Detection*. June 2017 (cited on page 17).

[50] Adel Aldalbahi et al. 'Visible Light Communication Module: An Open Source Extension to the ns3 Network Simulator With Real System Validation'. In: *IEEE Access* 5 (2017), pp. 22144–22158. DOI: 10.1109/ACCESS.2017.2759779 (cited on pages 17, 22, 39, 60).

[51] Sheng-Hong Lin et al. 'Outage performance analysis for outdoor vehicular visible light communications'. In: *2017 9th International Conference on Wireless Communications and Signal Processing (WCSP)*. 2017, pp. 1–5. DOI: 10.1109/WCSP.2017.8170939 (cited on pages 18, 22, 23, 31).

[52] T. Komine and M. Nakagawa. 'Fundamental analysis for visible-light communication system using LED lights'. In: *IEEE Transactions on Consumer Electronics* 50.1 (2004), pp. 100–107. DOI: 10.1109/TCE.2004.1277847 (cited on page 18).

[53] Alison Fields, Steven Linnville, and Robert Hoyt. 'Correlation of objectively measured light exposure and serum vitamin D in men aged over 60 years'. In: *Health Psychology Open* 3 (May 2016). DOI: 10.1177/2055102916648679 (cited on page 19).

[54] *ns3 Network Simulator*. https://www.nsnam.org/. Updated: 2022 (cited on page 21).

[55] *ns3 statistics*. https://www.nsnam.org/about/statistics/. Updated: 1/22/18 (cited on page 21).

[56] Adel Aldalbahi et al. 'Extending ns3 to simulate visible light communication at network-level'. In: *2016 23rd International Conference on Telecommunications (ICT)*. IEEE. 2016, pp. 1–6 (cited on pages 21, 22, 34, 46).

[57] Caixia Song. 'Performance Analysis of the IEEE 802.11p Multichannel MAC Protocol in Vehicular Ad Hoc Networks'. In: *Sensors* 17.12 (2017). DOI: 10.3390/s17122890 (cited on pages 22, 32, 39).

[58] Barbara M. Masini, Alessandro Bazzi, and Alberto Zanella. 'Vehicular visible light networks with full duplex communications'. In: *2017 5th IEEE International Conference on Models and Technologies for Intelligent Transportation Systems (MT-ITS)*. 2017, pp. 98–103. DOI: 10.1109/MTITS.2017.8005646 (cited on page 29).

[59] Anna Maria Vegni, Marwan Hammouda, and Valeria Loscrí. 'A VLC-based Footprinting Localization Algorithm for Internet of Underwater Things in 6G networks'. In: *2021 17th International Symposium on Wireless Communication Systems (ISWCS)*. 2021, pp. 1–6. DOI: 10.1109/ISWCS49558.2021.9562170 (cited on page 29).

[60] R Green and M Leeson. 'The optical wireless channel'. In: *Proc. Adv. Opt. Wireless Commun. Syst.* 2012, pp. 240–272 (cited on page 30).

[61] Lin Cheng et al. 'Comparison of Radio Frequency and Visible Light Propagation Channels for Vehicular Communications'. In: *IEEE Access* 6 (2018), pp. 2634–2644. DOI: 10.1109/ACCESS.2017.2784620 (cited on page 30).

[62] Dang Quang Hien and Myungsik Yoo. 'Handover in outdoor Visible Light Communication system'. In: *2017 International Conference on Information Networking (ICOIN)*. 2017, pp. 67–69. DOI: 10.1109/ICOIN.2017.7899477 (cited on pages 30, 36).

[63] Ali Safa Sadiq et al. 'An Intelligent Vertical Handover Scheme for Audio and Video Streaming in Heterogeneous Vehicular Networks'. In: *Mobile Networks and Applications* 18.12 (2013). DOI: 10.1007/s11036-013-0465-8 (cited on pages 33, 39).

[64] 'IEEE Standard for Local and Metropolitan Area Networks–Part 15.7: Short-Range Wireless Optical Communication Using Visible Light'. In: *IEEE Std 802.15.7-2011* (2011), pp. 1–309. DOI: 10.1109/IEEESTD.2011.6016195 (cited on page 36).

[65] Md Saifuddin et al. 'Performance analysis of cellular-v2x with adaptive & selective power control'. In: *2020 IEEE 3rd Connected and Automated Vehicles Symposium (CAVS)*. IEEE. 2020, pp. 1–7 (cited on page 45).

[66] Alaa Alsaeedy and Edwin Chong. 'A review of mobility management entity in LTE networks: Power consumption and signaling overhead'. In: *International Journal of Network Management* 30 (Nov. 2019). DOI: 10.1002/nem.2088 (cited on page 46).

[67] Rafael Molina-Masegosa, Javier Gozalvez, and Miguel Sepulcre. 'Comparison of IEEE 802.11p and LTE-V2X: An Evaluation With Periodic and Aperiodic Messages of Constant and Variable Size'. In: *IEEE Access* 8 (2020), pp. 121526–121548. DOI: 10.1109/ACCESS.2020.3007115 (cited on page 47).

[68] 3GPP TS 36.213. *LTE; Evolved Universal Terrestrial Radio Access (E-UTRA); Physical layer procedure*. ETSI TS 136 213. Sophia Antipolis Cedex, FRANCE: ETSI(European Telecommunications Standards Institute), Sept. 2019 (cited on page 47).

[69] Fabian Eckermann, Moritz Kahlert, and Christian Wietfeld. 'Performance analysis of C-V2X mode 4 communication introducing an open-source C-V2X simulator'. In: *2019 IEEE 90th Vehicular Technology Conference (VTC2019-Fall)*. IEEE. 2019, pp. 1–5 (cited on pages 48, 57).

[70] Anders R. Jensen et al. 'LTE UE Power Consumption Model: For System Level Energy and Performance Optimization'. In: *2012 IEEE Vehicular Technology Conference (VTC Fall)*. 2012, pp. 1–5. DOI: 10.1109/VTCFall.2012.6399281 (cited on page 48).

[71] 3GPP. *Multiplexing and channel coding*. ETSI TS 36 212. Sophia Antipolis Cedex, FRANCE: ETSI(European Telecommunications Standards Institute), Sept. 2010 (cited on page 49).

[72] 3GPP. *UE radio transmission and reception*. ETSI TS 36 101. Sophia Antipolis Cedex, FRANCE: ETSI(European Telecommunications Standards Institute), Sept. 2012 (cited on page 49).

[73] Anthony Ghiotto et al. 'Dual-Mode Power Amplifier Module with In-Band Reconfigurable Output Power for Multifunctional Radar and Radio Communication Systems'. In: *2014 International Radar Conference, Radar 2014* (Oct. 2014). DOI: 10.1109/RADAR.2014.7060397 (cited on page 49).

[74] Yan Li et al. 'A SiGe envelope-tracking power amplifier with an integrated CMOS envelope modulator for Mobile WiMAX/3GPP LTE transmitters'. In: *Microwave Theory and Techniques, IEEE Transactions on* 59 (Nov. 2011), pp. 2525–2536. DOI: 10.1109/TMTT.2011.2164550 (cited on page 49).

[75] Cristian Anghel, Cristian Stanciu, and Constantin Paleologu. 'LTE Turbo Decoding Parallel Architecture with Single Interleaver Implemented on FPGA'. In: *Circuits Syst. Signal Process.* 36.4 (2017), pp. 1455–1475. DOI: 10.1007/s00034-016-0362-z (cited on page 50).

[76] Claude Desset et al. 'Flexible power modeling of LTE base stations'. In: *2012 IEEE Wireless Communications and Networking Conference (WCNC)*. 2012, pp. 2858–2862. DOI: 10.1109/WCNC.2012.6214289 (cited on pages 50, 55).

[77] A.A. Abidi. 'Direct-conversion radio transceivers for digital communications'. In: *IEEE Journal of Solid-State Circuits* 30.12 (1995), pp. 1399–1410. DOI: 10.1109/4.482187 (cited on page 51).

[78] Lingjing Kong et al. 'Power Consumption Evaluation in High Speed Visible Light Communication Systems'. In: *2018 IEEE Global Communications Conference (GLOBECOM)*. 2018, pp. 1–6. DOI: 10.1109/GLOCOM.2018.8647711 (cited on pages 52, 53, 57).

[79] Hauke Holtkamp et al. 'A Parameterized Base Station Power Model'. In: *Communications Letters, IEEE* 17 (Nov. 2013), pp. 2033–2035. DOI: 10.1109/LCOMM.2013.091213.131042 (cited on page 53).

[80] Marco Malinverno et al. 'A Multi-Stack Simulation Framework for Vehicular Applications Testing'. In: *Proceedings of the 10th ACM Symposium on Design and Analysis of Intelligent Vehicular Networks and Applications*. DIVANet '20. Alicante, Spain: Association for Computing Machinery, 2020, pp. 17–24. DOI: 10.1145/3416014.3424603 (cited on page 54).

[81] Rafael Molina-Masegosa et al. 'Empirical Models for the Realistic Generation of Cooperative Awareness Messages in Vehicular Networks'. In: *IEEE Transactions on Vehicular Technology* 69.5 (2020), pp. 5713–5717. DOI: 10.1109/TVT.2020.2979232 (cited on page 55).

[82] José Santa et al. 'Experimental evaluation of CAM and DENM messaging services in vehicular communications'. In: *Transportation Research Part C: Emerging Technologies* 46 (2014), pp. 98–120. DOI: https://doi.org/10.1016/j.trc.2014.05.006 (cited on page 55).

[83] A.S. Chekkouri, A. Ezzouhairi, and S. Pierre. '10 - Connected vehicles in an intelligent transport system'. In: *Vehicular Communications and Networks*. Ed. by Wai Chen. Woodhead Publishing Series in Electronic and Optical Materials. Woodhead Publishing, 2015, pp. 193–221. DOI: https://doi.org/10.1016/B978-1-78242-211-2.00010-6 (cited on page 56).

[84] Rafael Molina-Masegosa, Javier Gozalvez, and Miguel Sepulcre. 'Configuration of the C-V2X mode 4 sidelink PC5 interface for vehicular communication'. In: *2018 14th International conference on mobile ad-hoc and sensor networks (MSN)*. IEEE. 2018, pp. 43–48 (cited on page 56).

[85] *Lighting Design Guidance*. https://globaldesigningcities.org/publication/global-street-design-guide/utilities-and-infrastructure/lighting-and-technology/lighting-design-guidance/. Posted: May 18, 2022 (cited on page 57).

[86] *Speed Limits*. https://www1.nyc.gov/html/dot/downloads/pdf/current-pre-vision-zero-speed-limit-maps.pdf. Updated: June, 2014 (cited on page 57).

[87] ETSI. *Intelligent Transport Systems (ITS) Vehicular Communications Basic Set of Applications (Specification of Cooperative Awareness Basic Service)*. ETSI TS 102 637-2. Sophia Antipolis Cedex, FRANCE: ETSI(European Telecommunications Standards Institute, Mar. 2011 (cited on page 57).

[88] *Traffic Density U.S. Environmental Protection Agency*. https://www.epa.gov/system/files/documents/2022-03/traffic-density-indicator-reference-sheet-20220306_0.pdf. Indicator Reference Sheet – March 6, 2022 (cited on page 58).

[89] *Lighting design guidance Global Designing Cities Initiative*. https://globaldesigningcities.org/publication/global-street-design-guide/utilities-and-infrastructure/lighting-and-technology/lighting-design-guidance//. Dimensions and Spacing – May 18, 2022 (cited on pages 60, 61).

[90] Cen B. Liu, Bahareh Sadeghi, and Edward W. Knightly. 'Enabling Vehicular Visible Light Communication (V2LC) Networks'. In: *Proceedings of the Eighth ACM International Workshop on Vehicular Inter-Networking*. VANET '11. Las Vegas, Nevada, USA: Association for Computing Machinery, 2011, pp. 41–50. DOI: 10.1145/2030698.2030705 (cited on page 62).